

2005

Characterization and Design of a Molecular Imprinted Polymer for Cinchona Alkaloids

William P. Fish
Seton Hall University

Follow this and additional works at: <https://scholarship.shu.edu/dissertations>

 Part of the [Analytical Chemistry Commons](#)

Recommended Citation

Fish, William P, "Characterization and Design of a Molecular Imprinted Polymer for Cinchona Alkaloids" (2005). *Seton Hall University Dissertations and Theses (ETDs)*. 318.
<https://scholarship.shu.edu/dissertations/318>

**Characterization and Design of a Molecular Imprinted
Polymer for *Cinchona* Alkaloids**

By:

William P. Fish

Dissertation submitted to the Department of Chemistry and Biochemistry of Seton Hall
University in partial fulfillment of the requirements for the degree of

DOCTOR OF PHILOSOPHY

in

Chemistry

May, 2003

We certify that we have read this thesis and that, in our opinion, it is adequate in scope and quality as a dissertation for the degree of Doctor of Philosophy.

APPROVED:




Nicholas H. Snow, Ph.D.
Research Mentor



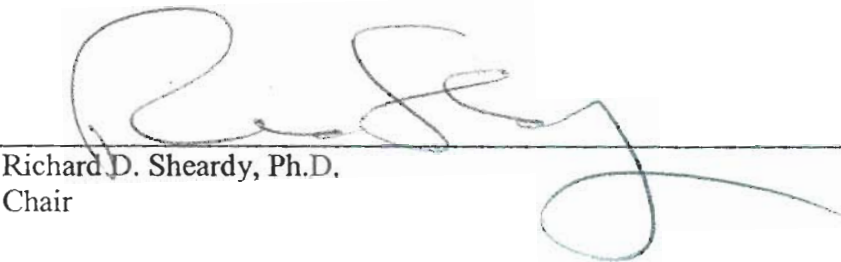
Yuri Kazakevich, Ph.D.
Member of Dissertation Committee



Cecilia H. Marzabadi, Ph.D.
Member of Dissertation Committee



Thomas P. O'Brien, Ph.D.
Member of Dissertation Committee



Richard D. Sheardy, Ph.D.
Chair

Acknowledgements

My wife, Emily, and daughter, Caroline, for always being there with unconditional love and support. I would not have made it this far without either of you.

My parents, siblings, and in-laws for all of their words of encouragement and support.

Dr. Nicholas H. Snow for all his patience, guidance as well as financial support. Thank you for letting me take this research in any direction I wanted and for being there when experiments failed. Also, extra thanks from my wife and I for all of your support these past two years.

Dr. Yuri Kazakevich, Dr. Cecilia Marzabadi, and Dr. Thomas O'Brien for all of their encouragement and words of wisdom over these past years. Thank you for all the tough questions over the years as well as pushing me to do my best every day.

The Department of Chemistry and Biochemistry faculty and graduate students of Seton Hall University for all of their ideas and support over the past years.

Maureen Grutt for all her help in dealing with the paperwork every year.

Seton Hall University for their financial support.

Merck Research Laboratories for providing materials, equipment, and lab space to perform some of the work in this dissertation.

Matt and Staci Mongelli for everything over these past four years. Thank you!

Dedication

In memory of my grandfather, Dr. William A. Fish for sowing the seeds of science at an early age.

In memory of Dr. Anthony R. J. Andrews, whose time on earth was short, but whose spirit lives on his students.

Table of Contents

Acknowledgements	i
Dedication	ii
Table of Contents	iii
List of Figures	vii
List of Tables	xii
Chapter 1	
Introduction	1
Types of Imprinting	4
Covalent Molecular Imprinting	4
Non-Covalent Molecular Imprinting	5
Applications	9
Antibody/Immunoassay	12
MIP Based Sensors	21
Enzyme Mimics/Catalysis	35
Solid-Phase Extraction	43
Chromatography	55
Conclusion	64
Chapter 2	
Introduction	68
Functional Group Arrangement and Shape Selectivity	68
Polymerization Solvent and Temperature	73

Influence of Functional Monomer	81
Recent Developements	84
Novel Polymerizations	84
Multi-Step Swelling	86
Surface Imprinting	89
Microgel Spheres	91
Covalent/Non-Covalent	94
Novel Monomers	101
Monomer/Template Ratio	109
Chapter 3	
Introduction	117
Experimental	131
Reagents	131
Instrumentation	131
Polymer Synthesis, Column and Sample Preparation	132
Attenuated Total Reflectance-Infrared Spectroscopy Studies	135
Binding Studies: Theory	135
Binding Studies: Sample Preparation	137
Isothermal Titration Calorimetry: Cinchonidine-MAA System	138
Results	138
ATR-IR Studies: Evaluation of Method	138

Isothermal Titration Calorimetry: Indinavir-MAA System	149
Polymer Selectivity	154
Isothermal Titration Calorimetry: Indinavir	161
Conclusion	170
Chapter 4	
Introduction	172
Experimental	180
Reagents	180
Instrumentation	181
Polymer Synthesis	182
Molecular Imprinted Polymer-Solid Phase Extraction	182
Preparation of MIP-SPE cartridges	182
Breakthrough Volume: Theory	182
Breakthrough Volume: Sample Preparation	185
Batch Binding Studies	185
Results and Discussion	186
Molecular Imprinted Polymer-Solid Phase Extraction	186
Cartridge Inertness	186
Breakthrough Volume Curves	186
Mobile Phase Competitor Studies	190
Recovery Studies	193
Comparison between Blank and Imprinted Polymer	201

Scatchard Plot Analysis	205
Conclusion	216
Chapter 5. Overall Conclusions	218
List of References	219

List of Figures

1-1. Lock and Key Principle	2
1-2. Imprinting of silica gels	3
1-3. Formation of monomer-template complex in covalent imprinting	6
1-4. Covalent imprinting of D-mannopyranoside	7
1-5. Several functional monomers used in non-covalent imprinting	8
1-6. Non-covalent imprinting of cinchonidine	10
1-7. Published literature concerning molecular imprinting	11
1-8. Binding isotherm for a (S)-propranolol imprinted polymer	16
1-9. Flow-through sensor for chloramphenicol	19
1-10. Synthesis of the CAP-DANS molecule	20
1-11. Chromatogram obtained from chloramphenicol flow-through sensor	22
1-12. Response curve of an epinephrine selective sensor	25
1-13. Response curve of several different nicotine selective sensor	30
1-14. Response of interferants to a nicotine selective sensor	32
1-15. Results obtained for a MIP catalyzed dehydrofluorination reaction	37
1-16. Ultra-violet-visible spectra of a MIP catalyzed dehydrofluorination reaction	39
1-17. Schematic of a catalytic fixed bed reactor	40
1-18. Ultra-violet-visible spectra from fixed bed reactor	41
1-19. Synthesis of phosphotriesterase enzyme mimic	42
1-20. Results of MIP facilitated paraoxon hydrolysis	44
1-21. Synthesis of a pentamidine imprinted polymer	47
1-22. Desorption profile for pentamidine	49

1-23. Chromatograms of MIP extracted ginko leaf hydrolyzate	50
1-24. Structures of several nerve agent degradation products	51
1-25. Chromatograms of a nerve agent solution before and after MIP extraction	54
1-26. Separation of a racemic naproxen mixture on a (S)-naproxen imprinted polymer	56
1-27. Separation of several NSAID compounds on a (S)-naproxen imprinted polymer	57
1-28. Preparation of a MIP capillary electrophoresis column selective for L-phenylalanine anilide	58
1-29. MIP capillary electrophoresis separation of D,L-phenylalanine anilide	60
1-30. MIP capillary electrophoresis separation of several anaesthetics on a (S)-ropivacaine imprinted polymer.	61
1-31. Supercritical fluid separation of D,L-phenylalanine anilide on a L-phenylalanine imprinted polymer	63
1-32. Thin layer chromatography separation using a (-)-norephedrine imprinted polymer	67
2-1. Structures and selectivities of several amino acid derivatives	69
2-2. Scatchard plots for a ricin imprinted polymer	74
2-3. Scatchard plots for a Ricin A and Ricin B imprinted polymers	75
2-4. Schematic of the multi-swelling polymer synthesis	87
2-5. Separation of several NSAIDS on a multi-swelled (S)-ibuprofen imprinted polymer	88
2-6. Surface imprinting polymerization	90
2-7. Binding data for a Z-glutamic acid imprinted polymer prepared by surface imprinting	92
2-8. General morphology diagram for crosslinked polymers	93
2-9. Binding studies on a theophylline imprinted microsphere	95
2-10. Synthesis of a cholesterol imprinted polymer using the covalent/non-covalent technique	98

2-11. Binding studies on a covalent/non-covalent prepared polymer selective for cholesterol	99
2-12. Imprinting of a diurea template	100
2-13. Separation of racemic DNB on a polymer prepared using a chiral monomer	106
2-14. Binding of theophylline to polymers prepared with different amounts of monomer	110
2-15. Selectivity of several nicotine imprinted polymers prepared with different amounts of monomer	113
2-16. Effects of sample load on selectivity for several different nicotine imprinted polymers	114
3-1. Effect of increasing monomer concentration of ¹H NMR line widths	120
3-2. Effect of increasing monomer concentration on a ultraviolet-visible spectra of	121
3-3. Structure of Indinavir	124
3-4. Scatchard plot describing the binding between methacrylic acid and Indinavir	125
3-5. <i>Cinchona</i> Alkaloids	129
3-6. Structures of synthesis materials	133
3-7. Schematic of column packing system	134
3-8. ATR-FTIR spectra of methacrylic acid	136
3-9. FTIR spectra of cinchonidine	141
3-10. ATR-FTIR of methacrylic acid standards	142
3-11. Methacrylic acid calibration curve	143
3-12. ATR-FTIR spectra of methacrylic acid-cinchonidine solutions	144
3-13. Scatchard plot describing the binding between methacrylic acid and cinchonidine	147
3-14. Isothermal titration calorimeter schematic	150
3-15. ITC plot for $\frac{1}{2}$ equivalent titration of cinchonidine with methacrylic acid	152

3-16. ITC plot for ¼ equivalent titration of cinchonidine with methacrylic acid	153
3-17. Separation between cinchonine and cinchonidine on a 1:1 methacrylic acid:cinchonidine imprinted polymer	156
3-18. Separation between cinchonine and cinchonidine on a 1:1 methacrylic acid:cinchonidine imprinted polymer	157
3-19. Separation between cinchonine and cinchonidine on a 1:1 methacrylic acid:cinchonidine imprinted polymer	158
3-20. Separation between cinchonine and cinchonidine on a 1:1 methacrylic acid:cinchonidine imprinted polymer	159
3-21. ITC plot for ¼ equivalent titration of Indinavir with methyl methacrylate	163
3-22. ITC plot for ¼ equivalent titration of Indinavir with 4-vinyl pyridine	164
3-23. ITC plot for the ¼ equivalent titration of Indinavir with methacrylic acid.	165
3-24. Separation between Indinavir and its epi-carboxamide isomer on a 7:1 methacrylic acid:Indinavir imprinted polymer.	169
4-1. Schematic of a solid-phase extraction cartridge	173
4-2. Basic process of solid-phase extraction	174
4-3. Theoretical breakthrough volume curve for a SPE cartridge	184
4-4. Initial cinchonidine breakthrough volume curve	188
4-5. Initial cinchonine breakthrough volume curve	189
4-6. Complete set of breakthrough volume curves for cinchonidine	191
4-7. Complete set of breakthrough volume curves for cinchonine	192
4-8. HPLC chromatogram of cinchonidine obtained using 20/80 THF/Water (v/v) as the sample diluent	197
4-9. HPLC chromatogram of cinchonidine obtained using 30/70 THF/Water (v/v) as the sample diluent	198
4-10. HPLC chromatogram of cinchonidine obtained using 50/50 THF/Water (v/v) as the sample diluent	199

4-11. HPLC chromatogram of cinchonidine obtained using 30/70 ACN/Water (v/v) as the sample diluent	202
4-12. Binding isotherms for a 4:1 imprinted and blank polymer	204
4-13. Calibration curve for cinchonidine used in batch binding analysis	206
4-14. Binding isotherms for cinchonidine on a blank and 4:1 imprinted polymer	207
4-15. Scatchard plots for cinchonidine on a blank and 4:1 imprinted polymer	208
4-16. Calibration curve for cinchonine used in batch binding analysis	211
4-17. Binding isotherms for cinchonine on a blank and a 4:1 imprinted polymer	212
4-18. Scatchard plots for cinchonine on a blank and a 4:1 imprinted polymer	214

List of Tables

1-1.	List of MIP based assay systems	13
1-2.	IC ₅₀ values for a (S)-propranolol imprinted polymer	14
1-3.	Apparent binding constants for Ricin based imprinted polymers	17
1-4.	List of MIP based sensor applications	23
1-5.	Response of epinephrine sensor to different interferents	26
1-6.	Recovery tests for an epinephrine selective sensor	28
1-7.	Comparison between an epinephrine selective sensor and other analytical methods	29
1-8.	Recovery tests for a nicotine selective sensor	33
1-9.	Comparison of a nicotine selective sensor and other analytical methods	34
1-10.	List of MIP based enzyme mimic/catalysis applications	36
1-11.	List of MIP based solid phase extraction applications	46
1-12.	Recovery of nerve agent degradation products	53
1-13.	R _f values for a TLC plate prepared with a (-)-pseudoephedrine imprinted polymer	65
1-14.	R _f values for a TLC plate prepared with a (-)-norephedrine imprinted polymer	66
2-1.	Selectivity of several phenyl alanine derivatives	71
2-2.	Morphology characteristics for a L-Phenylalanine anilide polymer prepared in different solvents	77
2-3.	Selectivity of several L-phenylalanine anilide polymers prepared in different solvents	78
2-4.	Selectivity of several L-phenylalanine anilide polymers prepared at different temperatures	79
2-5.	Retention factors of several small molecules on an imprinted polymer selective for phenol	102

2-6.	Retention factors on a alloxan imprinted polymer	104
2-7.	Retention factors for several triazine herbicides on three different triazine herbicide imprinted polymers	108
2-8.	Apparent disassociation constants for different nicotine imprinted polymers	111
3-1.	Selectivity of several Indinavir imprinted polymers	127
3-2.	Reported retention factors for <i>cinchona</i> alkaloids	130
3-3.	Methacrylic acid/cinchonidine ratios used in ATR-FTIR studies	139
3-4.	Chromatographic selectivity for a series of cinchonidine imprinted polymers	155
3-5.	ITC results for the Indinavir polymer system	167
4-1.	Retention factors obtained on a 4:1 methacrylic acid/cinchonidine imprinted polymer	187
4-2.	Mobile phase competitor studies	194
4-3.	Recovery studies using THF and water	196
4-4.	Recovery studies using acetonitrile and water	201
4-5.	Batch binding results under optimum condition	203
4-6.	Results from cinchonidine scatchard plot analysis	210
4-7.	Results from cinchonine scatchard plot analysis	215

Chapter 1. Historical Perspective and Common Applications

Introduction

Molecular imprinting is the process by which a block copolymer that possesses specific sites of recognition for a particular analyte is created. This is accomplished by placing the desired analyte molecule, known as the template, into a suitable solvent, or poragen, and adding to that a ligand, or functional monomer, that will interact, through the formation of a chemical bond or through intermolecular interactions, with the template to form a multimolecular complex. A sufficient amount of crosslinker is added, along with an initiator, and the solution then reacts to yield the solid polymer. Extraction of the template from the polymer matrix leaves behind binding sites that are complementary in stereochemistry and functionality to the template.

The origins for this technique can be traced back to the early theories on the functions of enzymes and antibodies.¹ In the 1890's Fischer, proposed that the specificity exhibited by enzymes towards a specific substrate was analogous to that of a "lock and key". As illustrated in Fig 1-1, the enzyme, or "key" is only able to interact with one substrate, or "lock", that in turn allows for a chemical reaction to occur.¹

Molecular imprinting was first investigated in the 1950's by Dickey, whose work focused on precipitating silica gels in the presence of organic dyes, as demonstrated in Figure 1-2.² Upon removal of the dye compound, he observed that the silica gels preferentially rebound the organic dye in which it was prepared. Shortly thereafter, Curti et. al., published their work on D, L-camphorsulfonic acid, in which they demonstrated that the silica gels, when used as a crude purification column, could separate the two enantiomers.³ Unfortunately, the selectivity

Figure 1-1. Schematic depicting Emil Fischer's "Lock and Key" principle. Adapted from Reference #1

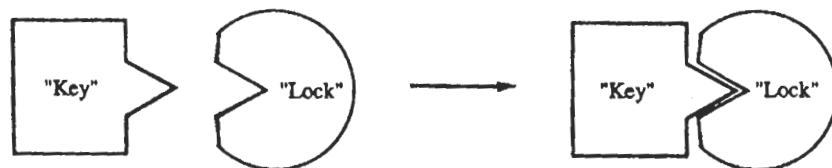
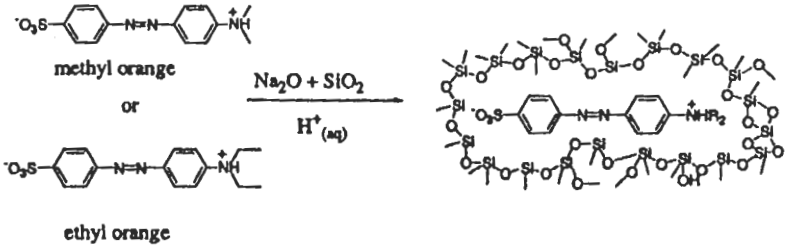


Figure 1-2. Dickey's method of imprinting silica gels selective for organic dyes. Adapted from Reference #2



achieved by these types of gels was not sufficient for the majority of applications at the time, and as such, the technique slowly dwindled out.

In the early 1970's, Wulff et. al., published work showing that efficient molecular recognition could be achieved by the introduction of functional groups into the imprinted cavity through the use of covalent bonds.⁴ This eventually would become known as the covalent method of preparing imprinted polymers. Shortly, thereafter Mosbach et. al. showed that it was possible to introduce functional groups into the binding cavity through the use of non-covalent interactions.⁵ This method, called non-covalent imprinting, forms the basis by which most imprinted polymers are prepared.

Types of imprinting

In order to effectively generate a successful imprint of a template molecule, the creation of a monomer-template complex must occur. This can be successfully accomplished by optimizing the conditions under which the monomer will most strongly interact with the template. Currently, there are two main techniques that are utilized to prepare imprinted polymers, covalent imprinting and non-covalent imprinting.

Covalent Molecular Imprinting

In covalent imprinting, reversible covalent bonds between the template molecule and the functional monomer are utilized to create a stable monomer-template complex. Following polymerization, the covalent bond is cleaved, allowing the template to be extracted from the polymer matrix. Upon reintroduction of the template into the polymer matrix, the covalent bond will reform within the binding site and then, given the kinetics associated with bond formation

and breaking, will break apart and the template will be released from the cavity.⁶ This approach has been used for several kinds of molecules, such as sugars,⁷⁻⁹ ketones,^{10,11} aldehydes,¹² and glyceric acid.^{13,14} The main advantage to this approach is that the resulting polymer will possess a more homogeneous distribution of binding sites. However, this technique is limited to templates and monomers that form covalent bonds whose formation kinetics are sufficiently fast in order to allow for use in many common separation techniques.¹⁵

The most common templates used in covalent imprinting are sugar molecules.⁶ A common example is the imprinting of phenyl- α -D-mannopyranoside. Generally, 4-vinylphenylboronic acid is used as the functional monomer, which will easily react with the D-mannopyranoside sugar hydroxyl groups to form ester linkages, as shown in Figure 1-3.⁶ Once the template is formed, a crosslinker, such as ethylene glycol dimethacrylate is added to the mixture along with an initiator and the mixture is polymerized through thermal initiation. Subsequent cleaving of the ester linkages allows for the removal of the sugar molecule and generates the selective binding site. This process is depicted in Figure 1-4.

Non-Covalent Imprinting

In non-covalent imprinting, intermolecular interactions, such as hydrogen bonding, that will cause the functional monomer to associate with the template molecule are utilized.¹⁶ Methacrylic acid (MAA) is the most common functional monomer used in this approach, although, as shown in Figure 1-5, several others have also been used.¹⁷ The extensive use of MAA as a functional monomer is due to its ability to interact with a variety of functional groups, such as acids, esters, amides, and amine substituents.⁶ Amino acids are often used as templates

Figure 1-3. Synthesis of a phenyl- α -D-mannopyranoside prior to covalent imprinting. Adapted from Reference # 6

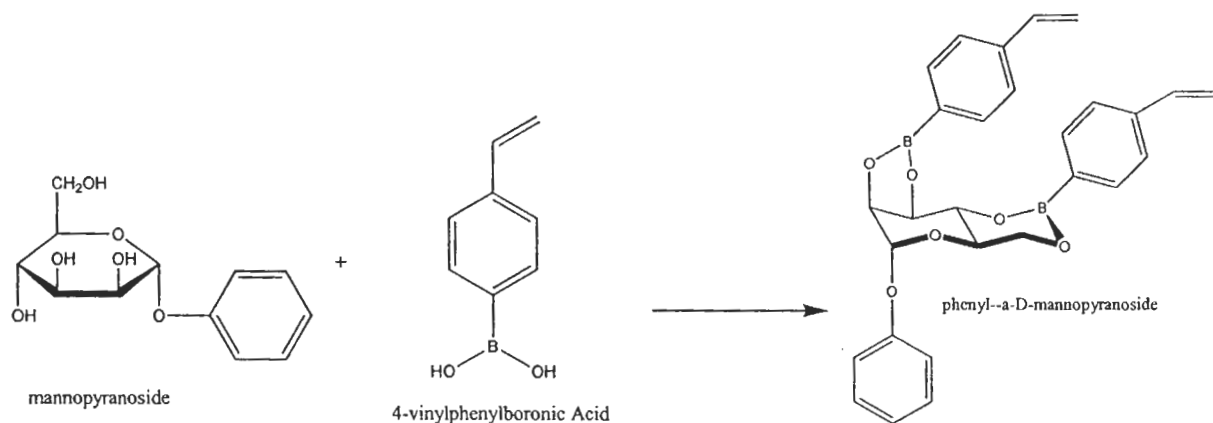


Figure 1-4. Covalent imprinting of phenyl- α -D-mannopyranoside. Adapted from Reference #6

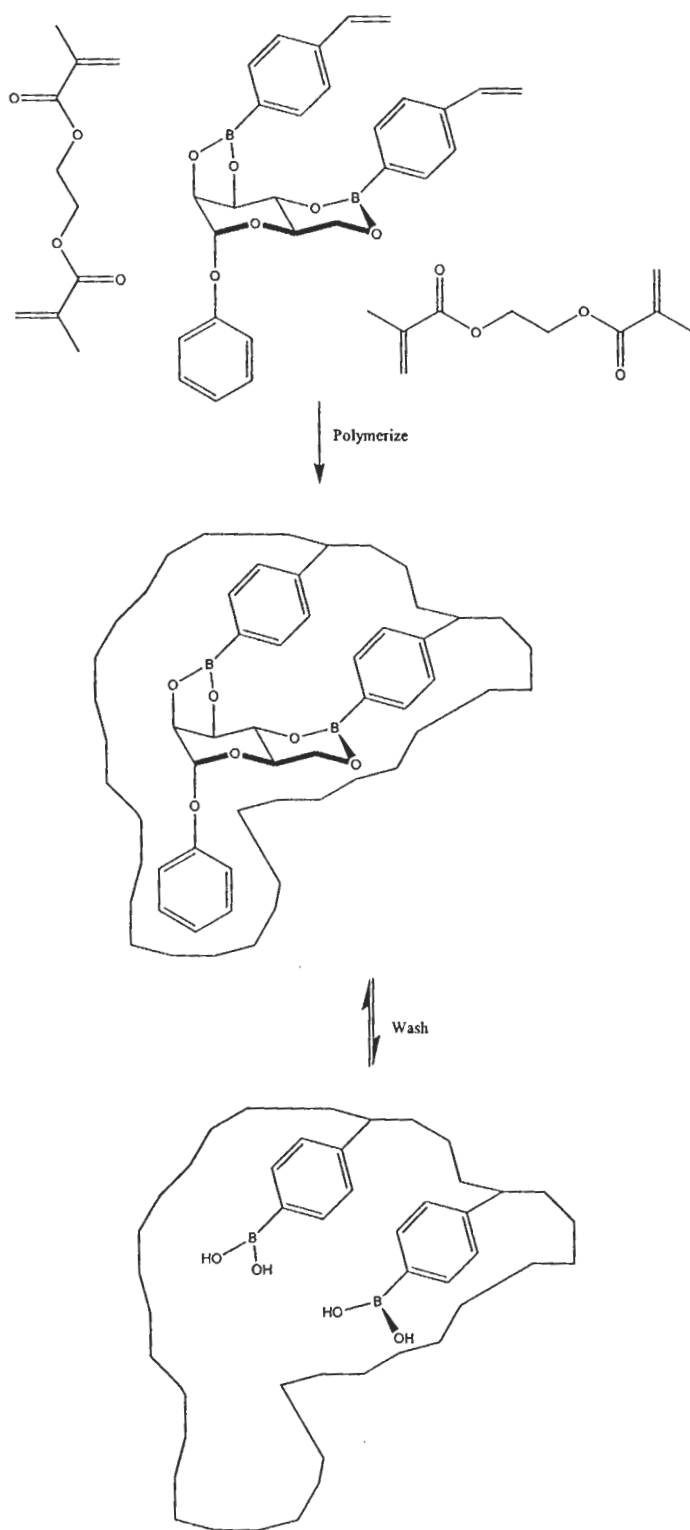
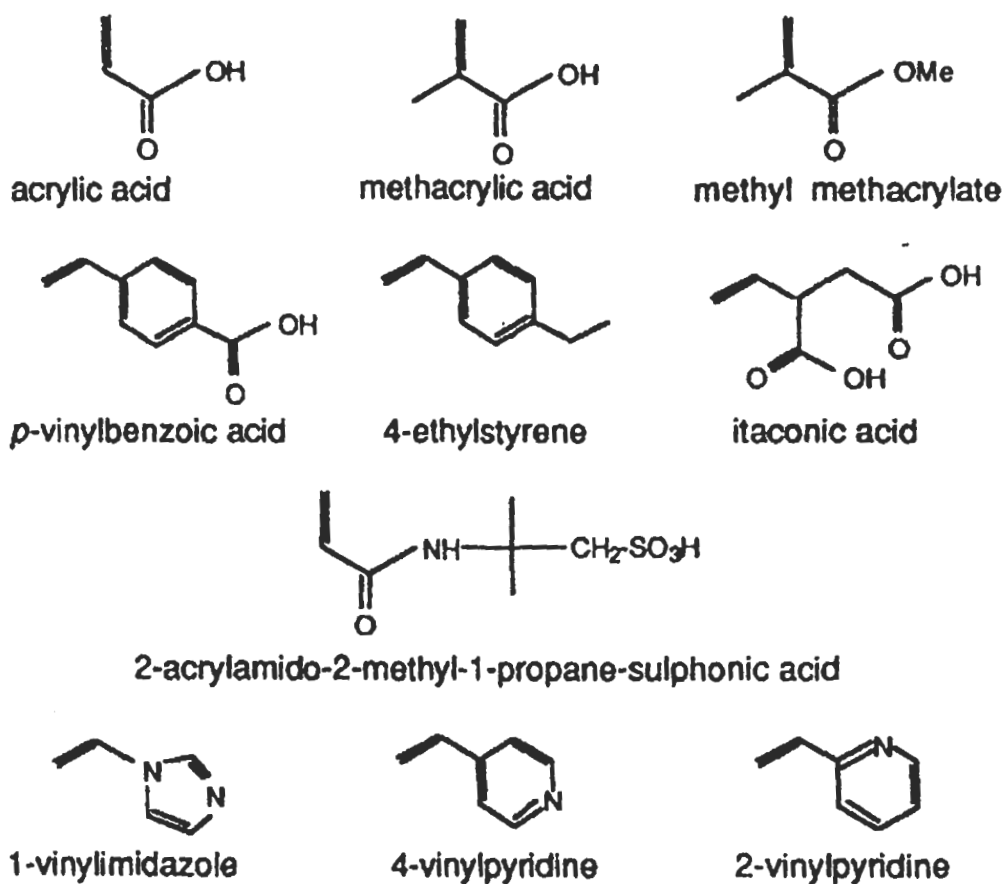


Figure 1-5. Structures of several different functional monomers that are used in non-covalent imprinting. Adapted from Reference #17



for non-covalent imprinting, since they often possess functional groups that interact strongly with MAA.^{16,18,19} Figure 1-6 depicts a typical non-covalent synthesis for cinchonidine.²⁰ The imprinting process begins with MAA interacting with the various template functional groups to form the multimolecular complex. Next, a suitable crosslinker, such as ethylene glycol dimethacrylate, is added along with an initiator and the resulting mixture is polymerized, locking the MAA into place in the correct stereochemical alignment. Finally, the polymer is washed, usually with a combination of acetic acid and acetonitrile or methanol, removing the template and generating a binding cavity. The advantage to this technique is that the intermolecular interactions used in the imprinting process have very fast formation kinetics, thus many different types of template can be imprinted. However, because the multi-molecular complex is based on weak interactions, the resulting polymer will contain a very large distribution of binding sites, resulting in an energetically heterogeneous surface.¹³

Applications of Molecular Imprinted Polymers

There are three particular features that have made MIP's very attractive materials:²¹

1. High affinity and selectivity similar to that of natural receptors
2. Superior stability in a variety of solvents and conditions, compared to natural biomolecules
3. Ease of preparation and adaptability to various applications, compared to natural biomolecules

As a result, the number of research groups, publications, and patents dealing with this material has increased significantly in the last few years, as shown in Figure 1-7.²¹ Currently MIP based materials have been applied to many different areas of chemistry. Within the analytical

Figure 1-6. Non-Covalent synthesis of MIP for Cinchonidine. Adapted from Reference #20.

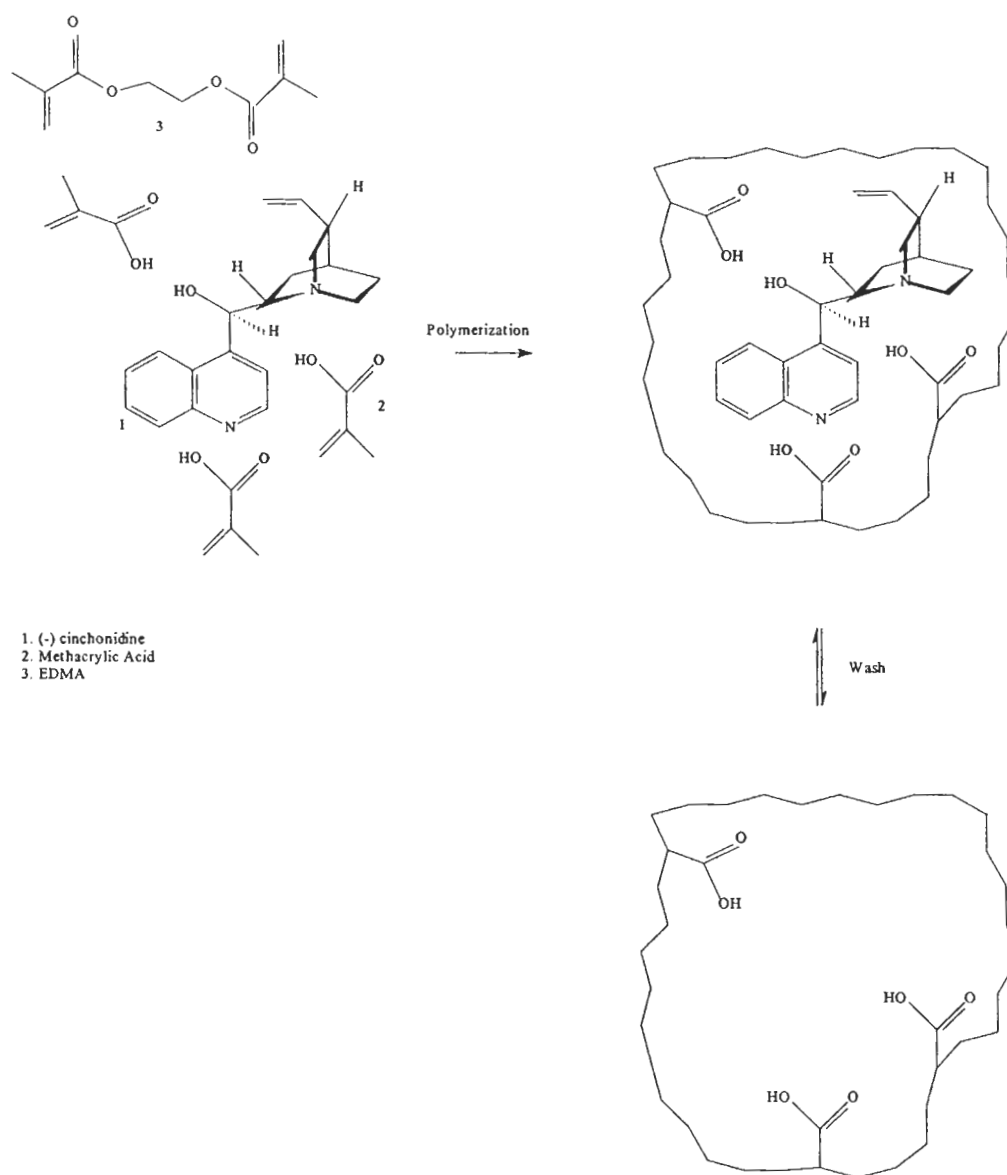
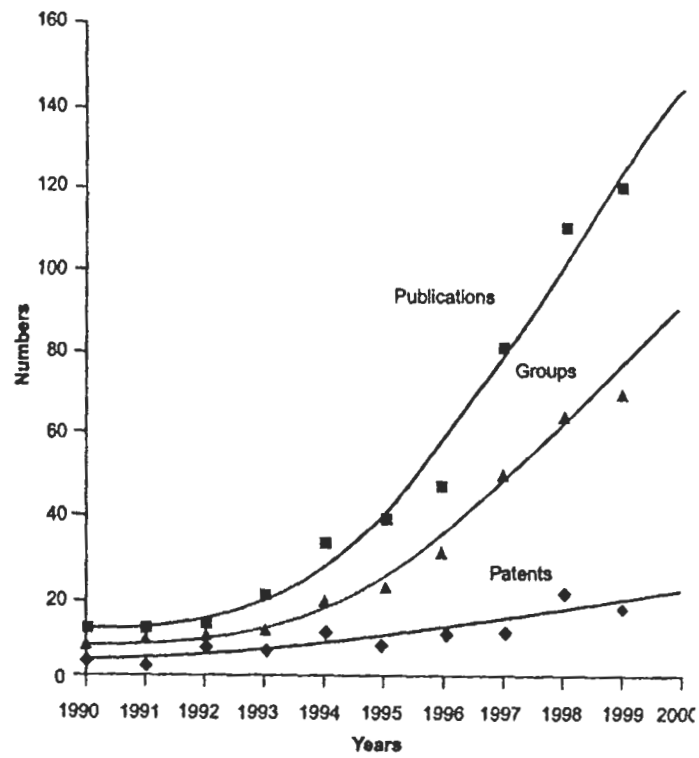


Figure 1-7. Published literature, patent applications, and research groups concerning MIP technology from 1990 through 2000. Adapted from Reference #21

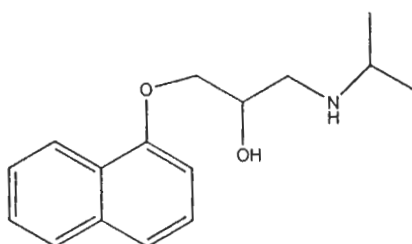


chemistry community, they have been used for immunoassay methods, sorbents for solid phase extraction, and stationary phases for a variety of separation techniques.

Antibody/Immunoassay

Antibodies are often used as analytical reagents in both clinical and research laboratories, primarily for immunoassays.²² The most common of these is the Enzyme-Linked Immuno-Assay (ELISA), and is used in a variety of analytical areas, such as environmental, clinical, forensic, and agricultural.²³ While it has been shown that ELISA methods are rapid, sensitive, and selective, the problems associated with reagent stability and antibody production suggest the need for new materials.²³ MIP's are an excellent choice for this type of application, as the common denominator between ELISA and MIP's is that both materials that will selectively rebind an analyte, through a site specific recognition for the analyte.²² In recent years, the use of imprinted polymers as antibody mimics for various assays is increasing as shown in Table 1-1.

For example, Andersson demonstrated the use of MIP's in radioligand assay analysis by using an MIP selective for S-propranolol, (*I*) a β -adrenergic antagonist (beta blocker) used in the



(*I*)

treatment of hypertension and angina pectoris.²⁴ As shown in Table 1-2, (S)-propranolol demonstrated the lowest IC_{50} values, amount of added analyte needed to displace 50% of an already bound ligand, for all polymers. Based on this, the MIP system of MAA and EDGMA was utilized for further study because of lower cross reactivity with other structural

Table 1-1. List of MIP based assay systems

<u>Analyte</u>	<u>Detection Method</u>	<u>Reference #</u>
Epinephrine	Enzyme Linked	23
Atrazine	Fluorescence	23
Proteins	Enzyme Linked	23
(S)-Propranolol	Radio assay	24
Ricin	Fluorescence	25
Chloramphenicol	Fluorescence	26
2,2-dichlorophenoxyacetic acid	Electrochemical	27
2,2-dichlorophenoxyacetic acid	Chemiluminescence	27
2,2-dichlorophenoxyacetic acid	Fluorescence	27, 29
Theophylline	Radio Assay	28
17 β -estradiol	Radio Assay	28
Biotin Methyl Ester	UV/VIS	30
N-bezylidene pyridine	Fluorescence	31
2-carboxamidrazones	Fluorescence	31

Table 1-2. IC₅₀ values obtained from binding studies on (S)-Propranolol polymers using several beta blockers. Adapted from Reference #24

Copolymer	Solvent	Ligand				
		(S)- Propranolol (μM)	(R)- Propranolol (μM)	(R,S)- Metoprolol (μM)	(R,S)- Timolol (μM)	(S)- Atenolol (μM)
MAA/EGDMA	Water	0.52	3.0	76	170	770
MAA/EGDMA	Toluene	0.29	20	4.6	38	1.6
MAA/EGDMA*	Water	0.43	1.22	64	250	1010
MAA/TRIM	Water	2.6	4.7	77	121	1720 ^a
MAA/TRIM	Toluene	0.16	3.3	1.5	8.1	0.51
MAA/TRIM	Water	0.91	2.1	86	106	960

*Prepared with Racemic Propranolol

^a Extrapolated value

components, as shown by the higher IC_{50} values for both aqueous and organic solvents. After optimizing the binding solution conditions, including pH, ionic strength, and organic content, the authors were able to achieve good discrimination, illustrated in Figure 1-8, between (R) and (S)-propranolol as well as between other structural analogs. Several important conclusions can be made from this work.²⁴ First, the concentration range at which maximum discrimination occurred was between 10-100 nM of (S)-propranolol, which the author noted, allows for this technique to be used in pharmacokinetic studies for (S)-propranolol, which has clinical concentrations typically between 5-200 nM. Second, most of the studies were performed using 50 μ g of polymer or less, thus a typical batch for prepared for (S)-propranolol would allow for around 100,000 individual assays, excluding any process by which the polymer is recovered, washed and used again.²⁴

Another interesting application of MIP's in immunoassays is for a fluorescent-based assay for Ricin, a very potent toxin that comes from the castor bean.²⁵ Ricin is composed of two polypeptide chains (A & B) that are linked by a disulfide bond and it has been utilized as a biological warfare agent. Therefore the need for a selective and sensitive biological assay is of great interest.²⁵ Four sets of imprinted polymers were prepared, utilizing Ricin, Ricin chain A, Ricin chain B, and bovine serum albumin (BSA) as the template molecules, and were constructed on the surface of silica particles. The particles were then exposed to solutions containing the analytes of interest, processed and analyzed by fluorescence spectroscopy.²⁵

The results in Table 1-3 show the calculated binding constants for each analyte on the various polymers. From the data, it is illustrated that the Ricin B chain can significantly interact with each imprinted polymer regardless of the Ricin template is used. This is important, given that Ricin is unlikely to be in its original molecular structure in the human body, rather it is

Figure 1-8. Binding study data for a (S)-propranolol imprinted polymer. Adapted from Reference #24

(S)-propranolol (\square) (R)-propranolol (\blacksquare) (R,S)-metoprolol (\bullet) (R,S)-timolol (\triangle) (R,S)-atenolol (\circ)

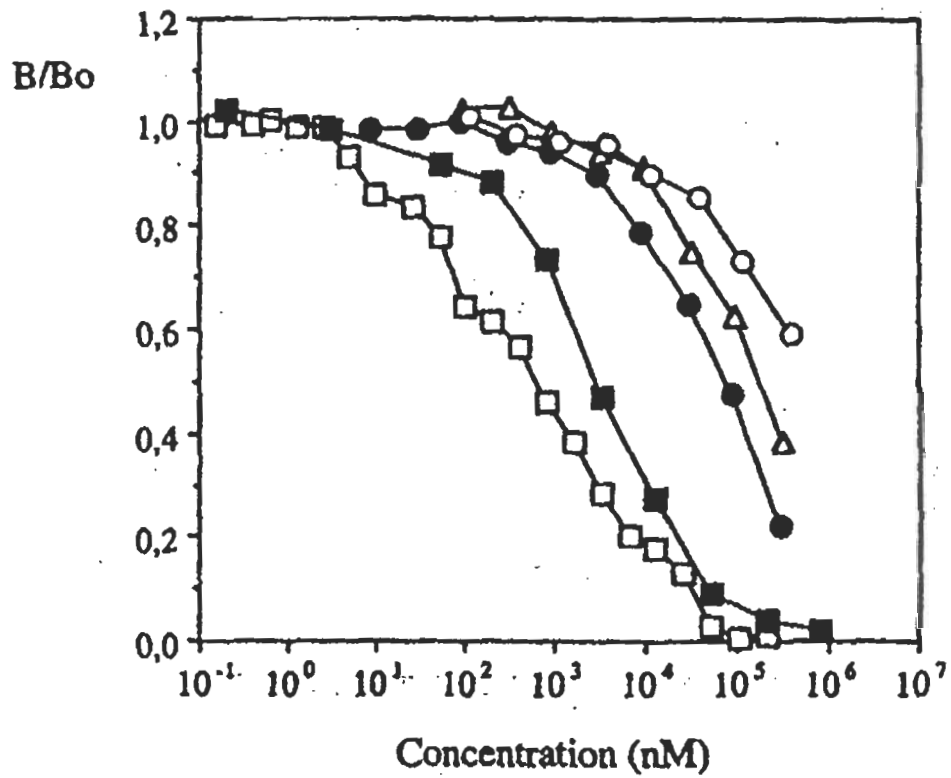


Table 1-3. Comparison of binding constants (K_d) for Ricin based imprinted polymers.
Adapted from Reference #25

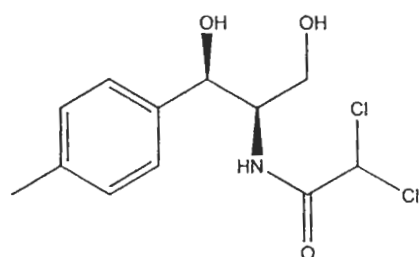
K_d ($\times 10^9$ M)				
Ligands	Templates used in Imprinting			
	Ricin	Ricin A	Ricin B	BSA
Ricin	33.8 ± 2.5 , 319.2 ± 14.3	NB	NB	NB
Ricin A	NB	107.3 ± 11.2	NB	NB
Ricin B	33.8 ± 2.5 , 319.2 ± 14.3	8.89 ± 0.85	105.5 ± 12.3	NB
BSA	NB	NB	NB	ND

NB = No binding (Specific binding – blank)

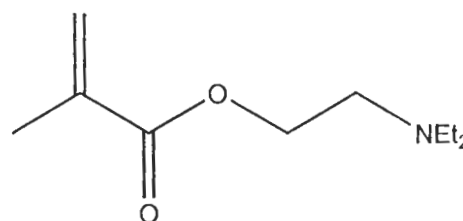
ND = Not determined

reasonable to suggest that the metabolic processing of Ricin will break it down to its two chains and other derivatives. Thus utilizing Ricin B as the template for an imprinted polymer should allow for the development of a very sensitive assay capable of identifying and quantitating Ricin.²⁵ Finally, it is interesting to note that two binding constants were calculated for both Ricin and Ricin B on the Ricin imprint, while only a single binding constant was calculated for the others, an explanation for this phenomenon will be discussed later

Finally, a sensitive fluorescent assay system was developed for chloramphenicol, an antibiotic used to treat a variety of diseases, such as typhoid fever and meningitis.²⁶ The extreme toxicity of chloramphenicol towards humans has relegated its use to only eye drops and veterinary medicines. Thus very sensitive methods for analysis are required to ensure strict control. Chloramphenicol (CAP) (2) was imprinted using a mixture of diethylaminoethyl methacrylate (3) and 2-vinyl-pyridine as functional monomers with EGDMA as a crosslinker.



(2)



(3)

The resulting polymer was processed and packed into a fluorescence flow-through cell as illustrated in Figure 1-9, such that it was contained prior to the optical path, and then placed into the detector completing the flow through system. Prior to analysis, a labeled version of CAP had to be prepared such that it would bind to the CAP polymer but with a binding strength significantly less than that of CAP. This was performed by attaching a dansyl group to 2-amino-1-(4-nitrophenyl)-1,3-propanediol to form CAP-dans as shown in Figure 1-10.

Figure 1-9. Schematic of flow-through fluorescent sensor for Chloramphenicol. Adapted from Reference #26.

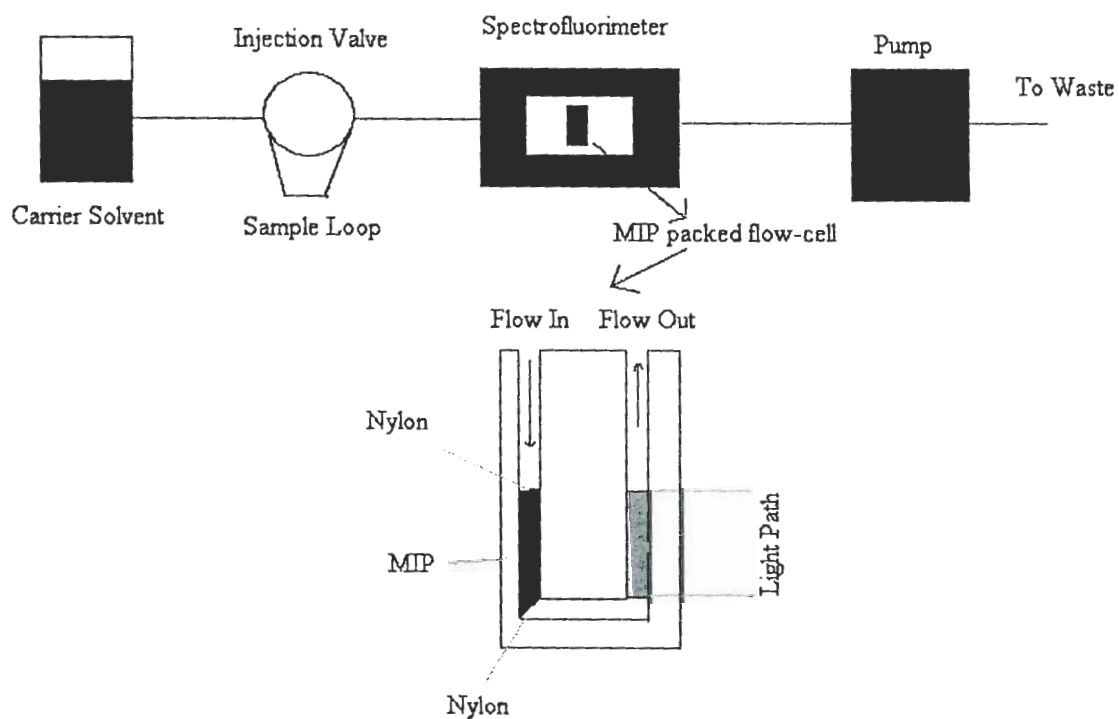


Figure 1-10. Synthesis of CAP-Dans molecule. Adapted from Reference #26

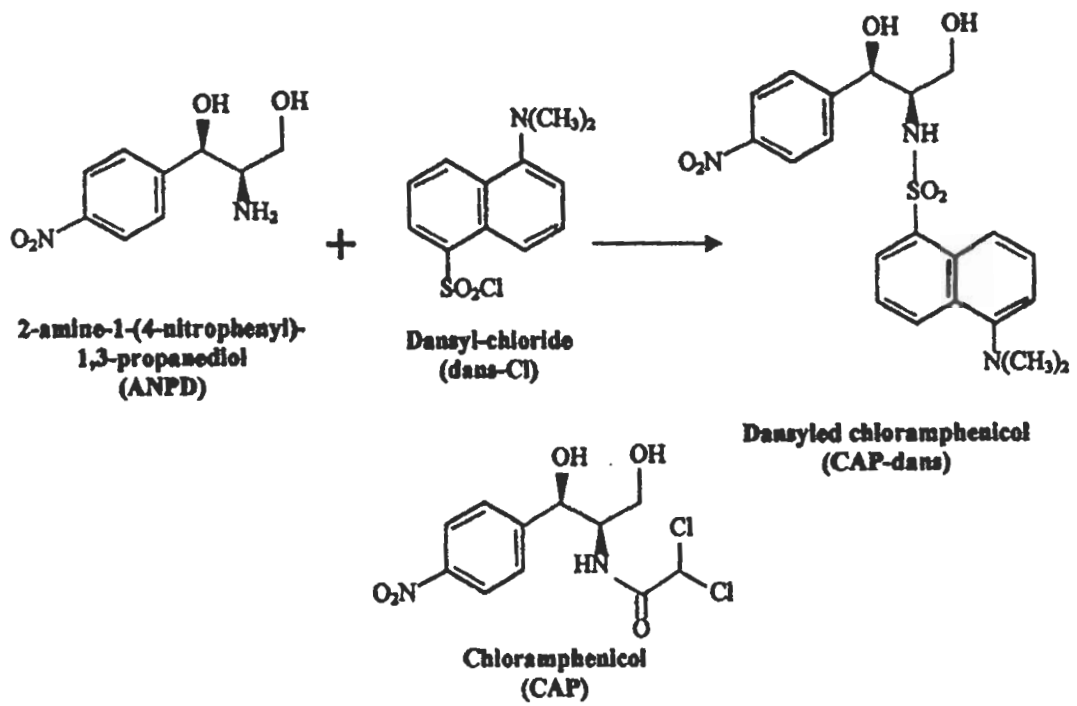


Figure 1-11 illustrates the process by which the assay was performed. First, the acetonitrile mobile phase, containing a dilute concentration, 4 $\mu\text{g/mL}$, of CAP-dans was pumped through the system, saturating the CAP polymer within the flow cell, creating a steady state concentration of CAP-dans. Next, an acetonitrile solution containing CAP was loaded in the sample loop and injected. As CAP reached the polymer, it displaced the CAP-dans from the polymer as its binding constant is higher, causing an increase in the concentration of CAP-dans downstream from the polymer just prior to the optical path. This increased CAP-dans concentration resulted in an increase in signal, producing the peak shown, which is directly proportional to the concentration of CAP injected. Since the mobile phase was still moving, CAP-dans will begin to displace the CAP from the polymer causing a decrease in CAP-dans concentration and will result in the negative peak of the chromatogram. Eventually, the CAP-dans returned to a steady state concentration and another injection could be performed. After optimizing certain parameters, such as flow rates, sample loop size, and Cap-dans concentration, the authors were able to achieve a detection limit of 8 $\mu\text{g/mL}$ with a working concentration range up to 100 $\mu\text{g/mL}$ with reproducibility better than 3%.

MIP Based Sensors

Sensor technology incorporating MIP materials is growing, as shown in Table 1-4. The advantages of using an MIP based sensor over conventional analytical techniques are many. First, high selectivity for a particular analyte eliminates the need to extract and separate sample components prior to quantitation, allowing for increased sample throughput and efficiency.³⁵ Second, the materials used to build the sensors are very inexpensive, compared to other instrumental techniques, such as gas chromatography.³⁵ Lastly, the procedures used for

Figure 1-11. Chromatogram obtained from the flow-injection CAP sensor. Adapted from Reference #26

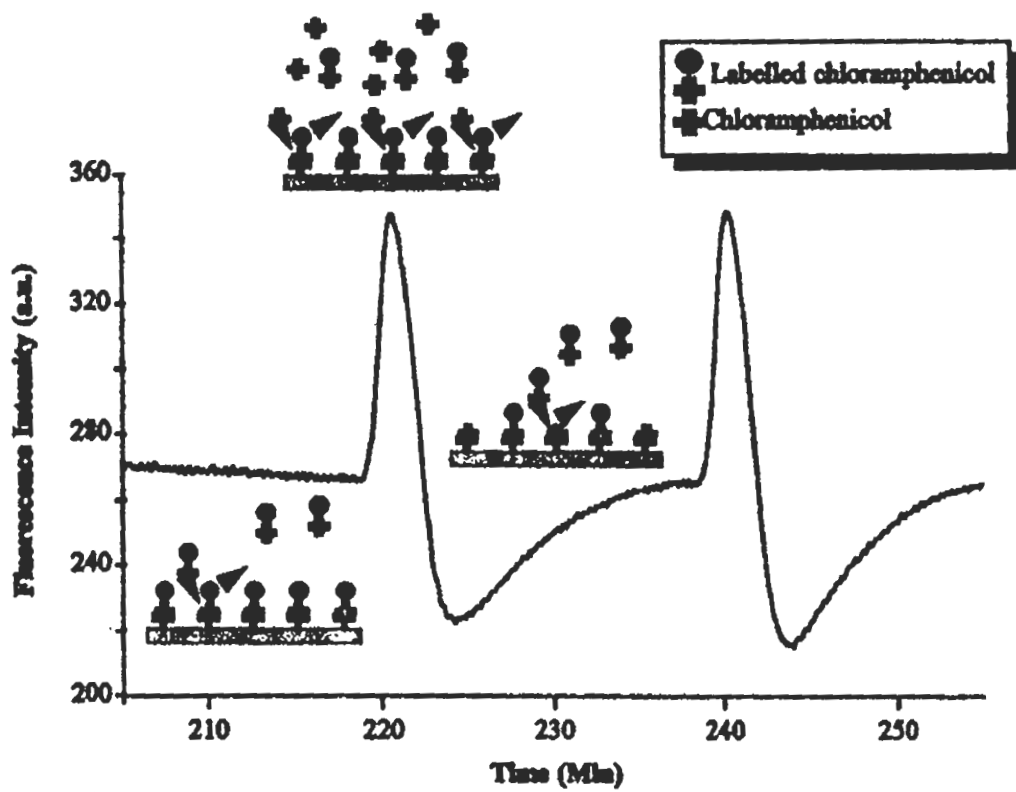
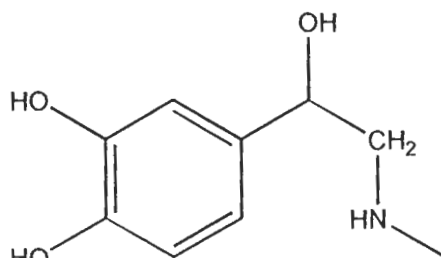


Table 1-4. List of selective sensors utilizing MIP materials.

<u>Analyte</u>	<u>Reference #</u>
Review articles	32,33,34
Nicotine	35
Epinephrine	36
Atrazine	37,49
Morphine	38
Dansyl-L-Phenylalanine	39
Benyl triphenylphosphonium	40
Chloramphenicol	41
Adenosine 3',5'-cyclic monophosphate	42
Flavonol	43
Polycyclic Aromatic Hydrocarbon	44,46
2-methylisoborneol	45
Clenbuterol	47
Glucose	48
Desmetryn	50
Carbohydrates	51
2,4-dichlorophenoxyacetic acid	52
Homocysteine	53
Histamine	54

synthesizing and coating the polymer are fairly straightforward, allowing for good batch to batch reproducibility.³⁵

A bulk acoustic wave (BAW) sensor for the measurement of epinephrine (**4**) was developed by Liang et. al.³⁶ The polymer was prepared by using MAA as a functional monomer,

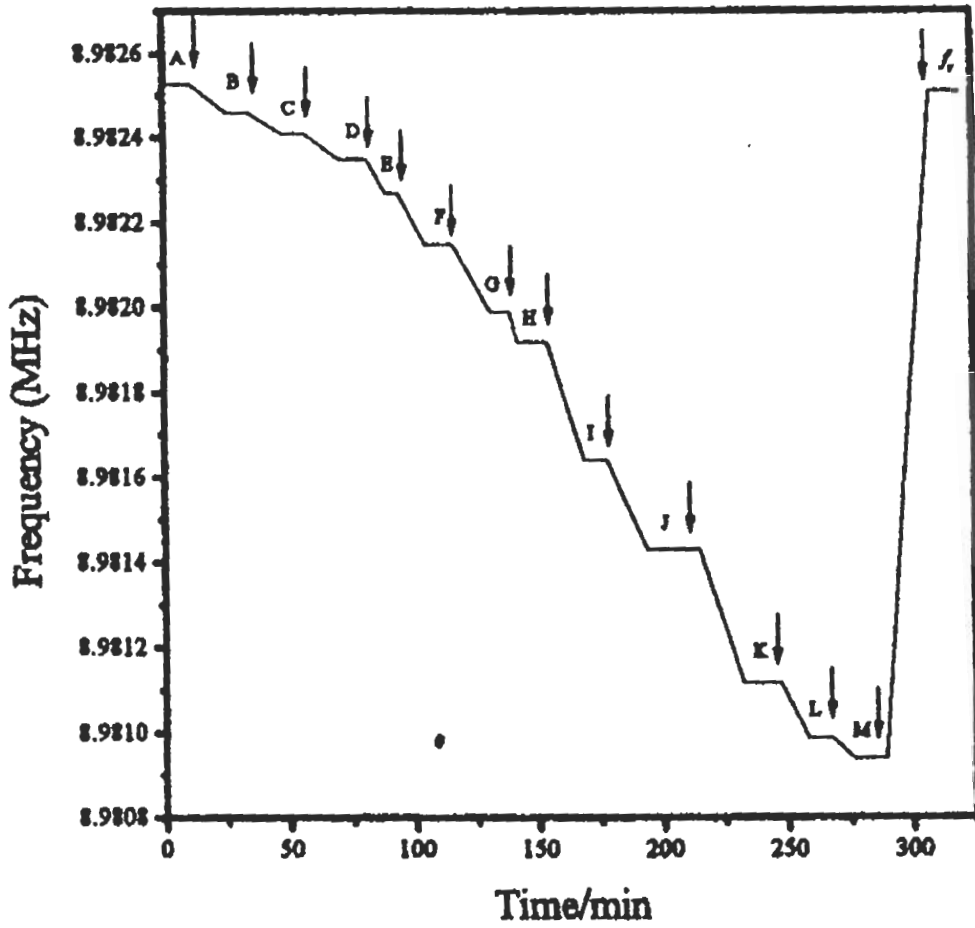


(4)

ethylene glycol dimethacrylate as a crosslinker and polymerizing at 50 °C in 3:2 acetonitrile:benzoic alcohol poragen. The resulting polymer was repeatedly ground, sieved, sedimented, and centrifuged until a suitable amount of particles with a size range of 0.8-1.2 μm were obtained, in 3:2 acetonitrile:benzoic alcohol poragen. The polymer particles were suspended in tetrahydrofuran and then coated onto the raw BAW sensor.³⁶

Figure 1-12 shows the response generated for standard solutions of epinephrine for both the imprinted polymer sensor and a non-imprinted sensor. Upon immersion in the epinephrine solution, a decrease in the frequency will occur, finally reaching a plateau signifying that the sensor is stable. The frequency at which the plateau occurs is reported as the reading for that particular epinephrine solution. It is clear that the sensor is selective for epinephrine as shown by the dramatic differences in response to epinephrine as well as the fairly linear decrease in frequency with increasing epinephrine concentration. In order to further assess selectivity, the sensor was used in standard solutions of other components representing a broad range of possible interferences. The results, shown in Table 1-5, reveal that the sensor demonstrates minimal

Figure 1-12. Response of a BAW sensor coated with a MIP selective for epinephrine. Adapted from Reference #36



Letter	Concentration (M)	Letter	Concentration (M)
A	2.0E-08	H	5.3E-06
B	5.0E-08	I	9.5E-06
C	9.0E-08	J	9.5E-06
D	1.6E-07	K	2.0E-05
E	4.8E-07	L	5.5E-05
F	8.9E-07	M	1.0E-04
G	1.1E-06		

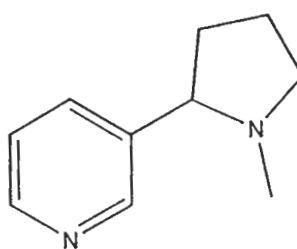
Table 1-5. Response of Epinephrine sensor to various interferents. Adapted from Reference # 36

Interferent	$k_{it} = \Delta f_i / \Delta f_t$	$K = k_{it}(M_t/M_i)$
Ammonium chloride	No interference	
Potassium chloride	No interference	
Magnesium sulfate	No interference	
Glucose	0.03	0.03
Urea	0.03	0.10
Methimazolium	0.04	0.08
Sulfadiazine	0.07	0.05
Procaine hydrochloride	0.05	0.03
Lactate	0.02	0.01
Caffeine	0.06	0.06
Ascorbic acid	0.04	0.04
Trimethoprim	0.13	0.08
Nicotinamide	0.05	0.08
Chlorophenamine maleate	0.07	0.03
Pymethamine	0.12	0.09
Analginum	0.09	0.05
Phenytoin sodium	0.03	0.02

f_i = response of sensor to 2×10^{-5} M interferent
 f_t = response of sensor to 2×10^{-5} M epinephrine
 M_i = molecular weight of interferent
 M_t = molecular weight of epinephrine

sensitivity to other components. After optimizing solvent conditions for analysis of epinephrine from serum and urine, recovery studies were performed by measuring the solutions of known concentrations of epinephrine and comparing the calculated value to the known value, as shown in Table 1-6. These results show that the sensor is accurate in determining the concentration of epinephrine given that the working environment is aqueous. Finally the authors compared their work to other established methods for epinephrine analysis, shown in Table 1-7, and found that the sensor demonstrated comparable sensitivity and recovery, illustrating the attractive nature of using MIP based sensors for analysis of biological fluids.

Using a similar synthesis procedure, a piezoelectric quartz crystal (PQC) thickness-shear mode (TSM) sensor was created using an MIP selective for nicotine (5). The polymer was



(5)

synthesized using MAA as the functional monomer, EGDMA as the crosslinker, and using chloroform as the poragen. The resulting polymer was repeatedly ground, sieved, and sedimented until suitable amount of particles, less than 1 μm in size, had been collected. The polymer particles were then suspended in tetrahydrofuran and coated onto the electrode surface to generate the final sensor.³⁵

Figure 1-13 shows the response of several different sensors, each possessing a different thickness, compared to that of the non-imprinted sensor. As illustrated, as coating thickness increases, the response increases as well, which is attributed to the fact that thicker coatings will possess more sites of recognition.³⁵ In all cases, there is a significant difference in response

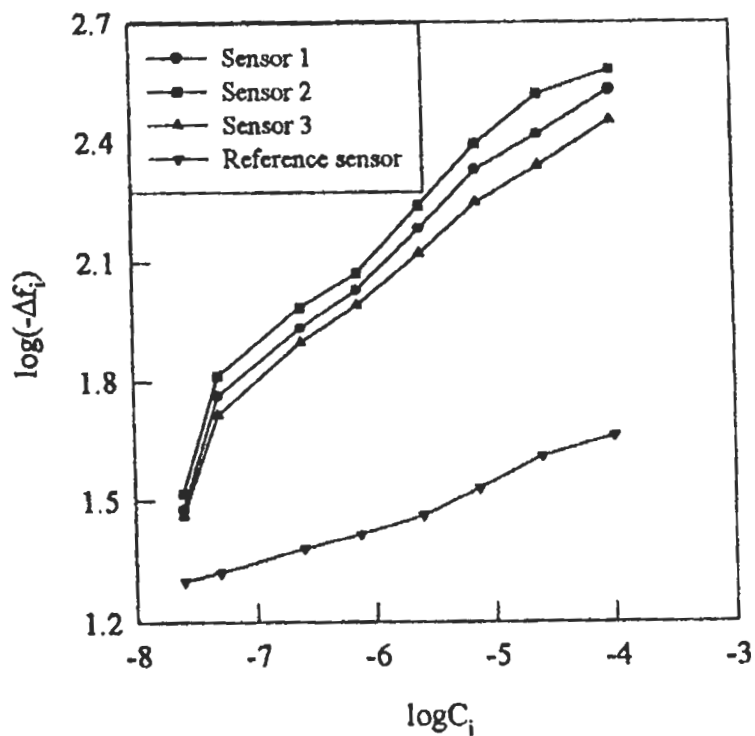
Table 1-6. Recovery test in serum and urine using an epinephrine selective sensor.
Adapted from Reference #36

Sample	Concentration (M)	Mean \pm RSD (M)	Recovery %
Serum	1.0×10^{-7}	$1.087 \times 10^{-7} \pm 3.17$	108.7
	5.5×10^{-7}	$5.56 \times 10^{-7} \pm 2.43$	101.1
	8.31×10^{-7}	$7.74 \times 10^{-7} \pm 2.14$	93.2
	1.19×10^{-6}	$1.17 \times 10^{-6} \pm 2.39$	98.0
Urine	1.69×10^{-7}	$1.65 \times 10^{-7} \pm 2.72$	97.6
	5.04×10^{-7}	$5.12 \times 10^{-7} \pm 2.51$	101.6
	7.19×10^{-7}	$7.44 \times 10^{-7} \pm 2.93$	103.5
	1.06×10^{-6}	$1.03 \times 10^{-6} \pm 1.99$	97.3

Table 1-7. Comparison of epinephrine sensor with other methods of analysis. Adapted from Reference # 36

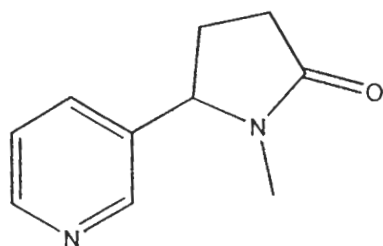
Method	Calibration Range	Detection Range	Recovery %	RSD (%)
HPLC	25.82-1032.56 pg/mL	12 pg/mL		13.09 (n=5)
CE	2-32 µg/mL	90 ng/mL	95	1.9 (n=6)
FIA	20-40 mg/L	0.02 mg/L		0.6 (n=28)
Fluorimetry	0.02-6 µM	9.3 nM	>94	≤ (n=5)
Trienzyme Sensor	30 nM-2.25 µM	30 nM		
MIP Sensor	$5.0 \times 10^{-8} - 2.0 \times 10^{-5} \text{ M}$	2.0×10^{-8}	93.2-108.7	3.17 (n=5)

Figure 1-13. Response curve of nicotine selective TSM sensors to various concentrations of nicotine. Adapted from Reference #35

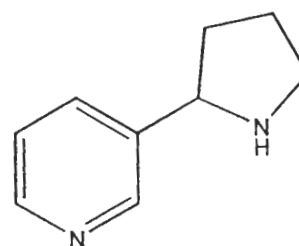


Sensor #	Thickness (-fΔ _{mod})
1	14574
2	99987
3	7237
Reference	10087

between the imprinted sensors and that of the non-imprinted. To further test selectivity, several studies were performed, by measuring the sensor's response in the presence of different structural analogs, specifically cotinine (6) and myosmine (7). As shown in Figure 1-14, the



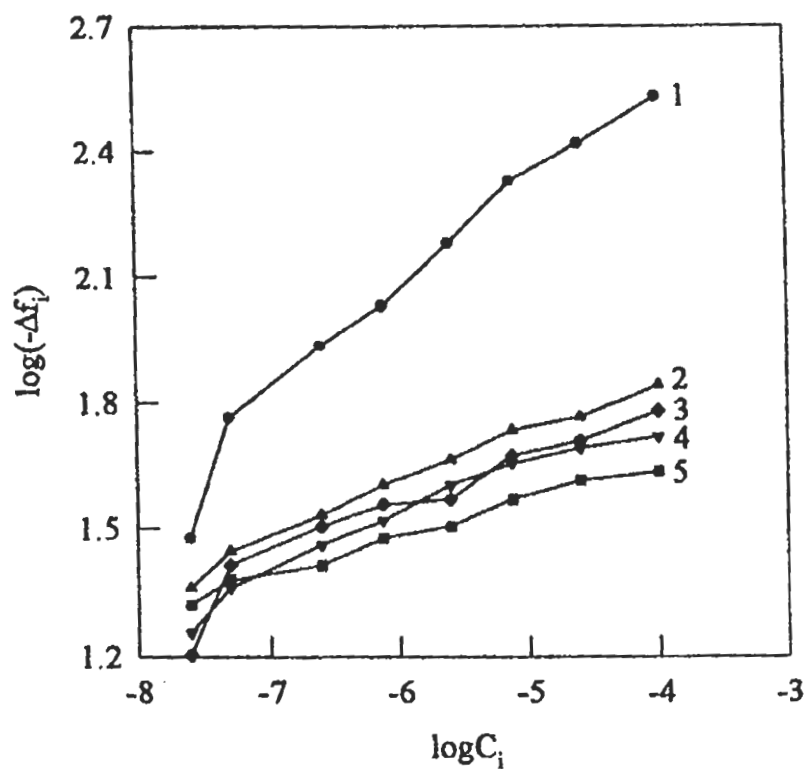
(6)



(7)

imprinted sensor displays increased selectivity for nicotine over both cotinine and myosmine such that the response is approximately equal to the response generated by cotinine and myosmine on the non-imprinted electrode. This suggests that the majority of the imprinted sensor's response is directly related to selective binding of nicotine to the polymer and not due to non-specific adsorption. Finally, the sensor was used to determine the concentration of nicotine in both urine and serum. The results, shown Table 1-8, indicate that the sensor demonstrates good recovery in both matrices as indicated by the average recoveries of 101.4% and 100.1% for serum and urine respectively.³⁵ Lastly, a comparison of this method to other reported methods of nicotine analysis seen in Table 1-9, reveals that this method is superior to most common analytical techniques. For example only gas chromatography-mass spectrometry demonstrated a slightly lower detection limit, however, the sensor had better reproducibility. Additionally, the recovery demonstrated by this method is comparable to other established techniques, proving that MIP based sensor material needs to be further investigated for biological sensors.

Figure 1-14. Response of nicotine sensor to nicotine, cotinine, and myosmine. Adapted from Reference #35



Line #	Polymer	Analyte
1	Imprinted	Nicotine
2	Imprinted	Cotinine
3	Imprinted	Myosmine
4	Reference	Myosmine
5	Reference	Cotinine

Table 1-8. Application of nicotine sensor to serum and urine samples. Adapted from Reference #35

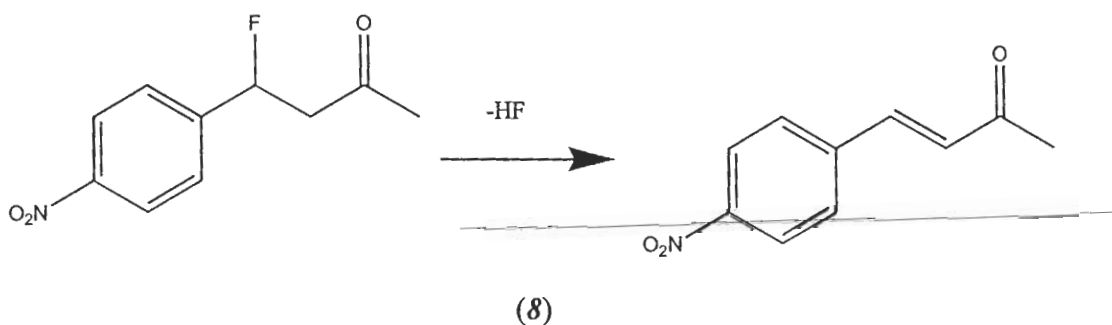
Serum			Urine		
Added (mg)	Found (mg)	Recovery (%)	Added (mg)	Found (mg)	Recovery (%)
1.6	1.7 ± 0.25	106.3	1.6	1.7 ± 0.10	106.3
3.2	3.3 ± 0.32	103.2	3.2	3.1 ± 0.20	96.9
4.8	4.7 ± 0.27	97.9	4.8	4.7 ± 0.26	97.9
6.4	6.2 ± 0.15	96.9	6.4	6.6 ± 0.34	103.1
8.0	8.2 ± 0.10	102.5	8.0	7.7 ± 0.36	96.3

Table 1-9. Comparison of Nicotine sensor to other methods of analysis. Adapted from Reference #35

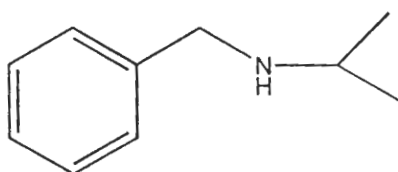
Method	Calibration Range (M)	Detection Limit (M)	Recovery %	RSD (%)
HPLC	6.8×10^{-6} - 3.4×10^{-5}	6.2×10^{-7}	99.1 – 100.6	0.8 – 2.3
GC	1.2×10^{-8} - 7.7×10^{-7}	3.1×10^{-9}	100 - 101	< 16.8
GC-MS	7.7×10^{-9} – 6.2×10^{-6}	9.8×10^{-10}		
SPE	Up to 1.2×10^{-6}	1.2×10^{-8}		< 4.0
CE	8.1×10^{-6} - 8.1×10^{-5}	3.8×10^{-7}		7.73 – 9.06
Spectrometry	Up to 7.4×10^{-5}			2.1 – 3.8
Flow Injection FTIR	0 – 5.8×10^{-2}	6.2×10^{-4}		
MIP Sensor	5.0×10^{-9} – 1.0×10^{-4}	2.5×10^{-9}	96.9 – 106.3	< 5.0

Enzyme Mimics/Catalysis

Catalyzed reactions are an important part of synthetic processes. Catalysts work by binding to a specific reaction substrate, such as a transition state intermediate, through specific sites of recognition. Subsequently, further reactions that occur with the substrate have lower activation energies, resulting in the start of a chemical reaction or an increase in the rate of product formation.⁵⁵ The use of MIP's in catalytic processes is desirable as MIPs are easy and inexpensive to make and demonstrate remarkable mechanical and thermal stability in a variety of working environments.⁵⁶ Table 1-10 provides a select list of the application of MIP's in catalytic processes. Recently, an MIP for a transition state analog (TSA) was imprinted for the dehydrofluorination of a 4-fluoro-4-(*p*-nitrophenyl)-2-butanone (**8**), which in this case was



N-benzylisopropylamine (**9**).⁵⁶ Preliminary batch binding experiments were performed in order

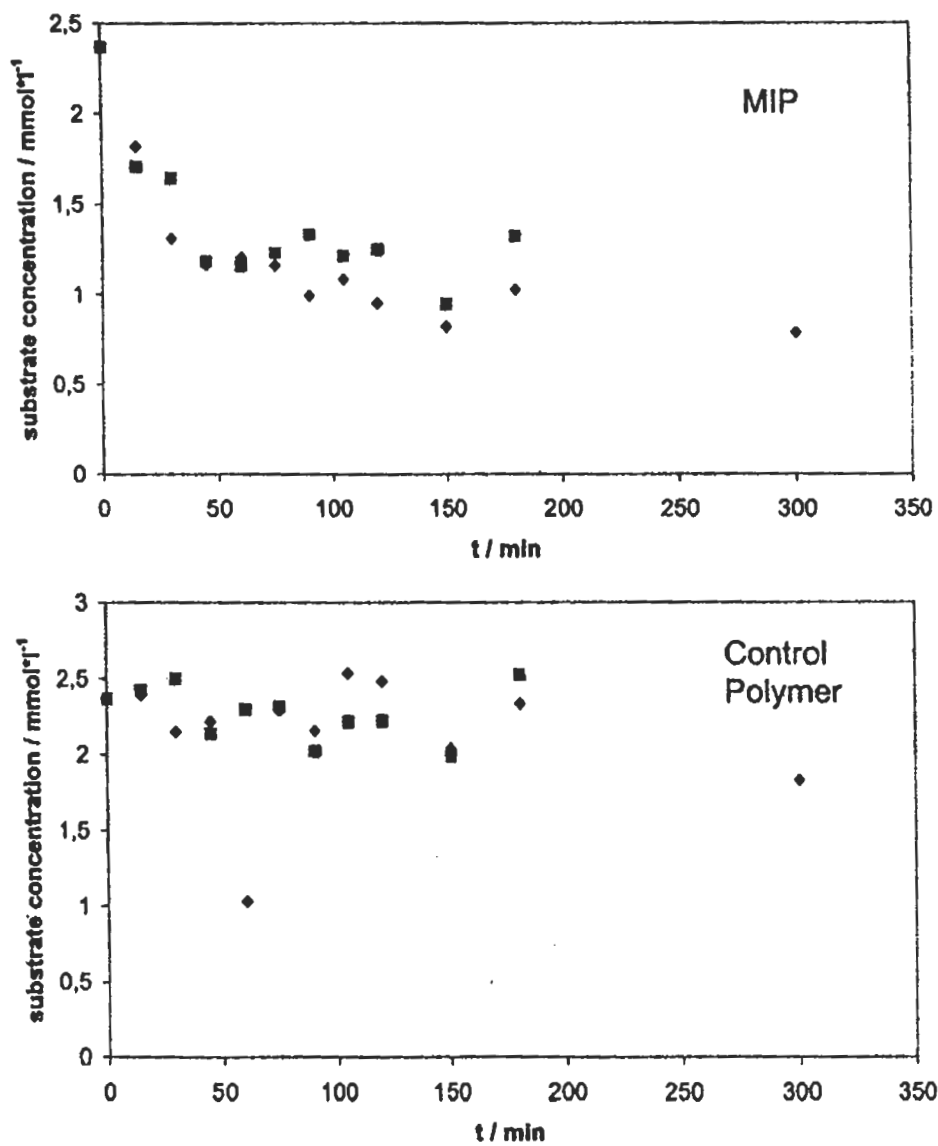


to assess whether or not the polymer could catalyze the reaction, and the results are summarized in Figure 1-15. As shown in the top portion of the figure, the substrate concentration is decreasing over time, contrasted to the results using the blank polymer, shown in the bottom

Table 1-10. List of MIP Enzyme Mimic/Catalysis applications.

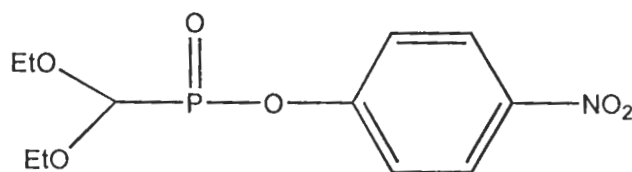
Enzyme Mimic/Catalyzed Reaction	Reference #
Dehydrofluorination	56, 59
Phosphotriesterase	57
Hydrolysis of amino acids	58, 60, 64
Carbonate ester hydrolysis	61
Synthesis of 1-(S)-phenylethanol	62
Release of p-nitrophenol	63

Figure 1-15. Comparison of batch binding results for the dehydrofluorination between an NBP and reference polymers. Adapted from Reference #56



portion of the figure, in which the substrate concentration remains fairly constant over the same range of time. These results show that dehydrofluorination is occurring and that it is occurring through the use of the MIP.⁵⁶ This was further proven, when the reaction was monitored by Ultraviolet-Visible spectroscopy (UV-VIS), shown in Figure 1-16. As the reaction proceeds, the absorption maximum shifts to higher wavelengths and greater intensity, compared to the spectra obtained prior to analysis. This is significant as it shows that the MIP is selectively catalyzing the reaction. To extend this further, the MIP was utilized in a continuously driven catalytic fixed-bed reactor, shown in Figure 1-17, which is commonly utilized in synthesis reactions.⁵⁶ Ultraviolet-Visible spectroscopy was used to analyze the effluent following passage through the reactor and the results are shown in Figure 1-18. The top portion is the spectra obtained on a reactor with the imprinted polymer. As with the preliminary batch binding studies, the UV-VIS spectra show a shift to higher wavelengths indicating that product formation is occurring. The bottom portion represents the spectra obtained on a reactor with a blank polymer. Here the spectra show no shift towards higher wavelengths, which suggests that no reaction is occurring.

In a second study, an imprinted polymer utilizing imidazole- Co^{2+} complex as a functional monomer was prepared. This done in an attempt to mimic the catalytic center of phosphotriesterase, an enzyme used to facilitate hydrolysis of organophosphotriester compounds, such as paraoxon (*10*).⁵⁷ Figure 1-19 shows the process by which the imprinted polymer



(10)

for paraoxon is created utilizing diethyl (4-nitrobenzyl) phosphonate (D4NP) (*11*) as the

Figure 1-16. Ultraviolet-Visible spectra for the catalyzed dehydrofluorination of FNPB.
Adapted from Reference #56

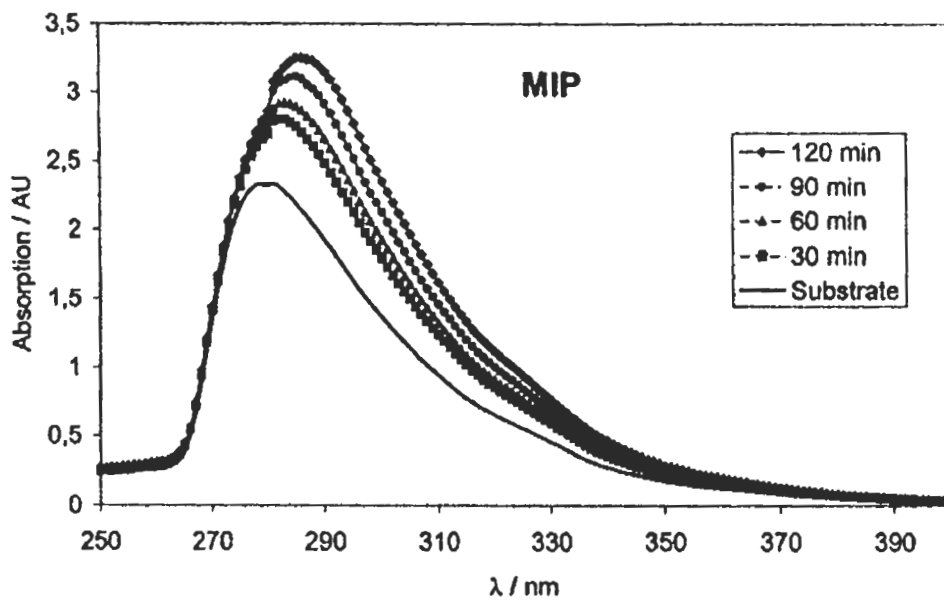


Figure 1-17. Schematic of a continuously driven catalytic fixed-bed reactor. Adapted from Reference #56

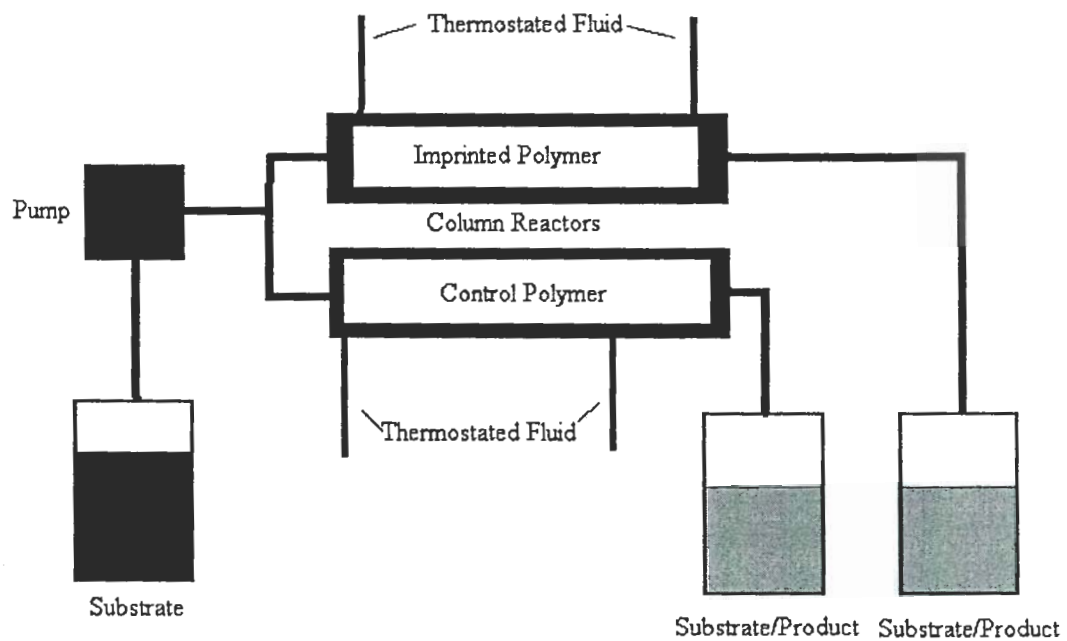


Figure 1-18. Ultraviolet-Visible spectra obtained from the catalytic reactor. Adapted from Reference #56

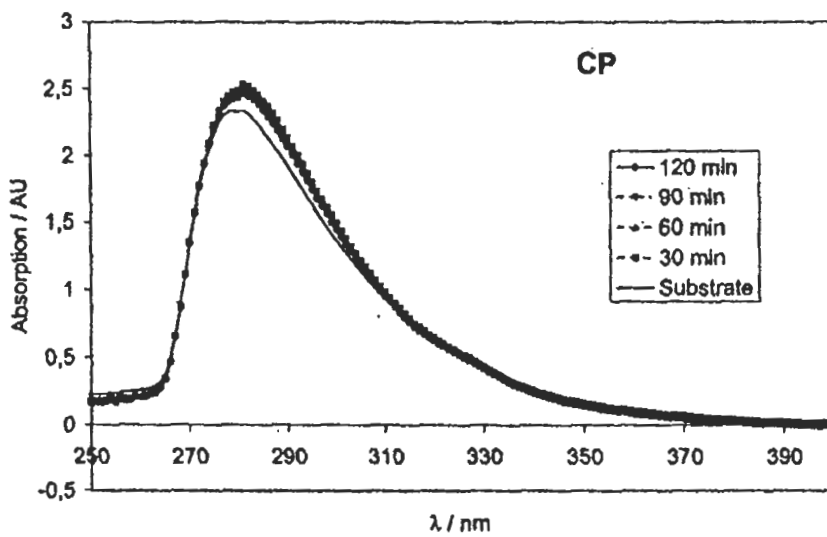
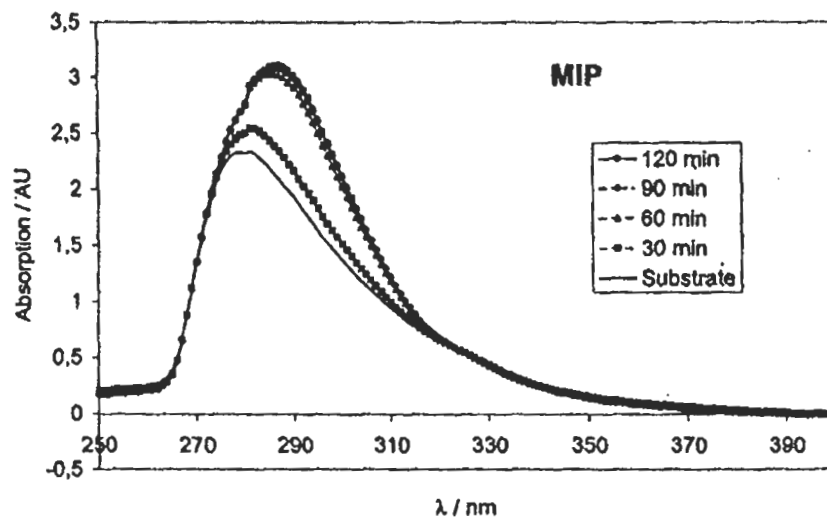
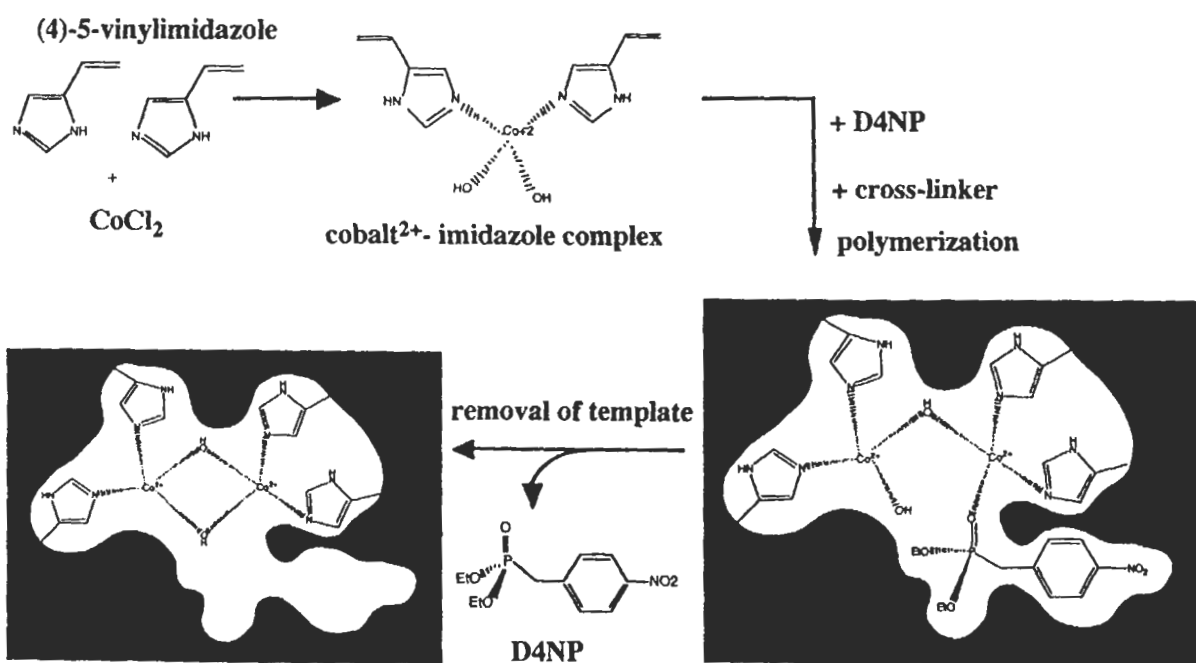
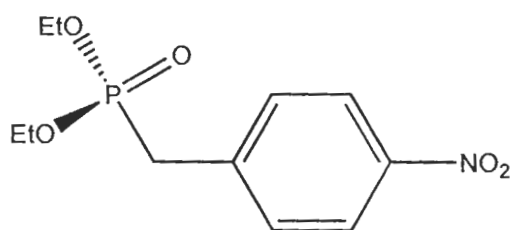


Figure 1-19. Synthesis of a phosphotriesterase mimic. Adapted from Reference #57



template. This molecule was chosen because it possesses a P-CH₂ bond contains a P-O bond,



(II)

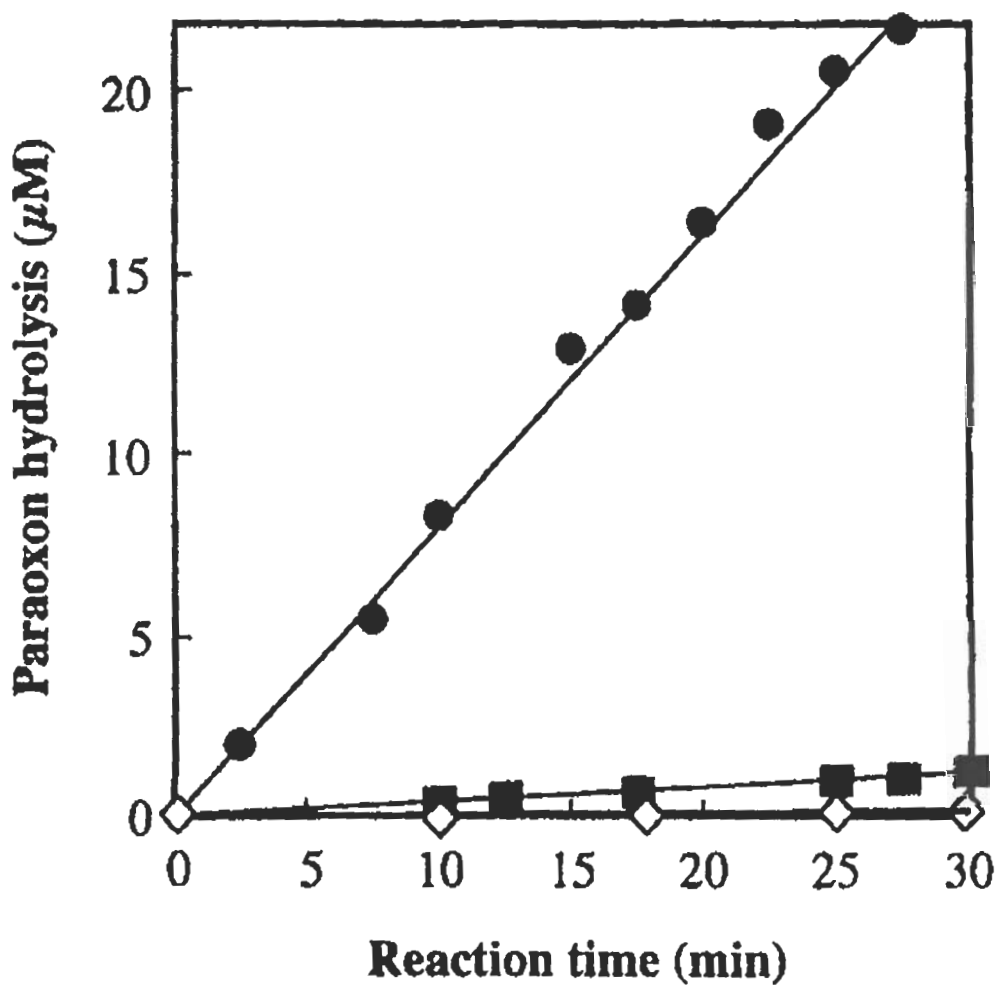
thus it was hypothesized that D4NP would not undergo hydrolysis, but rather serve to position the Co²⁺-imidazole complex within the polymer.⁵⁷

Figure 1-20 shows the results obtained for the hydrolysis of paraoxon on two imprinted polymers and a Co²⁺ solution. Clearly the Co²⁺-imidazole imprinted polymer demonstrates significant ability to hydrolyze paraoxon, approximately 20 times greater, compared to a polymer that contains imidazole and almost 100 times greater compared to hydrolysis performed in a Co²⁺ solution.⁵⁷ Furthermore, a turnover number (the number of substrate molecules converted into product per unit time when the enzyme is fully saturated with the substrate) of $5.6 \times 10^{-5} \text{ s}^{-1}$ for 1 mg of polymer, was calculated, however, when compared to the turnover number of phosphotriesterase, which is approximately 2200 s^{-1} , it is evident that significant improvement needs to be made.

Solid-Phase Extraction

Prior to performing quantitation, samples containing desired analytes often must undergo a pretreatment process. This process serves to not only isolate and remove the analyte from sample impurities, but also to pre-concentrate the analyte prior to analysis. Thus, the adsorbents used for this process are often selected based on their ability to retain and elute a particular

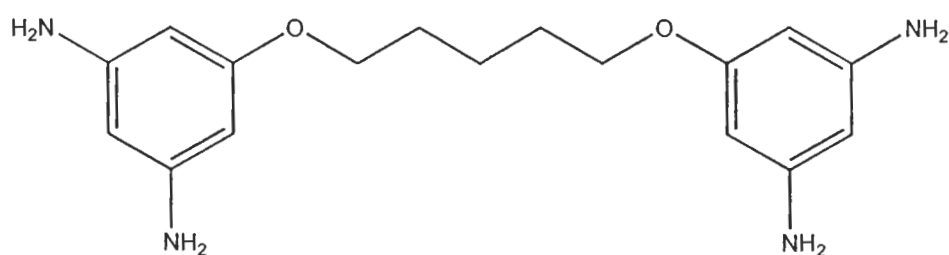
Figure 1-20. Results of paraoxon hydrolysis using a Co^{2+} -imidazole imprinted polymer.
Adapted from Reference #57



Polymer Prepared with Co^{2+} -imidazole Complex = •
Polymer prepared with Imidazole only = ■
Reaction in a 2.5 mM CoCl_2 Solution = ◇

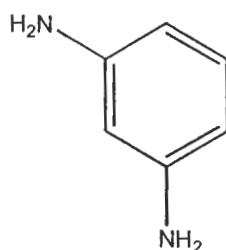
analyte. The high selectivity of imprinted polymers as well as their stability in a wide range of solvents and operating conditions, makes imprinted polymers very desirable phases for solid phase extraction. As shown in Table 1-11, the use of imprinted polymers in solid phase extraction is growing, as a number of MIP-SPE methods have been successfully developed for a variety of analytes in many different samples matrices.

One of the first MIP-SPE methods developed was for the enrichment of pentamidine (PAM) (*12*), a drug used to treat AIDS related disorders, from human urine.⁷² Two polymers



(12)

were prepared, one using PAM as the template and a reference polymer using benzamidine (BAM) (*13*) as the template, as shown in figure 1-21. By adjusting the pH of the mobile phase,



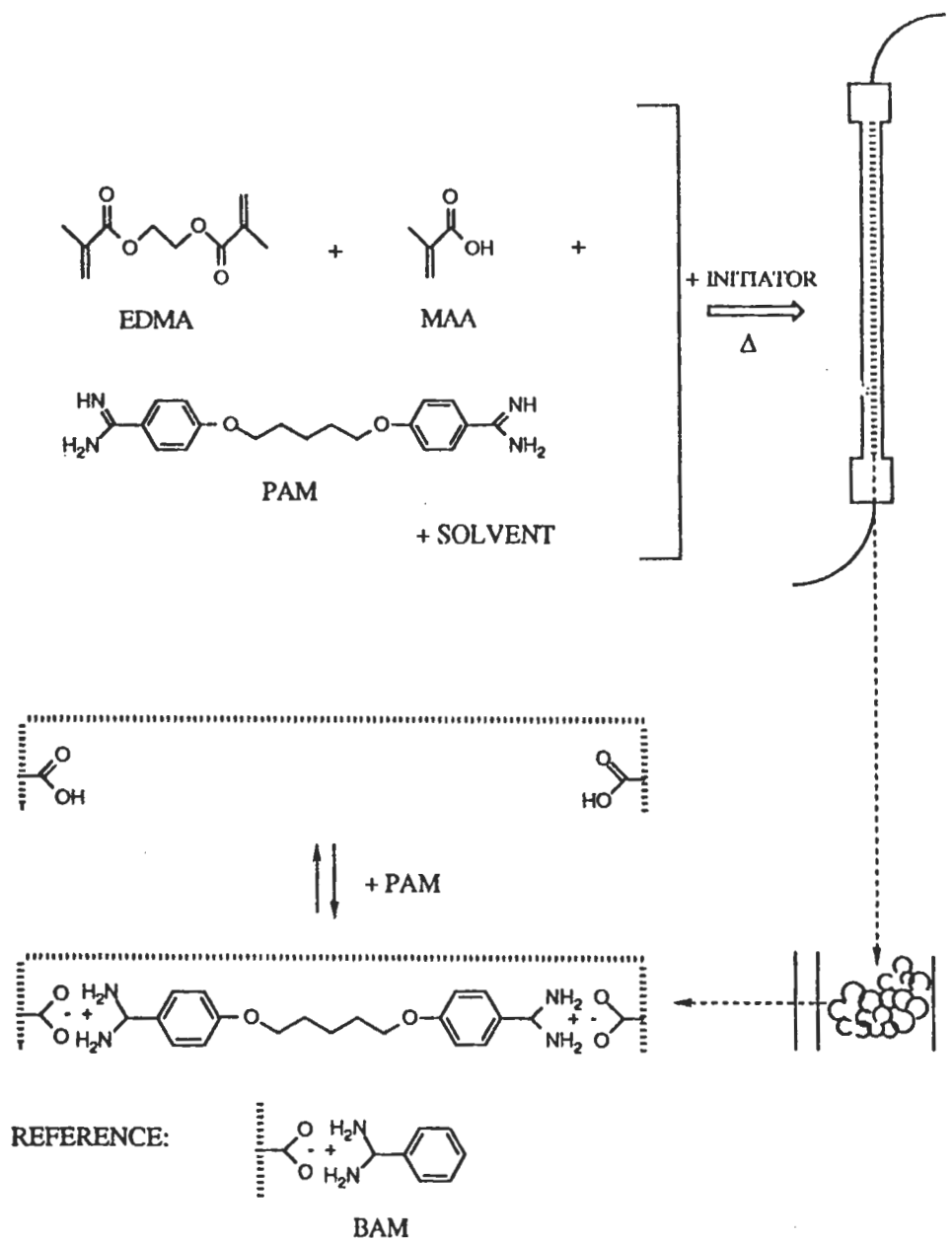
(13)

the retention and elution properties of PAM could be controlled, as the ionization states of the PAM amidine group and polymer carboxyl groups would be altered, allowing for increased (higher pH) or decreased (lower pH) electrostatic interactions between them.⁷² In this instance, a 100 mL urine sample containing 30 nM PAM was passed through the column with a mobile phase pH=5.0, retaining the PAM onto the column. The pH of the mobile phase was switched to

Table 1-11. Applications of MIP-SPE.

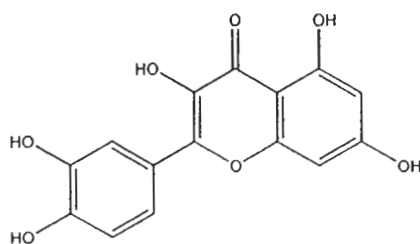
<u>Analyte</u>	<u>Matrix</u>	<u>Reference #</u>
Review Articles		65-71
Pentamidine	Urine	72
Theophylline	Serum	73, 85
Flavonoids	Ginko Leaves	74
Nerve Agents	Serum	75
Ochratoxin	Organic Solvent	76
4-nitrophenol	Water	77
Microcystin-LR	Water	78
Triazine herbicides	Water	79, 87, 89, 96, 101
7-hydroxy coumarin	Urine	80
Propranolol	Biological Fluids	81, 88, 91
Atrazine	Beef Liver	82
Sameridine	Plasma	83
Tamoxifen	Plasma/Liver	84
Nicotine	Chewing Gum	86
4-aminopyridine	Serum	90
Clenbuterol	Calf Urine	92, 95
Trögers Base	Acetonitrile	93
Phenytoin	Plasma	94
Flame retardants	Methanol	97
Phenoxy acids	Water	98
Pirimicarb	Water	99
2,6-pyridinedicarboxylic acid	Aqueous	100
Caffeine	Aqueous	102
Aterol	Methanol	103

Figure 1-21. Synthesis and preparation of Pentamidine MIP. Adapted from Reference #72



pH=2 and the PAM was desorbed from the column and determined directly by UV detection. Figure 1-22 shows the desorption profile of PAM on both the PAM and BAM imprinted polymers. Clearly, a selective enrichment of PAM is achieved, in this case by a factor of 4. Additionally, the authors noted that many of the sample interferences had been effectively removed from the urine sample, thus allowing for direct detection of PAM upon elution from the polymer.⁷²

In another method, Quercetin (*14*) was selectively extracted from ginkgo leaves.⁷⁴

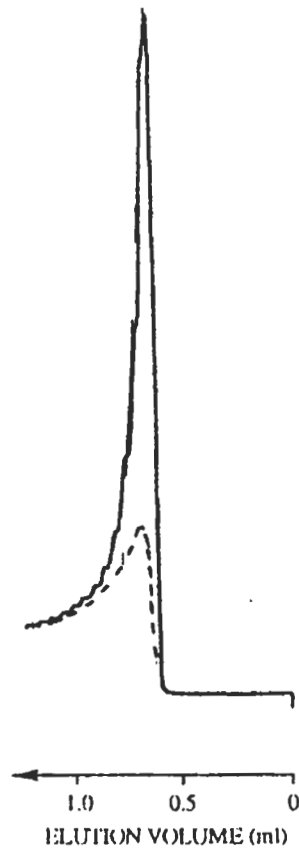


(14)

The imprinted polymer was prepared using acrylamide as the functional monomer and EGDMA as the crosslinker. Samples were prepared using the hydrolyzate of ginkgo leaves and were applied to cartridges containing approximately 0.4 g of polymer. MeOH was used as the wash solvent, followed by elution with 3 mL of MeOH/.Acetic Acid (9:1 v/v) and were analyzed by reverse phase HPLC.⁷⁴ The top portion of Figure 1-23 is a chromatogram of the ginkgo hydrolyzate solution without any sample pretreatment. Clearly, there are a number of sample components in the hydrolyzate, including significant amounts of kaempferol. The bottom portion of Figure 1-23 is the chromatogram of a sample that was extracted using the MIP phase prior to analysis. As shown, quercetin has been selectively removed and isolated from the other sample components, including significant removal of kaempferol.

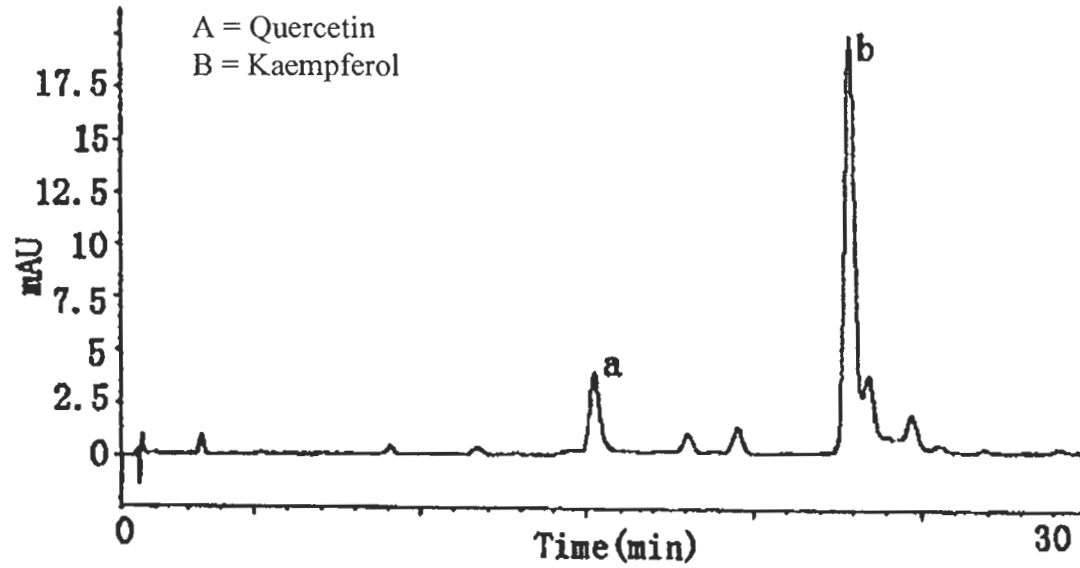
Recently, a MIP-SPE method for the selective extraction and analysis of chemical nerve agents was reported.⁷⁵ Figure 1-24 lists the structures of several degradation products and their

Figure 1-22. Desorption profile of PAM from both a non-imprinted and imprinted polymer.
Adapted from Reference #72

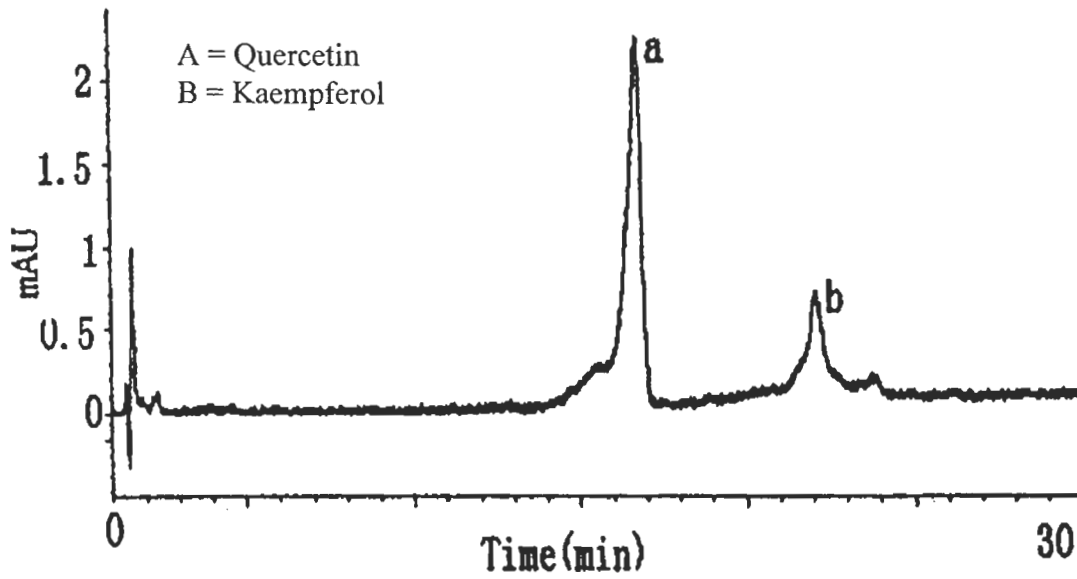


Non-Imprinted = -----
Imprinted = _____

Figure 1-23. Sample chromatogram of Ginkgo leaf hydrolzate solution before and after MIP extraction. Adapted from Reference #74

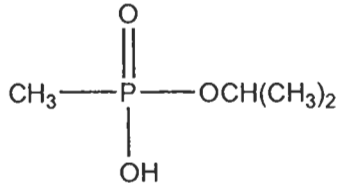


Prior to extraction

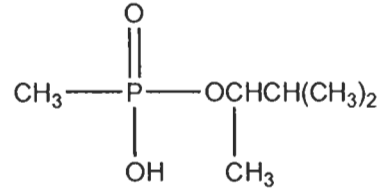


After Extraction

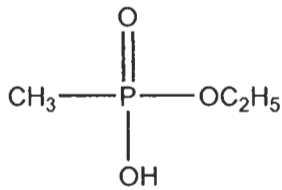
Figure 1-24. Structures of several nerve agents. Adapted from Reference #75



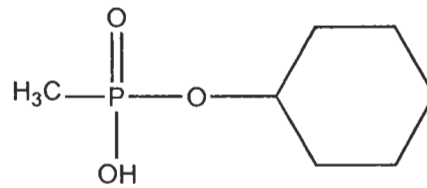
isopropyl methylphosphonate (IMPA)
Sarin Nerve Gas



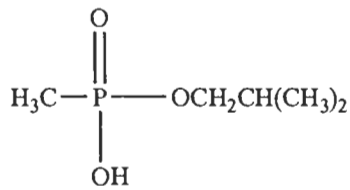
Pinacolyl methylphosphonate (PMPA)
Soman Nerve Gas



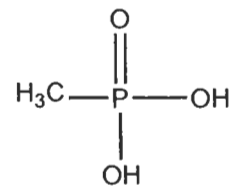
ethyl methylphosphonate (EMPA)
VX Nerve Gas



Cyclohexyl methylphosphonate (CMPA)
GF nerve Gas



Isobutyl methylphosphonate (BMPA)
Russian VX Nerve Gas



methylphosphonic acid (MPA)
Final nerve gas degradant

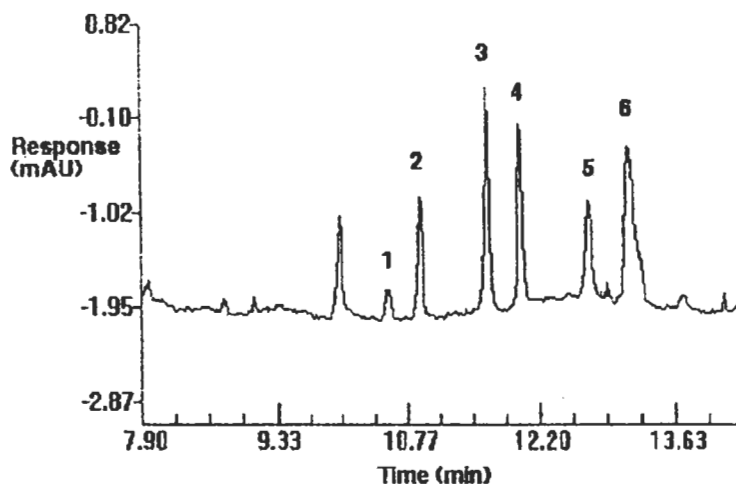
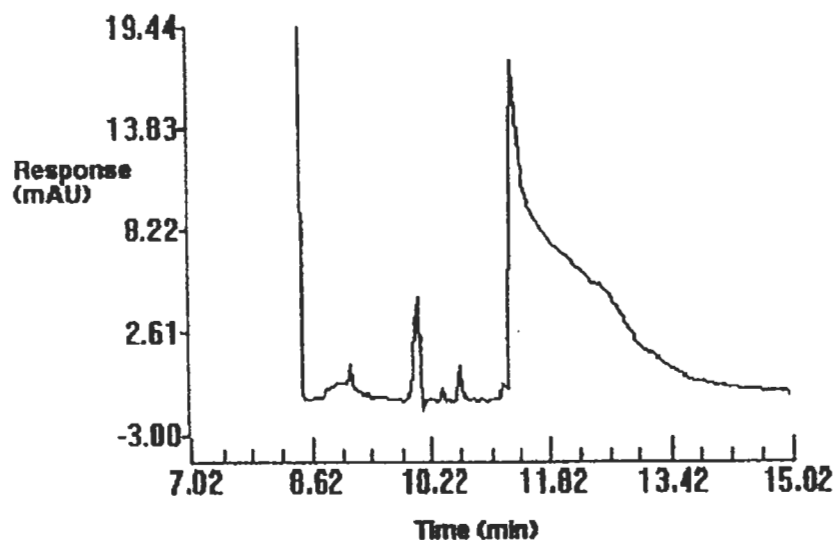
parent compounds. Imprinted polymers were prepared using PMPA, EMPA, and MPA were prepared using MAA as the functional monomer.⁷⁵ In addition, a blank polymer was prepared to serve as a control for the experiments. Initially, binding studies were performed in acetonitrile to compare selectivity of each imprinted polymer for the degradation products. Table 1-12 shows the recoveries of the various degradation products from the imprinted polymers. It was observed that good recovery was achieved using each imprinted polymer, while not shown, it was reported that the blank polymer did not exhibit any affinity for the analytes. Based on the above results, the imprinted polymer for PMPA was selected for use in further studies.⁷⁵

Extraction cartridges were prepared using 500 mg of PMPA imprinted polymer using acetonitrile and water as the loading and eluting solvents respectively. A 1 mL urine sample was spiked with the respective degradation products and extracted with acetonitrile. This was then passed through the MIP cartridge and followed by elution with 5, 2 mL portions of water. The elution portions were combined in a rotary evaporator, and evaporated until 1 mL remained. This was then injected a capillary electrophoresis system where separation and quantitation was completed. Figure 1-25 shows two electrochromatograms of the urine samples. The top electrochromatogram is that of the MIP extracted sample, while the bottom one is that of the acetonitrile extract of the urine sample. A comparison between the two chromatograms show that the MIP was successfully able to clean up the urine sample extract as shown by the baseline resolution achieved for all six compounds. This contrasts with to the electrochromatogram of the untreated extract, which was only able to separate MPA from the other analytes, which co-eluted.

Table 1-12. Recoveries of degradation products on several imprinted polymers. Adapted from Reference # 75

Template	PMPA	EMPA	MPA	IMPA	BMPA	CMPA
PMPA	83.3	98.9	97.4	99.2	97.5	78.5
EMPA	50.8	86.5	79.8	97.5	97.5	81.3
MPA	70.2	94.4	88.4	89.4	89.2	87.3

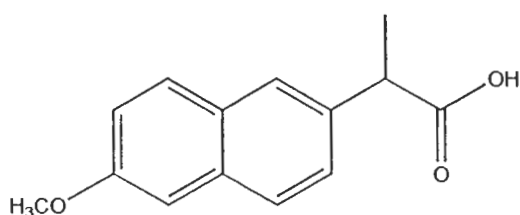
Figure 1-25. Chromatogram of a urine sample prior to and after extraction with a PMPA imprinted polymer. Adapted from Reference #75



1. MPA 2. EMPA 3. IMPA 4. BMPA 5. CMPA 6. PMPA

Chromatography

The use of imprinted polymers as chiral stationary phases in HPLC is the most common usage of MIP technology.^{6,15,17} In addition to their good mechanical and thermal stability, MIPs possess another advantage over conventional chiral phases, in that they have a predetermined elution order. This arises from the fact that the imprinted compound will always elute last compared to the other enantiomers or diastereomers present. Figure 1-26 shows the separation of (R,S)- Naproxen (**15**), a non-steroidal anti-inflammatory agent, on a (S)-Naproxen imprinted



(15)

polymer.¹⁰⁴ As shown, the imprinted analyte elutes last, even in the presence of multiple components as shown in Figure 1-27.¹⁰⁴ The broad peaks associated with each molecule, demonstrate the poor efficiency of MIP based phases.¹⁵ While some of the cause can be attributed to the irregular shapes of the packed particles, the majority is the result of different mass transfer rates between imprinted sites.¹⁵ Since the polymer surface possesses a heterogeneous distribution of binding sites, it is reasonable to believe that several different mass transfer rates will be present, with the high affinity binding sites possessing the slowest rates and the non-selective possessing the fastest rates.¹⁵

Recently, MIP's have become popular choices for stationary phases in capillary electrochromatography.¹⁰⁵⁻¹⁰⁹ Lin et. al. demonstrated a very simple separation of D,L-Phenylalanine anilide (D,L-PA) (**16**) using capillary electrophoresis.¹⁰⁵ Figure 1-28 shows the

Figure 1-26. Separation of R,S Naproxen on a (S)-Naproxen imprinted polymer. Adapted from Reference #104

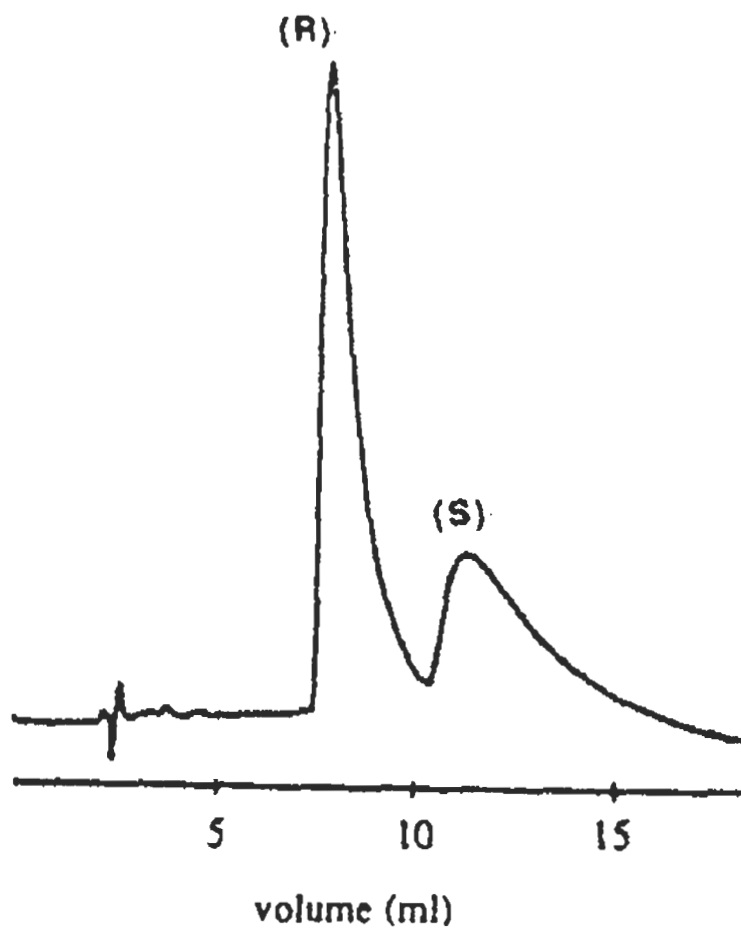
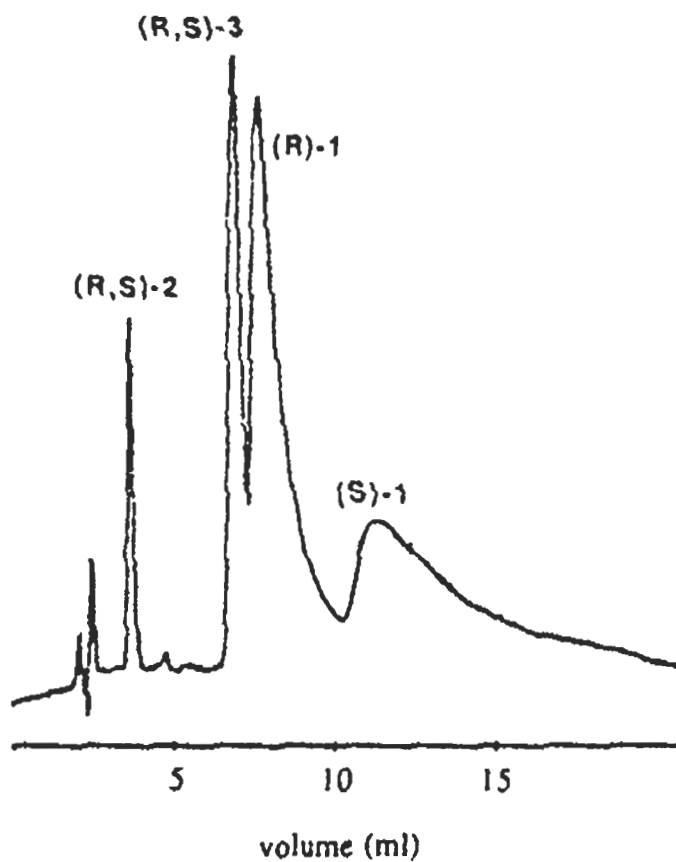
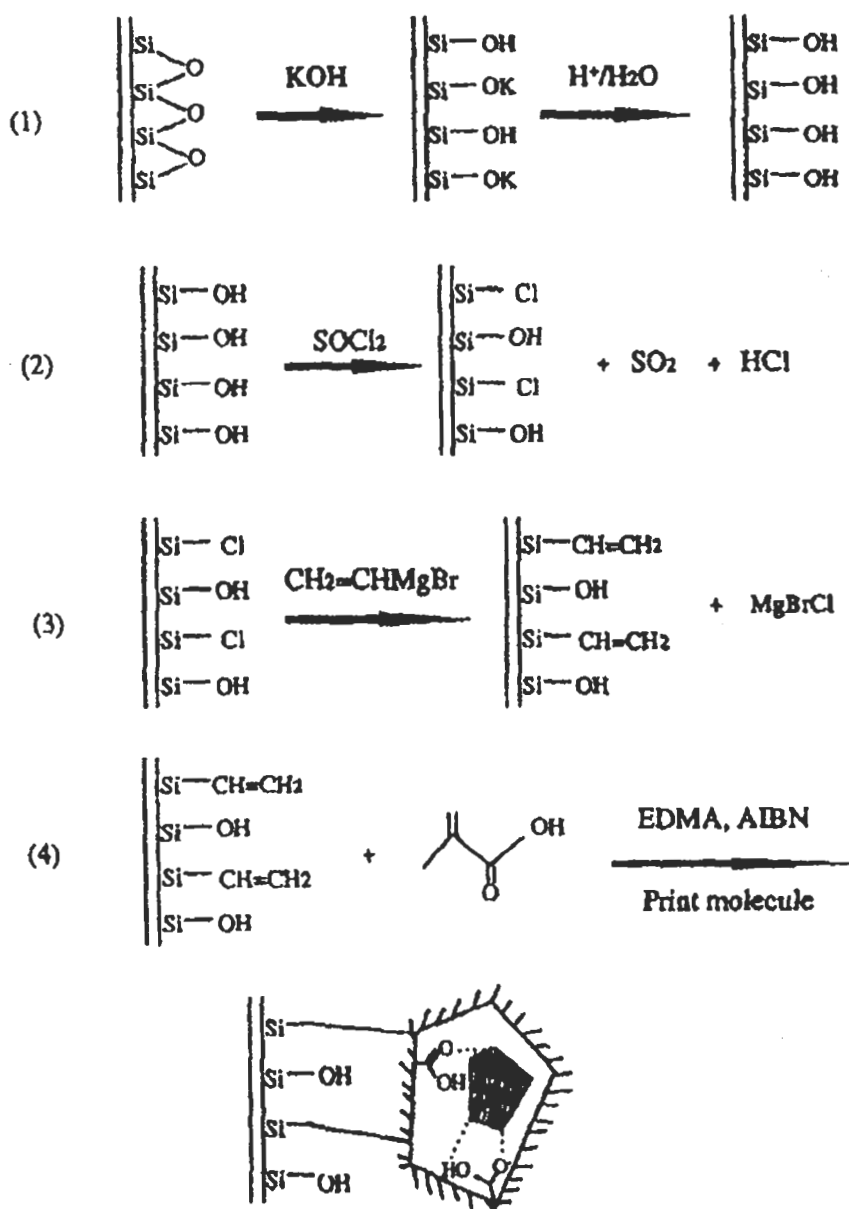


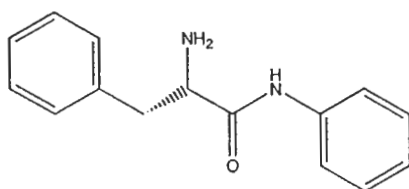
Figure 1-27. Separation of several NSAID on a (S)-Naproxen imprinted polymer. Adapted from Reference #104



Number	Compound
1	Naproxen
2	Ibuprofen
3	Ketoprofen

Figure 1-28. Synthesis and preparation of a capillary electrophoresis column imprinted with L-PA. Adapted from Reference # 105

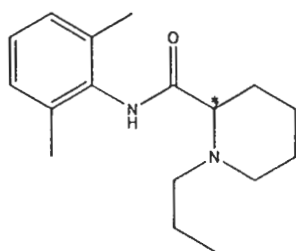




(16)

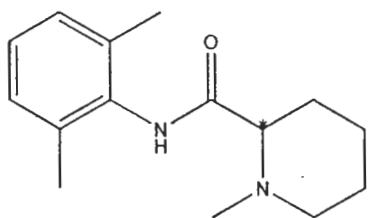
scheme by which the capillary column was prepared and Figure 1-29 shows a typical electrochromatogram for the separation of D,L-Phenylalanine anilide.¹⁰⁵

The local anesthetic (S)-ropivacaine (17) was used as a template to prepare a MIP

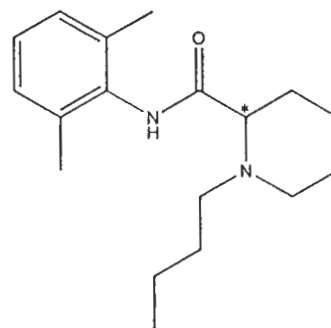


(17)

monolithic column.¹⁰⁶ The polymerization mixture was pushed into the fused silica capillary by a syringe and the ends capped with a soft rubber material. After low temperature polymerization, the caps were removed and the capillary was then flushed to remove the template and any unreacted monomers or initiator.¹⁰⁶ Figure 1-30 shows the separation achieved for racemic mixtures of ropivacaine, mepivacaine (18), and bupivacaine (19) on a



(18)



(19)

Figure 1-29. Separation of D,L-PA on a capillary electrophoresis column imprinted with L-PA.
Adapted from Reference #105

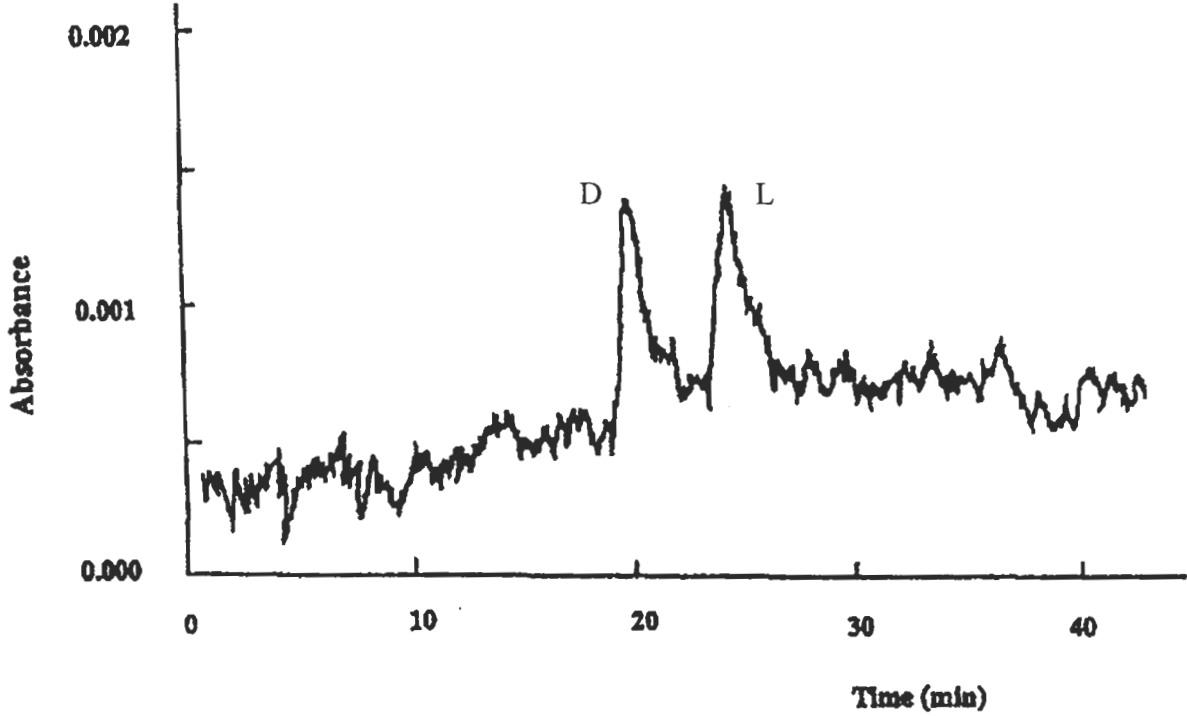
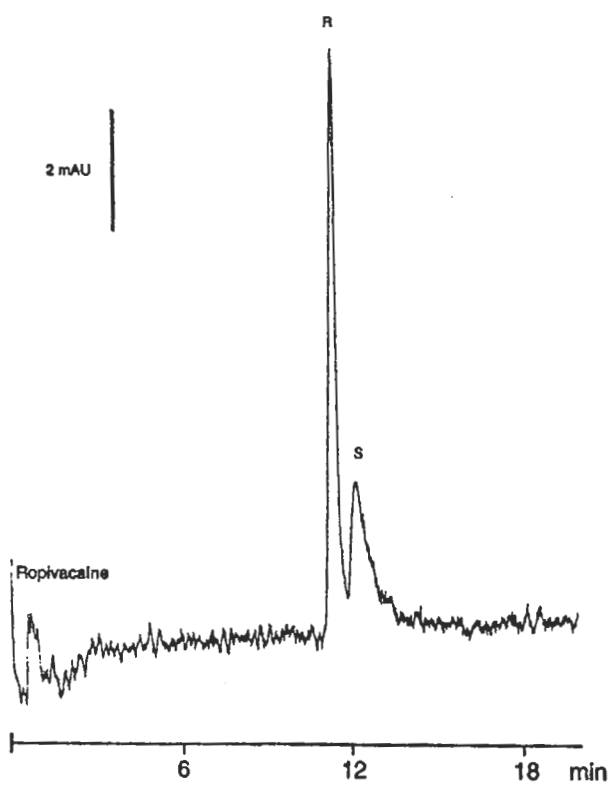
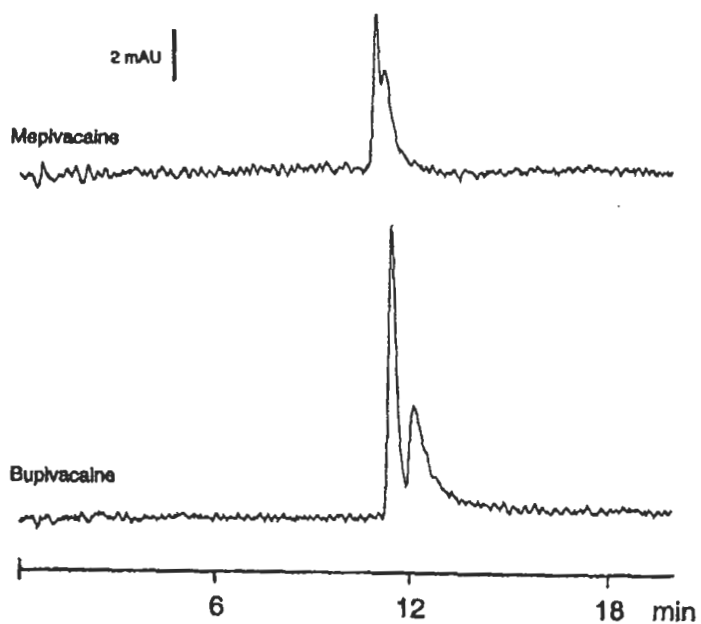


Figure 1-30. Separation of several anesthetics on a capillary electrophoresis monolithic column imprinted with (S)-ropivacaine. Adapted from Reference #106

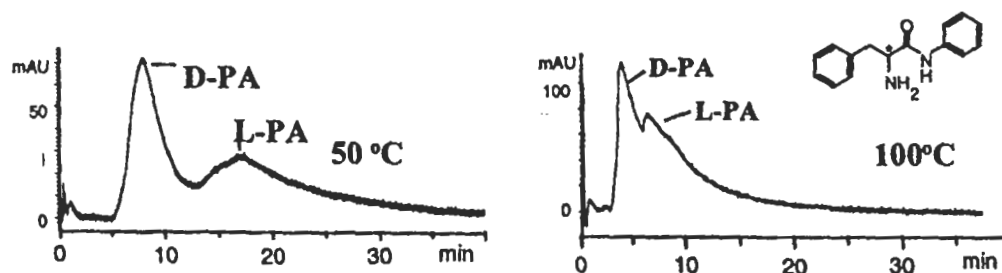


(S)-ropivacaine imprinted polymer. Upon examining the chromatogram obtained for the separation of racemic ropivacaine, the peak shapes of the imprinted enantiomer, (S)-ropivacaine are excellent compared to peak shapes usually obtained when using MIPs as stationary phases in HPLC. While the selectivity is not very large, sufficient resolution was obtained to clearly identify the two enantiomers. Similarly, bupivacaine exhibits the same characteristics as ropivacaine, mostly likely do to the fact that they differ in structure by one additional methyl group on the alkyl chain. The poor separation of mepivacaine can be attributed to the fact that it lacks an extended alkyl chain, thus its fit into the binding cavity is not ideal.¹⁰⁶

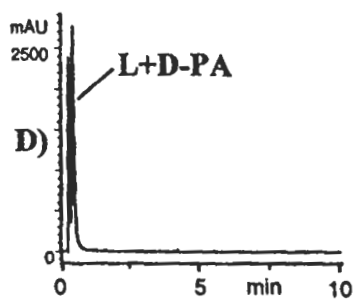
Recently, the use of imprinted polymers for supercritical fluid chromatography was explored.¹⁰⁹ This use is intriguing given the properties of supercritical fluid carbon dioxide. The advantages of using carbon dioxide as a mobile phase include viscosity that is an order of magnitude less than water as well as increased diffusion coefficients for dissolved compounds.¹⁰⁹ It was believed that this would help increase the mass transfer kinetics of imprinted polymers. Two different polymers were prepared, one by thermal polymerization for propranolol, and another by low temperature photoinitiation for L-phenylalanine. Figure 1-31 shows the SFC separation of D,L-PA at two different temperatures with the separation achieved on a blank polymer. Separation was accomplished, although after several days of operation, the chromatographic performance decreased and ultimately the polymer physically deteriorated so that it could no longer be used. This is interesting in that physical degradation of an imprinted polymer is very rare, however, supercritical CO₂ is considered a very strong “organic” solvent.. This would seem to suggest that different types of crosslinkers or monomers may be necessary for use in supercritical conditions.

In another interesting application, (-)-pseudoephedrine (**20**) and (-)-norephedrine (**21**)

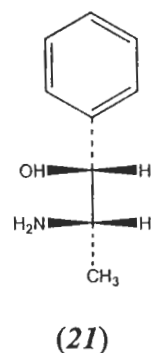
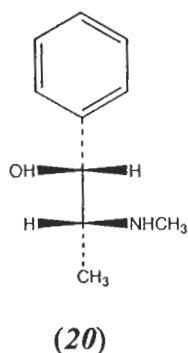
Figure 1-31. Separation D,L-PA on a L-PA imprinted polymer and a reference polymer using supercritical fluid conditions. Adapted from Reference #110



Outlet pressure 150 bar Flow rate 2.0 mL/min Oven temperature 50-100°C
Detection 260 nm Mobile Phase CO₂, 40 % MeOH/HOAc (95:5, v/v)



Outlet pressure 150 bar Flow rate 2.0 mL/min Oven temperature 50°C
Detection 260 nm Mobile Phase CO₂, 40 % MeOH/HOAc (95:5, v/v)



were used to prepare imprinted polymers for use as a stationary phase for thin-layer chromatography.¹¹¹ Table 1-13 shows the selectivity obtained for several components on (-)-pseudoephedrine imprinted with MAA and itaconic acid as functional monomers and Table 1-14 shows the selectivity obtained for the same components on a (-)-norephedrine imprinted polymer. It appears that some selectivity is obtained on both polymers imprinted with MAA, while better selectivity was observed on polymers prepared with itaconic acid. Finally, Figure 1-32 shows several TLC plates separated with a (-)-norephedrine imprinted polymer.

Conclusion

The origins of molecular imprinting were discussed and two general types of imprinting were presented. Covalent imprinting uses covalent bonds between the monomer and the template to provide a stable monomer-template complex, which results in a small distribution of binding sites. However, this technique is limited by the kinetics that are associated with the formation of different covalent bonds, thus only certain molecules may be imprinted. Non-covalent imprinting utilizes intra-molecular interactions, such as hydrogen bonding, to create the monomer-template complex. This allows for many different types of molecules to be used as templates, however, the resulting polymer will possess a large distribution of binding sites. Lastly, several different applications were examined and the impact and future potential of imprinted polymers was discussed.

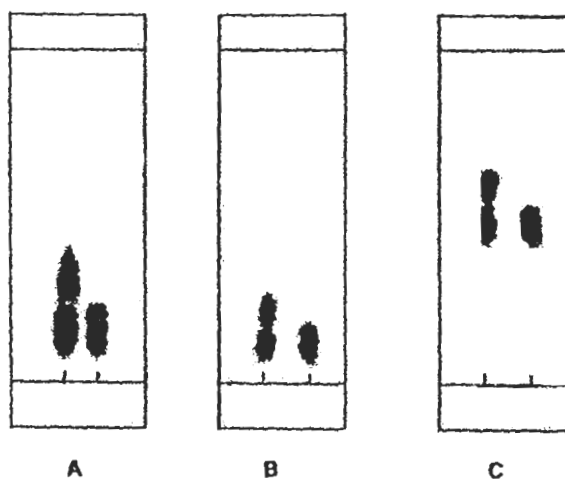
Table 1-13. R_f Values on a (-)-pseudoephedrine imprinted polymer. Adapted from Reference #111

Drug	% Acetic Acid	Methanol			Acetonitrile		
		$R_f(+)$	$R_f(-)$	α	$R_f(+)$	$R_f(-)$	α
Norephedrine	1	-	-	-	-	-	-
	5	0.32	0.32	1.0	0.18	0.18	1.0
	10	0.33	0.36	1.1	0.22	0.24	1.1
Epinephrine	1	0.26	0.38	1.5	-	-	-
	5	0.46	0.58	1.3	0.14	0.24	1.7
	10	0.56	0.64	1.1	0.44	0.54	1.2
Pseudoephedrine	1	0.28	0.30	1.1	0.10	0.10	1.0
	5	0.36	0.46	1.3	0.18	0.24	1.3
	10	0.40	0.50	1.3	0.20	0.29	1.5
Ephedrine	1	0.40	0.56	1.4	-	-	-
	5	0.44	0.56	1.3	0.28	0.38	1.4
	10	0.66	0.80	1.2	0.40	0.54	1.4

Table 1-14. R_f values obtained on a (-)-norephedrine imprinted polymer TLC plate. Adapted from Reference #111

Drug	% Acetic Acid	Methanol			Acetonitrile		
		$R_f(+)$	$R_f(-)$	α	$R_f(+)$	$R_f(-)$	α
Norephedrine	0	0.08	0.41	5.1	0.12	0.24	2.0
	1	0.55	0.67	1.2	0.52	0.70	1.4
	5	0.66	0.74	1.1	0.38	0.50	1.3
	10	0.74	0.84	1.1	0.83	0.97	1.2
Epinephrine	0	0.04	0.12	3.0	-	-	-
	1	0.50	0.60	1.1	0.08	0.20	2.5
	5	0.68	0.82	1.2	0.30	0.40	1.3
	10	0.88	0.94	1.1	0.34	0.44	1.3
Pseudoephedrine	10	-	-	-	0.74	0.88	1.4
Ephedrine	0	0.18	0.28	1.6	-	-	-
	1	0.54	0.64	1.2	-	-	-
	5	0.60	0.70	1.2	0.32	0.44	1.4
	10	0.70	0.78	1.1	0.36	0.44	1.2

Figure 1-32. TLC plates showing the separation of racemic norephedrine (left column) and (-)-norephedrine (right column). Adapted from Reference #111



A. Developed in MeOH B. Developed in 1% HOAc in acetonitrile C. Developed in 5% HOAc in acetonitrile

Chapter 2. Fundamentals of Imprinting and Novel Developments

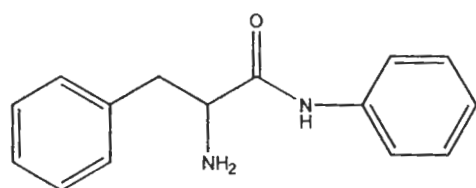
Introduction

In both of the two methods by which molecular imprinting occurs, intermolecular interactions, such as hydrogen bonding, are used that will cause the functional monomer to associate with the template molecule in a multi-molecular complex. In order to effectively generate a successful imprint of a template molecule, the creation of a monomer-template complex must therefore occur. Furthermore, this complex must remain stable while the polymerization process takes place. Therefore, optimizing the conditions under which the monomer will most strongly interact with the template throughout the polymerization process should result in the creation of a polymer that possesses selective binding sites for the template. There are several factors that must be considered prior to any attempts at imprinting. The following discussion examines several critical parameters that affect the quality of imprinted polymer, which will allow for a basic, fundamental understanding of the processes involved in molecular imprinting.

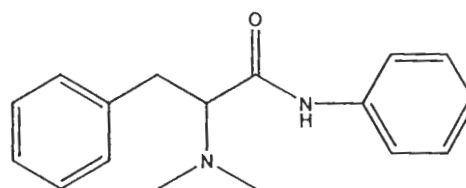
Functional Group Arrangement and Shape Selectivity

In non-covalent imprinting, it is reasonable to assume that the rebinding process will be kinetically more favorable than covalent imprinting. Therefore, additional points of interaction, either through a non-covalent interaction or a “shape” interaction, within the binding site, should lead to an increase in polymer selectivity. In a study performed on several amino acid derivatives, whose structures are depicted in Figure 2-1, variations were made to the number of functional groups as well as to the structural rigidity.¹¹² A comparison between the resulting polymer selectivities yields information about the

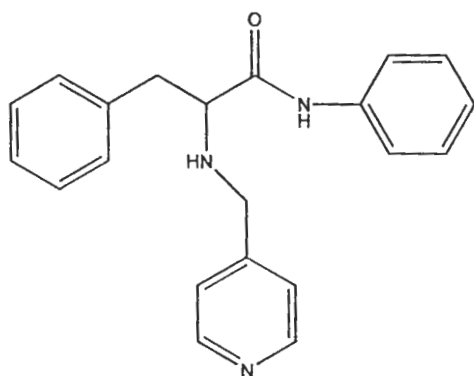
Figure 2-1. Structures and selectivities of several amino acid derivatives. Selectivity was determined by imprinting each polymer with the L form of amino acid. Adapted from Reference #112



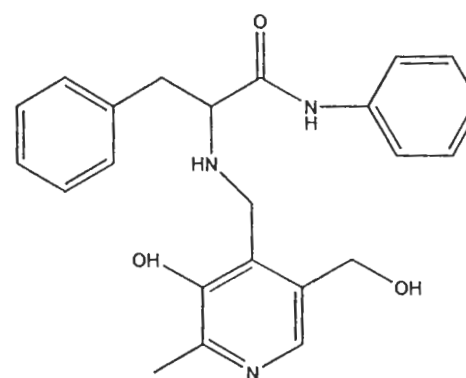
PheAN
4.1



Me₂PheAn
3.7



PyMePheAn
8.4



PLPheAn
2.7

effects of these additional interactions. A polymer prepared with L-phenylalanine anilide (PheAn), demonstrated a selectivity of 4.1 versus its enantiomer. By switching a primary amine to a tertiary amine to create N,N-dimethylphenylalanine anilide (Me₂PheAn), the resulting polymer enantioselectivity dropped slightly to 3.7. This could be attributed to the increase in steric bulk around the nitrogen, disrupting the interaction with MAA. Next, the dimethylamine group was replaced with a methyl pyridine group to form N-pyridylmethylphenylalanine anilide (PyMePheAn), resulting in an increase in selectivity to 8.4. This can be attributed to the addition of the pyridine ring, which is expected to interact strongly with MAA. Finally, two hydroxyl groups and a methyl group were substituted onto the ring, resulting in significant decrease in selectivity, down to 2.7. This could be attributed to an increase in the overall steric bulk, which would cause a misalignment between the template functional groups and the MAA residues within the binding cavity. Several other studies on amino acids¹¹³⁻¹¹⁶ demonstrated similar results to the above study, suggesting that both shape and functional group arrangement play a significant role in determining polymer selectivity.

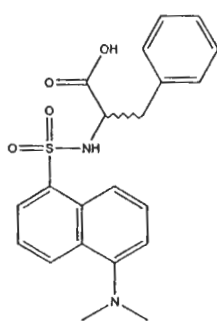
This concept is also illustrated in a recent study performed on a dansyl-L-phenylalanine (**22**) (Dns-Phe) imprinted polymer system utilizing both methacrylic acid and 2-vinyl pyridine as functional monomers.¹¹⁷ Two other amino acids were synthesized, Dansyl-phenylalanine methyl ester (**23**) (Dns-Phe-Me-ester) and Naphthyl-sulfonyl phenylalanine (**24**) (Naph-Phe) to test both the influence of the Dns-Phe carboxylic acid and dimethylamino group respectively.¹¹⁷ Table 2-1 shows the retention factors as well as the selectivity obtained on these polymers. By blocking the carboxylic

Table 2-1. Selectivity of different derivatives of the amino acid Phenylalanine. Adapted from Reference # 117.

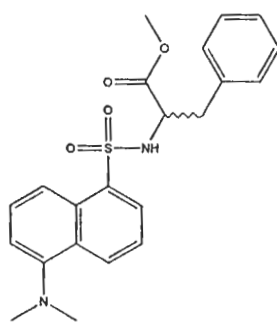
Top: Selectivity obtained by varying the functionality
 Bottom: Selectivity obtained by varying side chain length

Analyte	Dns-Phe	Dns-Phe-Me-ester	Napth-Phe
k' D-enantiomer	1.0	0.0	1.1
k' L-enantiomer	2.2	0.0	1.7
α	2.2	-	1.5

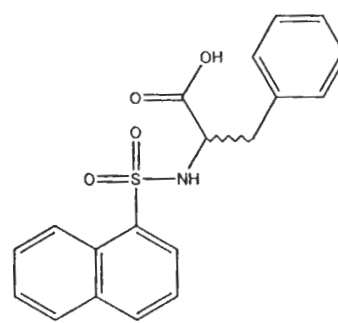
Analyte	Dns-Ala	Dns-Leu	Dns-Val
k' D-enantiomer	0.8	0.5	0.5
k' L-enantiomer	1.0	0.6	0.7
α	1.3	1.2	1.4



(22)



(23)



(24)

acid group on the Dns-Phe, (compare the structure of Dns-Phe and Dns-Phe-Me-ester), no enantioselectivity was observed, indicating that the interaction between the Dns-Phe carboxylic acid and the polymer pyridine groups is the primary interaction by which the polymer generates selectivity, which was further confirmed through additional HPLC and IR studies.¹¹⁷ A comparison between the Dns-Phe and Naph-Phe, in which the dimethylamino group has been removed, shows that the L enantiomer of Naph-Phe is retained, however the retention factor is significantly reduced compared to Dns-Phe. This allowed the authors to conclude that the interaction between the dimethylamino group on Dns-Phe and the MAA within the polymer provides a secondary, stabilizing interaction. Additionally, further studies using other amino acid derivatives of varying side chain lengths, whose chromatographic results are also shown Table 2-1, demonstrated that a tight steric fit between the polymer and side chain was necessary in order to generate selectivity. This was shown by the decreased selectivity for the various derivatives regardless of whether the side chains exhibited greater or lesser steric bulk than Dns-Phe. Based on this, it has been proposed that the enantioselective mechanism consists of a leading interaction between the template and polymer that initially retains the enantiomers. This is followed by secondary stabilizing interactions including weaker

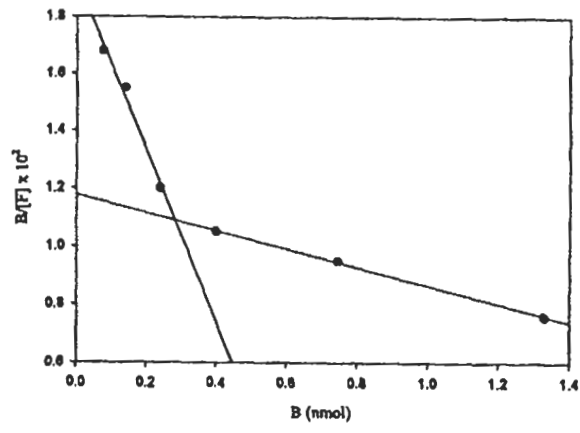
template-monomer interactions as well as a proper steric fit of the template into the binding site.

As described earlier, the puzzling binding patterns for a series of Ricin Imprinted polymers provides further insight into the role of shape interactions on generating selectivity.²⁵ An examination of the Ricin imprint scatchard plots,¹¹⁸ shown in Figure 2-2, shows two distinct classes of binding sites, which is consistent with other reported work utilizing scatchard plots with MIP's. Figure 2-3 is a scatchard plot for the binding of Ricin A and B to their respective imprints and is linear in both cases, which suggests that only one class of binding sites was created on these imprints. Thus to explain why Ricin B could bind to the Ricin polymer while Ricin A could not, it was proposed that the Ricin B chain, given its more random coil, is structurally more flexible and thus can conform to a variety of cavities, while the A chain, with extensive secondary sheet and helix structures can not conform to the binding cavity shape even though the imprinted polymer should possess recognition sites for both chains. This also explains the binding of Ricin B to Ricin A imprints as the smaller, flexible nature of B allows it to interact with the cavity created by imprinting A. Thus, in this situation, it appears that while interactions play a role in generating the initial binding, the shape interaction provides significant discrimination effects.²⁵

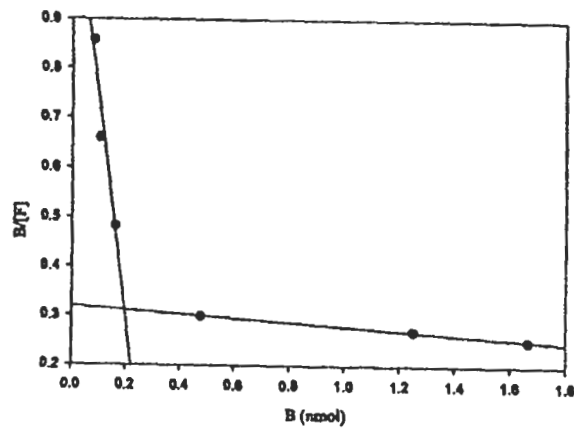
Polymerization Solvent and Temperature

The solvent, or porogen, utilized in the synthesis of imprinted polymers plays a significant role in the resulting polymer's physical properties and its ability to resolve enantiomers. In a authoritative investigation into the effect of porogens on polymer

Figure 2-2. Scatchard plots obtained using a Ricin imprinted polymer. Adapted from Reference #25

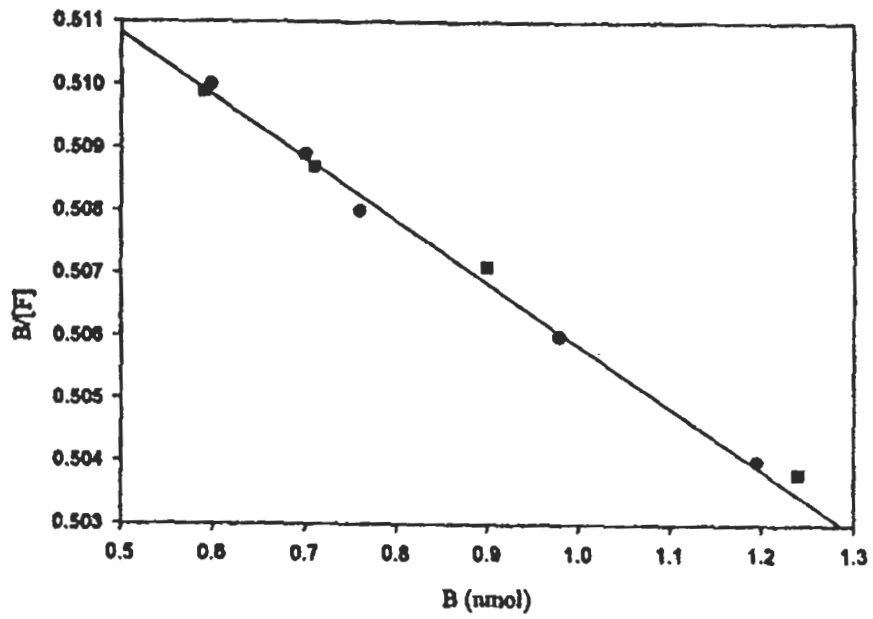


Scatchard plot of Ricin binding to Ricin imprinted polymer

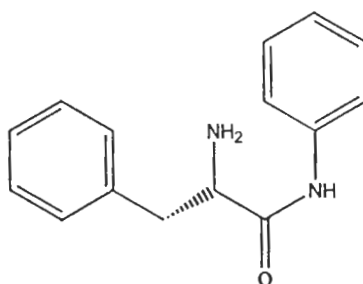


Scatchard plot of Ricin B chain to Ricin imprinted polymer

Figure 2-3. Scatchard plot obtained for the binding of Ricin Chain A (■) and Ricin B Chain (●) to their respective polymers. Adapted from Reference #25



selectivity, Sellergren and Shea,¹¹⁹ investigated a variety of different solvents utilized in the preparation of a L-phenylalanine anilide (**16**) (L-PA) imprinted polymer.



(16)

The authors performed a variety of studies aimed at complete characterization of the resulting polymer morphology, Table 2-2 being a representative example, and attempted to correlate the various morphological features to the resulting polymer chromatographic selectivity. In what was considered a surprise, they were able to conclusively show that the largest influence on polymer selectivity could be attributed directly to the porogens capacity to form hydrogen bonds, and not to any one particular morphological feature. An examination of Table 2-3 shows that the polymers prepared in poor hydrogen bonding solvents, such as chloroform, hexane, and acetonitrile, demonstrated greater chromatographic selectivity than those prepared in strong hydrogen bonding solvents such as isopropanol or acetic acid. Based on these results, it was concluded that, in general, imprinted polymer selectivity would be remarkably better if performed in low-hydrogen bonding capacity solvents.

Prior to the above study, O'Shannessy et. al. had reported the results of performing polymerizations at low temperatures using photolytic homolysis (photoinitiation) of azobisnitriles in the synthesis of an imprinted polymer for L-PA.¹²⁰ The results in Table 2-4 show chromatographic data obtained for four polymers. Two

Table 2-2. Several morphology characteristics for a L-phenylalanine anilide imprinted polymer prepared in several different solvents. Adapted from Reference #119

Poragen	Swelling (mL/mL)	Pore Volume (mL/g)	Surface Area (m ² /g)
MeCN	1.36	0.60	256
CHCl ₃	2.11	0.007	3.5
C ₆ H ₆	1.55	0.43	216
CH ₂ Cl ₂	2.01	0.007	3.8
DMF	1.97	0.17	157
THF	1.84	0.24	194
Isopropanol	1.10	0.86	49
Acetic Acid	1.45	0.52	267

Table 2-3. Selectivity of several L-phenylalanine anilide imprinted polymers prepared in various solvents. Adapted from Reference # 119

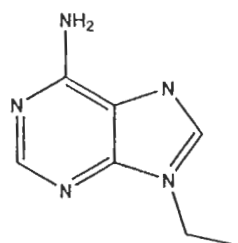
Poragen	H-Bond Type	Selectivity (α)
MeCN	Poor	5.8
CHCl ₃	Poor	4.5
C ₆ H ₆	Poor	6.8
CH ₂ Cl ₂	Poor	8.2
DMF	Medium	2.0
THF	Medium	4.1
Isopropanol	Strong	3.5
Acetic Acid	Strong	1.9

Table 2-4. Selectivity of L-phenylalanine anilide imprinted polymer prepared at two different temperatures. Adapted from Reference #120.

Polymer Preparation	k_D	k_L	α
Acetonitrile 60°C	1.058	1.667	1.57
Chloroform 60°C	2.395	4.814	2.01
Acetonitrile 0°C	1.081	2.459	2.275
Chloroform 0°C	1.4	3.15	2.25

polymers were prepared at low temperatures using photoinitiation, while the other two were prepared at 60 °C, using thermal initiation. The retention factors (k) for both D,L phenylalanine anilides were calculated, as well as the overall selectivity (α) for each polymer. The sufficient difference in selectivity clearly shows that using lower temperatures for performing the polymerization is desirable.¹²⁰

Overall, the two studies illustrate that increased selectivity will be obtained if the polymerization is performed at low temperatures, utilizing photo-initiation, in solvents of poor hydrogen bonding capacity. Finally, the above results were confirmed in a third study performed by Spivak et.al. who studied a MIP system for 9-ethyladenine (25).¹²¹



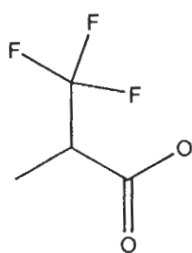
(25)

In addition to the above effects, they also observed that polymers displayed the greatest chromatographic selectivity when the mobile phase was also the poragen.¹²¹ In a related report, high pressure was examined in the formation of selective polymers.¹²² Two sets of polymers were prepared using 1 and 1000 bar for the two templates. Chromatographic determination revealed that one polymer displayed a “pressure” effect as evident by a slight increase in selectivity, however the other polymer system displayed no increase in selectivity, and thus the results were deemed inconclusive.¹²²

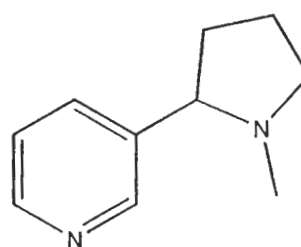
Influence of the Functional Monomer

Since non-covalent imprinting relies on the ability of the functional monomer to interact with the template, it is reasonable to believe that the strength of the interactions will vary. While MAA has been used to interact with a variety of functional groups, it was shown that 2-vinylpyridine (2-VP) interacts with carboxylic acid groups better than MAA.¹²³ In a Boc L-tryptophan system imprinted with 2-VP or MAA, it was shown that the 2-VP polymer generated a selectivity of 2.25 versus 1.90 achieved with MAA. Furthermore when a polymer was prepared using a mixture of MAA and 2-VP, a higher selectivity, 4.35, was achieved. This same effect was observed for several other amino acid derivatives studied. The authors believed that 2-VP and MAA preferred separate interactions on the amino acid, resulting in interactions that were maximized in terms of strength and number.¹²³

A second set of studies performed using either MAA or its analog trifluoromethyl acrylic acid (TFMAA) (**26**) demonstrated that the TFMAA generated



(26)

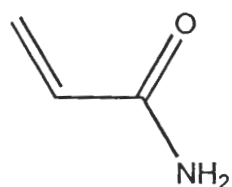


(27)

polymers that were more selective for nicotine (**27**).^{124,125} It was hypothesized that the trifluoromethyl functionality, through electron withdrawing effects, causes TFMAA to be more acidic, allowing it to generate greater interactions with the basic functional groups in nicotine.¹²⁴ However, another study demonstrated that MAA generated greater

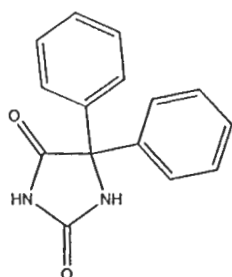
selectivity than a similar polymer prepared using TFMAA.¹²⁶ Since, neither study performed additional studies focusing on the strength of the monomer-template interactions prior to polymerization, valid conclusions cannot be readily drawn as to why there is a discrepancy.

Further adding to the uncertainty surrounding strengths of hydrogen bonds, are the studies performed using acrylamide (**28**) as a functional monomer. For a



(**28**)

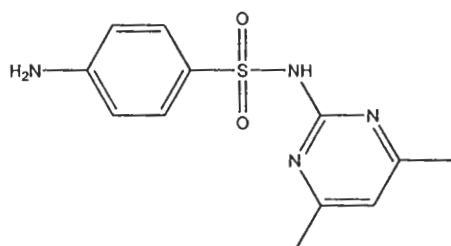
series of polymers prepared for several amino acid derivatives in both non-polar (chloroform) and polar (acetonitrile) organic solvents, greater enantioselectivity was observed on polymers utilizing acrylamide as the functional monomer.¹²⁷ A second study compared acrylamide and MAA polymers selective for 5,5-diphenylhydantoin, an acidic drug (**29**) that were prepared in tetrahydrofuran, a polar solvent.



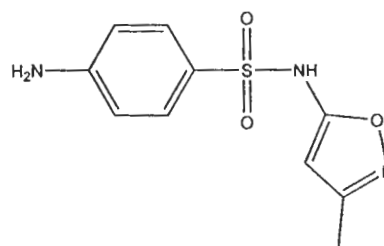
(**29**)

In binding studies, the acrylamide polymer was calculated to effectively bind 34 $\mu\text{mol/g}$ of template, while the MAA prepared polymer was only able to bind 7.1 $\mu\text{mol/g}$.¹²⁸ The above studies attribute acrylamide's superior performance to its ability to form stronger

hydrogen bonds in polar solvents than MAA. However, a new study in which acryamide/4-VP and MAA/4-VP polymers were prepared for sulfamethoxazole (SMO) (**30**) and sulfamethazine (SMZ) (**31**) in acetonitrile (polar organic), suggests that other



(30)



(31)

factors need to be considered.¹²⁹ When SMO was utilized as the template molecule, the acrylamide polymer generated greater chromatographic selectivity (2.4) vs. the MAA polymer (0.65). However, when SMZ was used as the template, the MAA polymer now demonstrated greater selectivity (2.84) than that of the acrylamide polymer (1.19).¹²⁹ This suggests that both the relative strengths of interactions between the monomer and the template as well as solvent polarity will play a role in facilitating non-covalent interactions.

Overall, one can state that there are no universal guidelines for the selection of a functional monomer. While poragen polarity and the acid/base nature of monomer and template can be used as a general guideline to narrow the choices down to a few, they cannot be used to predict the strength of the interactions. Thus, it is suggested that utilizing an independent technique, such as NMR or IR spectroscopy, to empirically determine the strengths of the resulting interactions prior to polymerization is a necessary step in the process of generating an imprinted polymer.

Recent Developments

The above sections provide insight into the basic fundamentals of molecular imprinting as well as several of the challenges that face researchers. In recent years there have been several developments in molecular imprinting, which we believe signify changing attitudes towards molecular imprinting. In past years, MIPs were a novel technique whose rapid growth can be attributed to the majority of researchers incorporating them into several different applications, regardless of whether or not current MIP technology permitted successful implementation.

Recently, this attitude has shifted to one of maturation, whose future growth will be dependent upon developing rational and efficient design processes that allow for not only a more complete understanding of the underlying chemical processes involved, but also the production of rugged and reliable materials that ultimately will allow MIPs to meet the regulatory guidelines that are required of many analytical techniques. The following section discusses several developing areas of MIP research that represent this changing attitude. Areas of particular interest are novel polymerization techniques, novel monomers, non-covalent/covalent imprinting, and changing monomer-template ratios.

Novel Polymerization Techniques

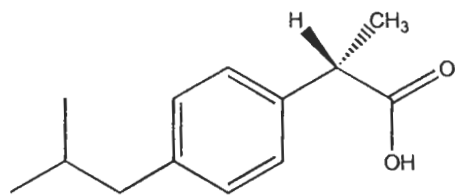
Currently, bulk polymerization is the most common form of polymerization used in molecular imprinting.¹³⁰ However, there are three main problems with this process that have been identified:¹³⁰

1. The grinding and sieving process employed to reduce the solid polymer into particles suitable for use is both extremely time consuming and inefficient, resulting in significant waste as a good portion of the polymer will be in an unusable form.¹³¹ Furthermore, this process is often done manually and would not lend itself to successful large scale processing. Finally, manual processing leads to batch to batch irreproducibility as it is very difficult to generate the same particle distribution each time.¹³⁰
2. Block polymers, such as the ones employed for imprinting, are highly crosslinked, which makes template recovery difficult. While some researchers have reported greater than 90% recovery, the vast majorities achieve much lower percentages. Thus for applications developed for pharmaceuticals, the cost of replacing lost template may become prohibitive, especially for preparatory scale.
3. There is little opportunity for tailoring these materials to give certain desirable properties. As illustrated above, the imprinting process requires poor hydrogen bonding solvents, limiting the number that can be used for polymerization and as a consequence limiting the types of solvents that analysis can be performed in.

In response to this criticism, several different polymerization techniques have been developed for molecular imprinting.

Multi-Step Swelling Polymerization

The research group of Haginaka et. al., in a series of publications, have developed a polymerization technique that produce uniform-sized beads that contained the imprinted polymer.¹³²⁻¹³⁶ They reasoned that this technique would allow for improved chromatographic performance as the stationary phase would now consist of spherical particles, approximately 6 μM in size.¹³² Additionally, this technique is performed by creating a micro-emulsion within an aqueous environment, thus it was also reasoned that this would allow for use in high aqueous environments.¹³² The general process by which this occurs is illustrated in Figure 2-4. The first swelling step prepares the polystyrene seed particles for further processing as the particles will uptake an activating agent. The second swelling step causes the seed particles to incorporate the porogen and initiator within the inside of the particle. In the third swelling step, the functional monomer, template, and crosslinker are added and incorporated into the seed particle. Finally, the fully swollen particle is polymerized and then washed to produce a uniform, spherical particle that has been selectively imprinted.¹³⁵ Figure 2-5 shows two separations achieved on a non-imprinted and a (S)-ibuprofen (32) imprinted polymer



(32)

prepared by this process. As shown the polymer has successfully separated the two enantiomers of ibuprofen in addition to successfully separating other structurally related compounds. Of interest is the mobile phase, which is a 55:45 20 mM phosphate buffer

Figure 2-4. Multi-step swelling technique for the preparation of imprinted polymers.
Adapted from Reference #132

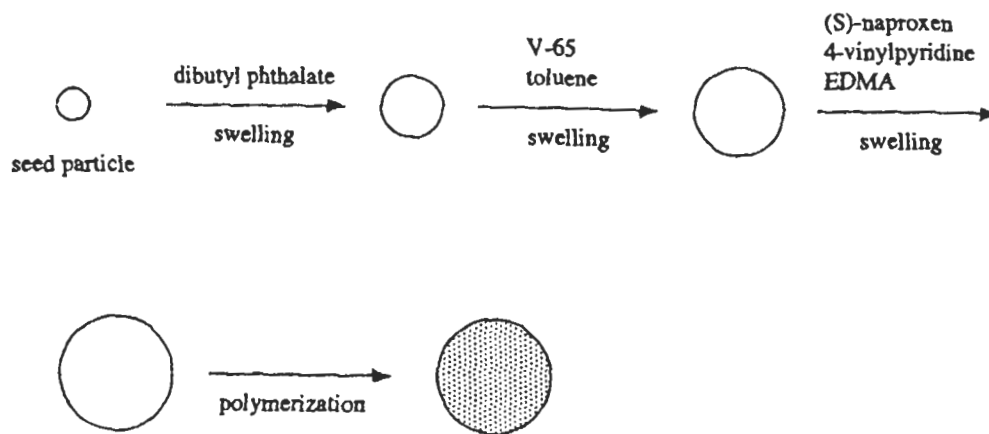
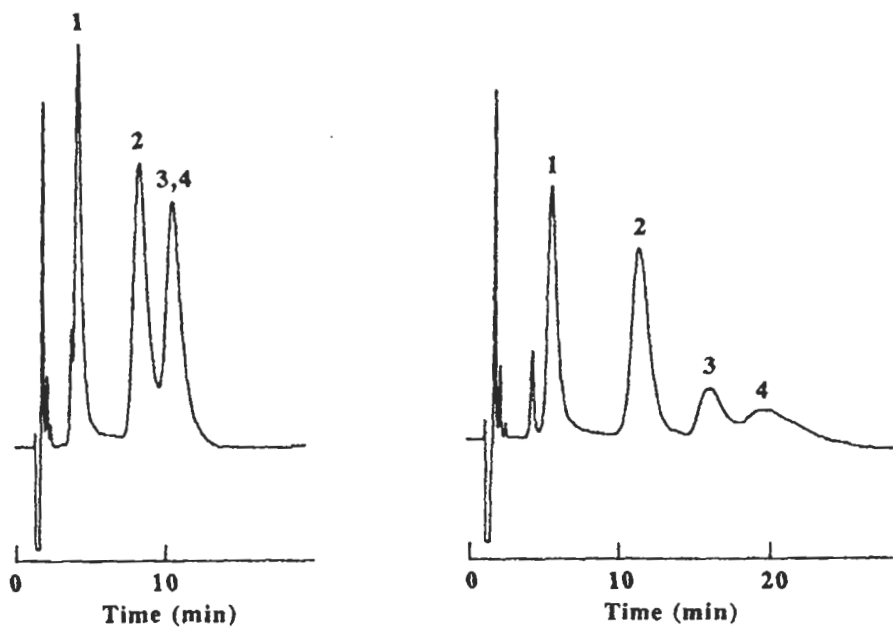


Figure 2-5. Separation of several NSAIDs on both a non-imprinted polymer and a (S)-ibuprofen. Adapted from Reference #134

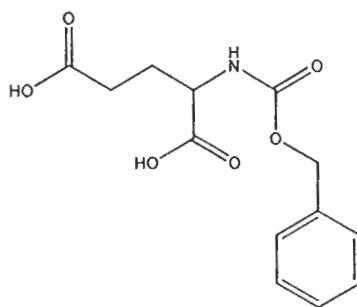


<u>Peak Number</u>	<u>Compound</u>
1	Pranoprofen
2	Ketoprofen
3	(R)-Ibuprofen
4	(S)-Ibuprofen

(pH= 3.2):acetonitrile mix. Clearly, this represents a marked improvement in the area of chiral separations using imprinted polymer stationary phases.

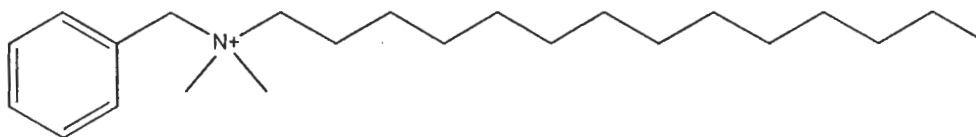
Surface Imprinting

Surface imprinting, developed in the last few years, is a technique that prepares block polymers much like the conventional technique, but rather than being performed in pure organic solvent, the process occurs in a water in oil emulsion.¹³⁷ Figure 2-6 illustrates this process for the preparation of a imprinted polymer for a N-benzyloxycarbonyl-glutamic acid (Z-Glu) (33). As shown in the first part, the Z-Glu will



(33)

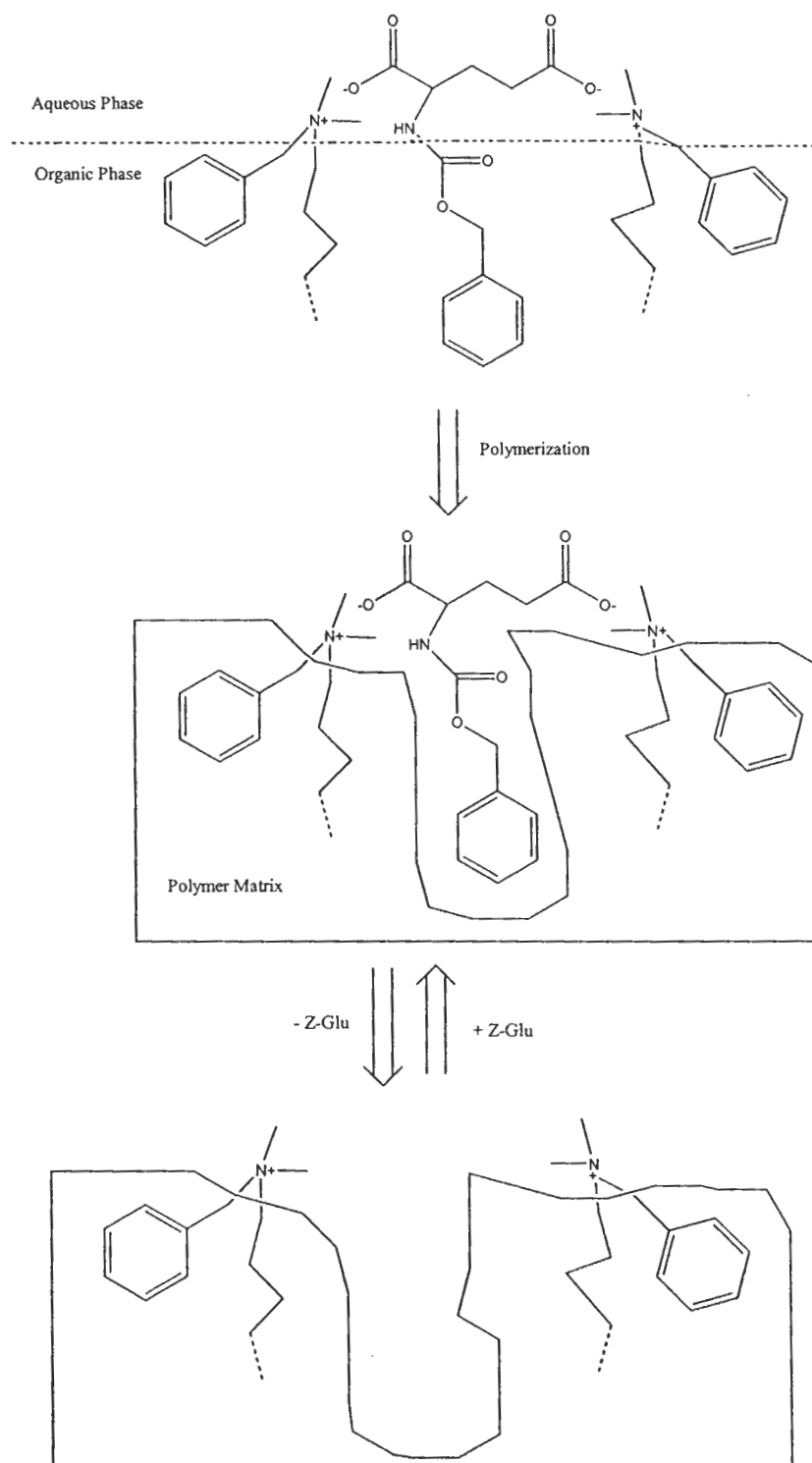
arrange itself such that the charged groups will be stabilized in the basic (pH = 8.9) aqueous phase, while the hydrophobic portion of the molecule will be stabilized in the organic phase.¹³⁷ The functional monomer, in this application a cationic surfactant called Zephiramine (34) or Zeph. (benzyltrimethyl-*n*-tetradecylammonium), must serve three



(34)

key functions. First it must strongly interact with the template, in this case via ionic interactions, to give a stable template-monomer complex. Second it must act as a

Figure 2-6. Synthesis of an imprinted polymer using the surface imprinting technique.
Adapted from Reference #137



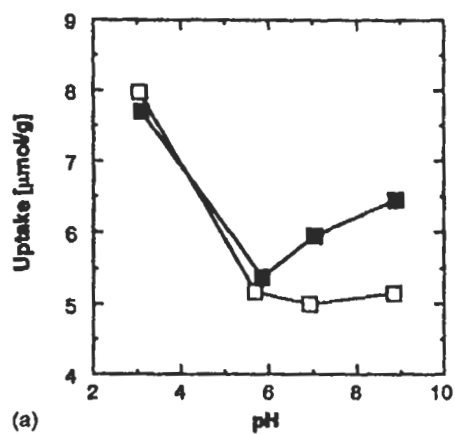
stabilizer in the resulting solid polymer matrix, thus these molecules often possess an aromatic ring system. Lastly, it also must be an efficient emulsion stabilizer that will provide stability at the water-oil interface.¹³⁷ Binding studies, shown in Figure 2-7, show that a selective phase was achieved as both imprinted polymers were able to selectively rebind its corresponding template. Furthermore, analysis of other structurally similar enantiomers revealed that the polymer possessed no cross reactivity as it didn't show any recognition towards other structural analogs.

What is intriguing about this work is that this system is analogous to a biological membrane interface. While not expressed by the authors of this work, we believe that this technique could provide a very efficient method for creating biological mimics that specifically could recreate binding sites on proteins and membranes, and warrant much closer scrutiny.

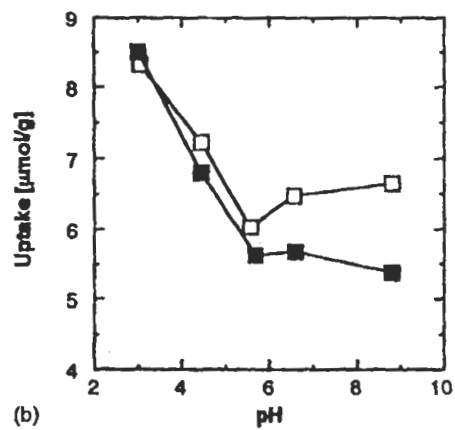
Microgel Spheres

Microgel spheres are created by using a precipitation based polymerization technique. This technique involves performing the polymerization in large amounts of solvent relative to the concentration of the template, crosslinker, and functional monomer.¹³⁸ It was reported that this was advantageous as the resulting polymers were generally obtained in good yields and possessed very uniform particle sizes.¹³⁹ This is caused by the fact that during normal MIP polymerizations, phase separation occurs, where as in this technique, the large volume of solvent prevents this from occurring. Phase separation occurs when the growing crosslinked polymer exceeds the solubility of the poragen and causes the polymer to precipitate.¹³⁸ Figure 2-8 is a

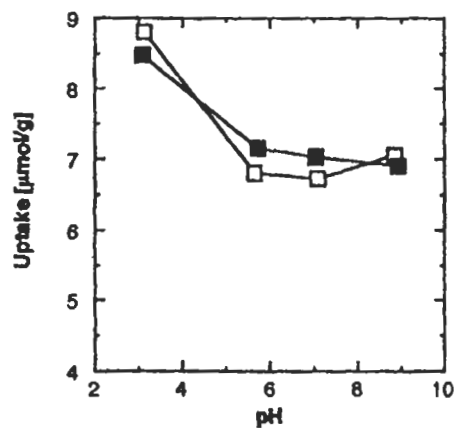
Figure 2-7. Binding studies on a Z-Glutamic acid imprinted polymer prepared by surface imprinting. Adapted from Reference #137
Z-L-Glu (■) Z-D-Glu (□)



(a)

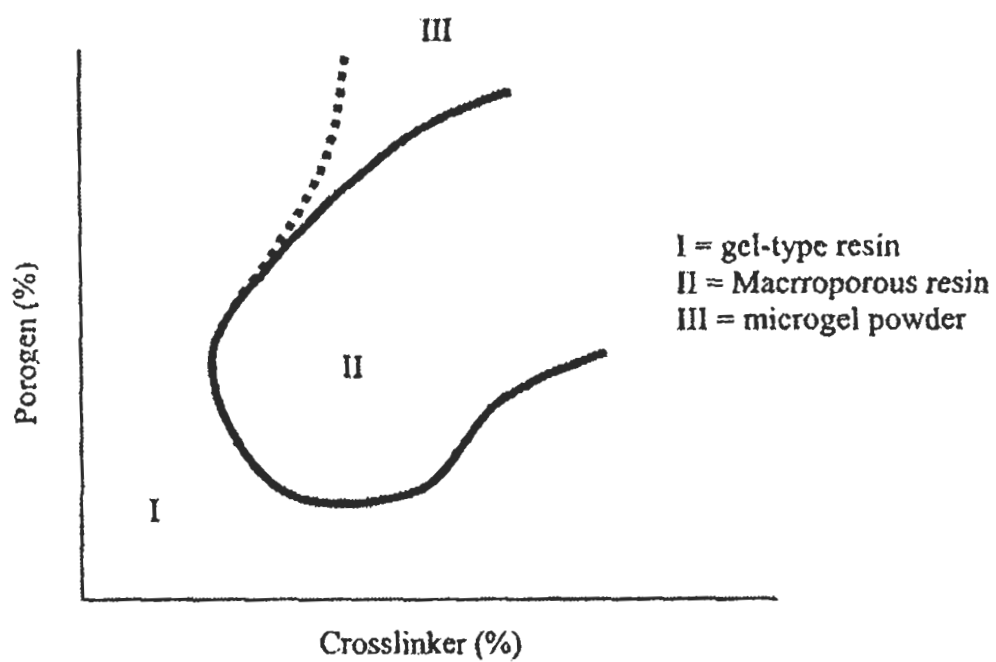


(b)



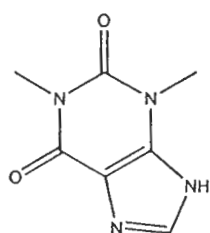
- A. Z-L-Glu Imprinted Polymer
- B. Z-D-Glu Imprinted Polymer
- C. Control Imprinted Polymer

Figure 2-8. General morphology diagram for crosslinked polymers. Adapted from Reference # 140

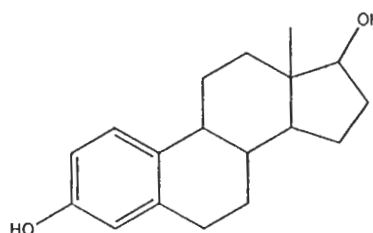


morphology diagram for crosslinked polymers described by D.C. Sherrington.¹⁴⁰

Typically, most imprinting is done with high amounts of crosslinker, often 80% or more, and the overall monomer volume (volume of crosslinker and functional monomer/s) is typically 50% of the total polymerization solution volume.¹³⁸ Thus, on the morphology diagram, this will yield polymers in region II, which yields the traditional solid block copolymer.¹⁴⁰ However, as Ye et. al demonstrated in their preparation of microspheres for theophylline (35) and 17 β -Estradiol (36), by increasing the volume of poragen used, polymers corresponding to region III on the morphology diagram could be synthesized,



(35)



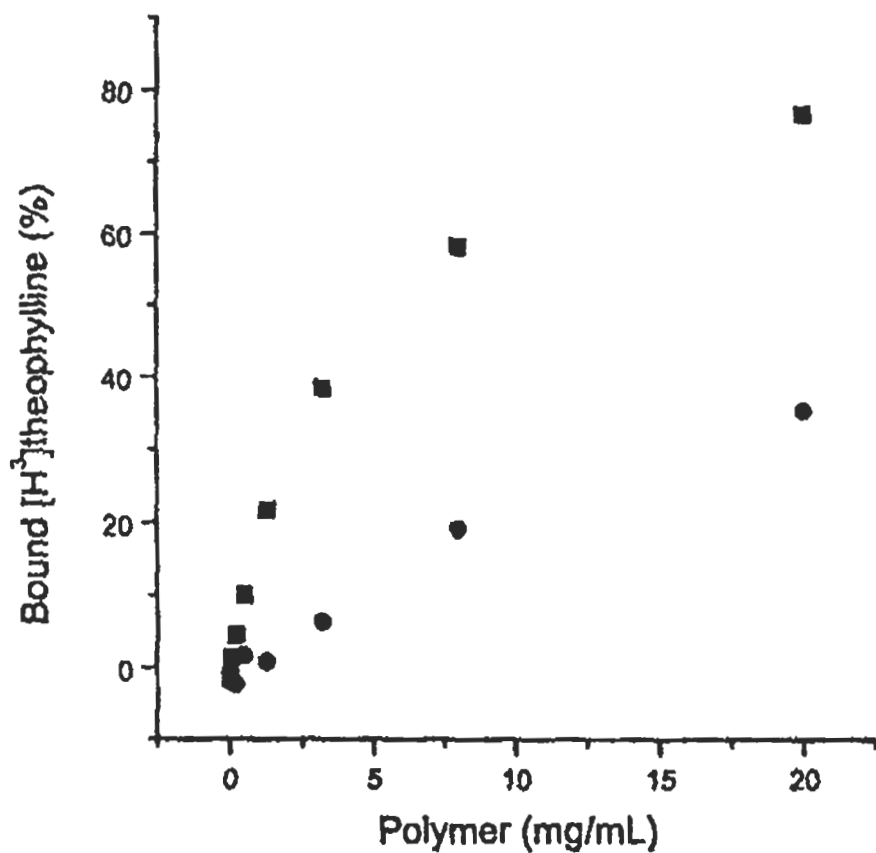
(36)

whose size depended upon how much poragen was added.¹³⁸ Binding experiments, shown in Figure 2-9, demonstrated that the microgel sphere had successfully been imprinted as it bound a greater amount of theophylline than a blank microgel sphere.¹³⁸

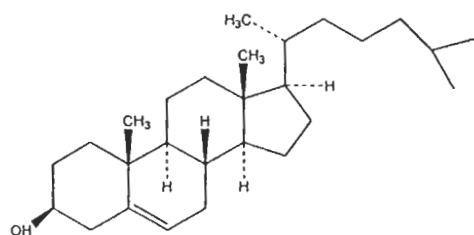
Covalent/Non-Covalent Imprinting

Recently, a hybrid technique, first demonstrated by Whitcombe et. al., has been developed that combines both covalent and non-covalent imprinting processes together.¹⁴¹ This hybrid method, also known as “sacrificial spacer”^{141,142} or “surface imprinting”,¹⁴³ involves covalently attaching a synthetic template mimic to the polymer structure followed by chemical modification after polymerization to yield an incorporated monomer capable of non-covalent interactions with the analyte of interest. Thus this

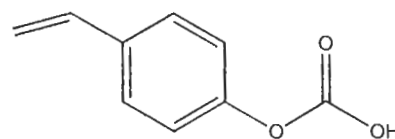
Figure 2-9. Binding studies utilizing a theophylline imprinted microsphere. Adapted from Reference #138
Imprinted Polymer (■) Non-Imprinted Polymer (●)



technique would allow for an imprinting process that incorporated the advantages of both covalent and non-covalent imprinting. Whitcombe et. al. prepared a MIP selective for cholesterol (37) utilizing 4-vinyl phenyl carbonate ester (38) as the functional

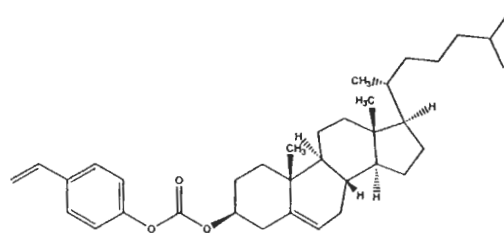


(37)



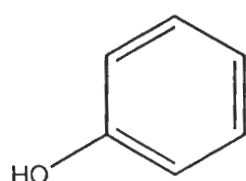
(38)

monomer.¹⁴¹ This was reacted with cholesterol to yield the final monomer-template molecule cholesteryl (4-vinyl)phenyl carbonate (39). Additionally, the monomer was

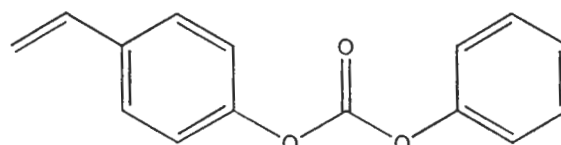


(39)

reacted with phenol (40) to yield phenyl (4-vinyl)phenyl (41) carbonate, to test the effect of the shape recognition of the resulting polymer. Following polymerization, the



(40)



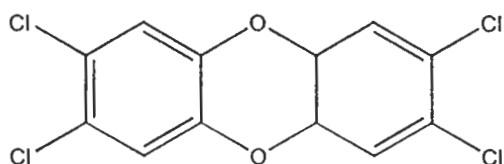
(41)

resulting polymers were then subjected to hydrolysis, which chemically cleaved the cholesterol or phenol from the polymer and generated the non-covalent moiety within the

polymer. This entire process is demonstrated in Figure 2-10, which represents the reaction utilized to generate the imprinted polymer for cholesterol.¹⁴¹

Binding studies, shown in Figure 2-11, demonstrated that the imprinted cholesterol polymer was indeed selective. A comparison between the hydrolyzed polymer (P4H) and the non-hydrolyzed polymer (P4) demonstrates that the hydrolysis process has generated a site of interaction within the polymer. Furthermore, when these results are compared to a blank polymer (P2H), it is shown that the non-hydrolyzed polymer exhibits slightly poorer selectivity indicating that no sites of interactions are present within the polymer. However, further studies revealed that the polymer demonstrated significant recognition for other structurally related compounds as well.

The group of Lübke et. al. extended this approach for their imprinted polymer system selective for 2,3,7,8-tetrachlorodibenzodioxin (TCDD) (**24**), a highly toxic



(**24**)

pesticide.¹⁴² In this work, the template-monomer molecule was created via a complex synthesis whose shape and functional group arrangement, upon chemical modification, would be complimentary to the functional groups and shape of TCDD in the resulting polymer as illustrated in Figure 2-12. Binding studies revealed that there were very small differences between the prepared blank polymers and their respective imprinted polymers, which is suggestive that some selective processes are occurring within the polymer, however, further work is needed to better optimize this process.¹⁴²

Figure 2-10. Synthesis of a cholesterol imprinted polymer using the covalent/non-covalent hybrid technique. Adapted from Reference #141

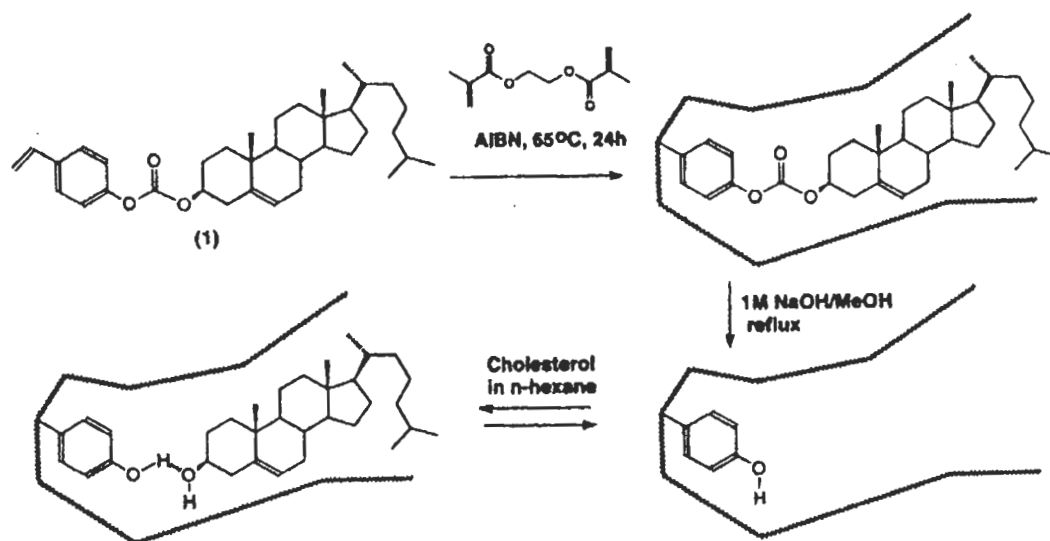


Figure 2-11. Binding study results achieved on a cholesterol imprinted polymer utilizing covalent/non-covalent imprinting. Adapted from Reference #141

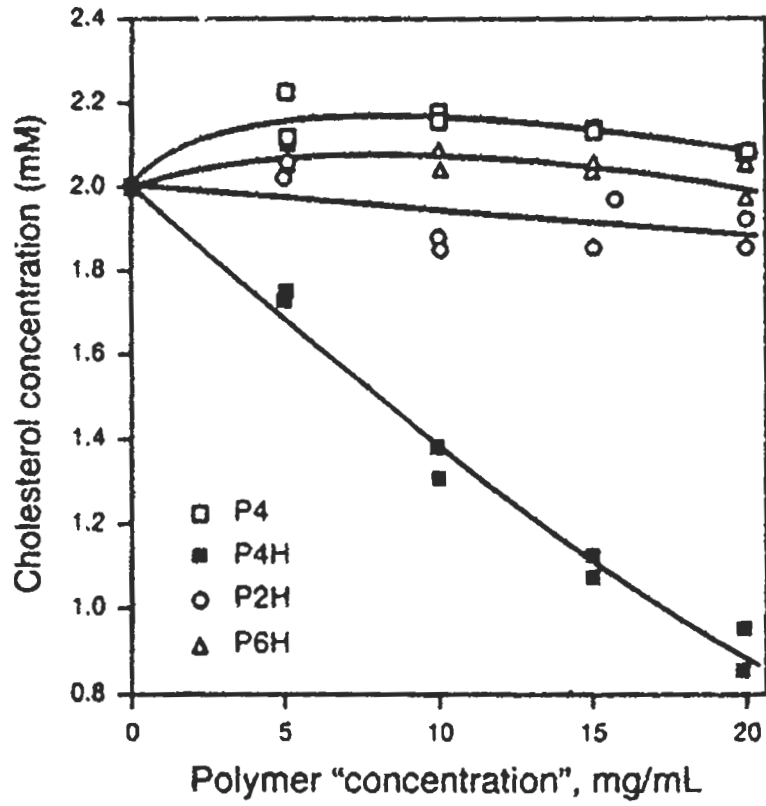
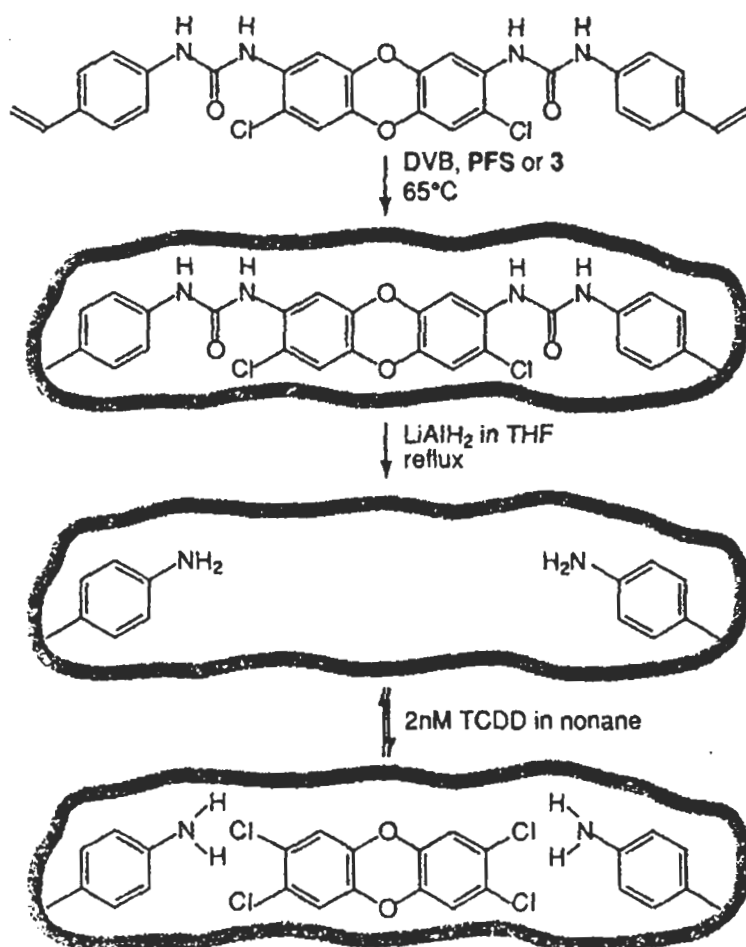


Figure 2-12. Imprinting synthesis utilized to create a polymer with specific recognition for TCDD. Adapted from Reference #142

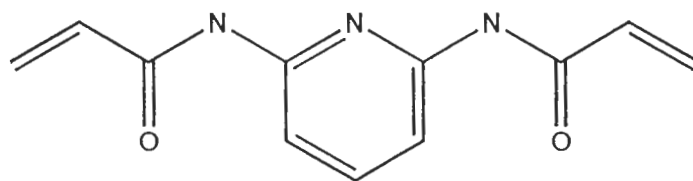


Finally, allyl phenyl disulfide was used to create an imprinted polymer that possessed a thiol group within the binding cavity for the analysis of phenol.¹⁴⁴ The allyl phenyl disulfide was incorporated into the polymer matrix and then cleaved leaving a thiol group within the cavity. A mixture of phenol, thiophenol, aniline, and pyridine was injected onto the resulting polymers and the retention factors calculated, which are shown in Table 2-5.¹⁴⁴ Surprisingly, only phenol demonstrated significant interactions with the imprinted polymer, however, it also demonstrated significant interactions with a polymer prepared with allyl mercaptan. This would indicate that a minimal imprinting effect has been achieved

Novel Monomers

Recently, several new monomers have been utilized in the synthesis of MIP's. While other techniques have employed new types of monomers, such as those used in covalent/non-covalent imprinting, this discussion focuses on novel monomers utilized with traditional imprinting procedures.

In one application, the molecule 2,6-bis(acrylamido)pyridine (BAP) (43) was



(43)

used as a functional monomer to prepare imprinted polymers for alloxan and cyclobarbital.¹⁴⁵ It was rationalized that since biological molecules interact with multiple

Table 2-5. Retention factors of several small molecule compounds. Adapted from Reference #144

Analyte	Imprinted	Reference	Blank
Phenol	5.64	4.20	1.80
Thiophenol	0.84	0.76	0.89
Aniline	0.84	0.97	1.63
Pyridine	1.01	1.14	1.59

Imprinted Polymer: Prepared with allyl phenyl disulfide

Reference Polymer: Prepared with allyl mercaptan

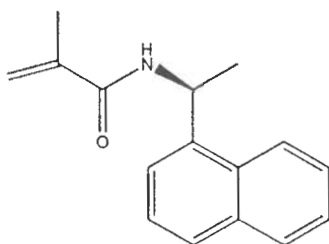
Blank Polymer: Prepared with no template

binding sites, such as the complementary base pairing exhibited by deoxyribose nucleic acids, that an imprinted polymer prepared with monomer that could form multiple interactions with the template would be a better biological mimic than other traditional monomers.¹⁴⁵ The results, shown in Table 2-6, reveal that the monomer interacts better than MAA for molecules containing imide functional groups. This is demonstrated by the difference in capacity factors for alloxan, thymine, theobromine, and uracil. Other molecules such as cytosine and adenine, demonstrate significantly better recognition on the traditional MAA polymer. Overall, the results suggest that multi hydrogen bonding monomers have the potential to be viable materials for the creation of artificial receptors. Given the difficulties in trying to place functional groups in proper spatial alignment, these monomers can readily mimic biological systems and still be used in easy polymerization techniques. This would allow for significant reduction in the amount of time expended for current design and synthesis processes.

Also of interest is the use of a chiral functional monomer in the imprinting process.¹⁴⁶ One of the disadvantages to molecular imprinting is that several grams of a pure enantiomer are necessary in order to synthesize sufficient quantities of polymer needed for various studies.¹⁴⁶ Potentially, the cost of obtaining the necessary amounts of material needed could be very high. However, if a selective polymer could be prepared using a chiral monomer, which was synthesized from commonly available chemicals, then a racemic mixture could be utilized as the template, keeping the cost of synthesis low. This study utilized (S)-(-)-N-methacryloyl-1-naphthylethylamine (**44**) as the

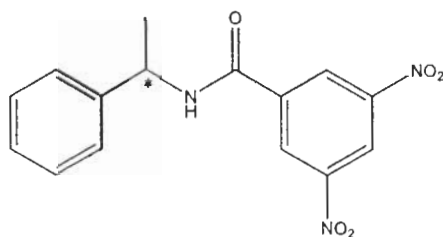
Table 2-6. Retention factors for several analytes on alloxan imprinted polymers prepared with BAP and MAA as a functional monomer. Adapted from Reference #145

Analyte	Capacity Factor	
	BAP Monomer	MAA Monomer
Adenine	0.26	0.93
Guanine	0.01	0.01
Cytosine	0.14	4.05
Thymine	4.84	0.21
Uracil	7.55	0.80
Theophylline	0.01	0.03
Theobromine	1.73	0.20
Alloxan	2.24	1.89
6-amino-1-methyluracil	13.8	1.20



(44)

functional monomer to prepare an imprinted polymer for the separation of N-(3,5-Dinitrobenzoyl)- α -methylbenzylamine (DNB) (45).¹⁴⁶

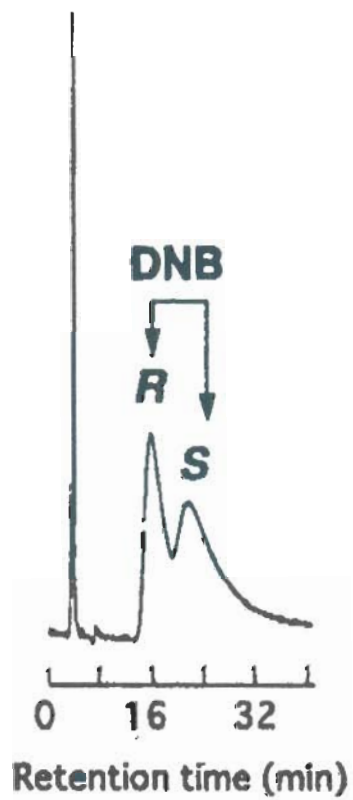


(45)

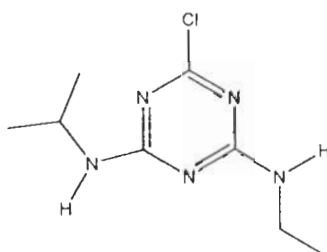
Figure 2-13 shows a chromatogram for the separation of the racemic DNB using the chiral monomer. While, the selectivity is not very high, the polymer does demonstrate some enantioselectivity towards the racemic DNB mixture. However, it was not surprising that imprinting with one of the DNB enantiomers gave better enantioselectivity than the polymer prepared with a racemic mixture. This can be attributed to the fact that the binding sites present on the polymer will be configured for only one enantiomer of DNB resulting in a more homogeneous surface compared to using racemic DNB, which will have binding sites configured for both enantiomers.

A third study performed by Matsui et. al, focused on solving the problem of embedded template molecules that slowly elute over time, commonly called template

Figure 2-13. Separation of racemic DNB on an imprinted polymer using a chiral monomer. Adapted from Reference #146

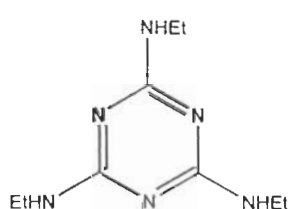


leakage, which often occurs in MIP-SPE applications, reducing sensitivity.¹⁴⁷ To do this, a 'dummy template', defined as a template that mimics the shape and functionality of the desired target analyte, was used to prepare an imprinted polymer selective for atrazine (46), a pesticide.

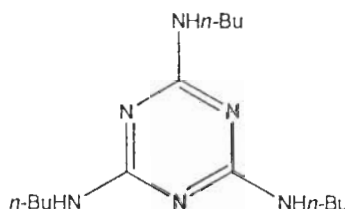


(46)

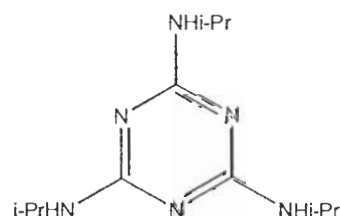
Three trialkylmelamines, Triethylmelamine (TEM) (47), tributylmelamine (TBM) (48), and triisopropylmelamine (TPM) (49), were used as possible dummy templates.



(47)



(48)



(49)

A series of polymers were prepared using the three trialkylmelamines as templates, including a blank polymer prepared with no template. Table 2-7 shows the retention factors calculated for several different triazine herbicides.

Based on these results, it is apparent that atrazine and simazine are significantly retained as demonstrated by the large retention factors. In addition, all polymers displayed moderate recognition for several other herbicides as almost all of the herbicides tested exhibited a significant retention factor, with TEM showing the greatest selectivity

Table 2-7. Retention factors obtained on several triazine herbicides imprinted polymers.
Adapted from Reference #147

Analyte	Polymer			
	P(TEM)	P(TBM)	P(TPM)	P(blank)
Atrazine	10.4	8.2	6.3	0.66
Simazine	11.5	8.8	6.4	0.75
Propazine	9.0	7.3	8.6	0.61
Cyanazine	6.7	5.3	5.3	0.62
Ametryn	9.9	6.6	9.0	0.88
Prometryn	6.9	5.2	7.5	0.77
Tertbutylazine	8.4	7.4	6.9	0.39
Tertbutryn	5.2	3.8	3.9	0.50
1,3,5-triazine	0.29	0.10	0.11	0.08

of the three dummy templates.

Monomer/Template Ratio

In recent years, increasing attention has focused on the effects of changing the monomer-template ratio. A current criticism of MIPs is that large amounts of template are often needed, particularly if the intended application is chromatography.¹⁴⁸ Several studies have attempted to address this concern. Yilmaz et. al. investigated a theophylline selective polymer prepared with M/T ratios ranging from 4:1 through 5000:1.¹⁴⁸ Figure 2-14 is a binding data obtained for these polymers. Interestingly, a polymer prepared with a 5000:1 ratio of monomer to template demonstrated some selective interactions compared to the control polymer. Also of interest is the fact that a 12:1 polymer demonstrated the greatest binding capacity, which is surprising given the fact that theophylline possesses four sites of possible interactions, it is unlikely that up to three equivalents of monomer would bind at each one possible site.

The authors, in explaining their results, proposed that the excess monomer present in solution, forced the equilibrium towards a complete multi-molecular complex formation, which would reduce the overall number of binding sites present, a greater of them would be high energy.¹⁴⁸ Indeed, when the authors calculated the apparent number of high energy sites, shown in Table 2-8, they found that the 12:1 has roughly double the number of high affinity sites than that of the 4:1 polymer.¹⁴⁸ However, it should be noted that addition of 100 equivalents of monomer generated worse performance than that of the 4:1 suggesting that there is practical limit as to the amount of monomer that can be used.

Figure 2-14. Binding data obtained for several different theophylline imprinted polymers. Adapted from Reference #148

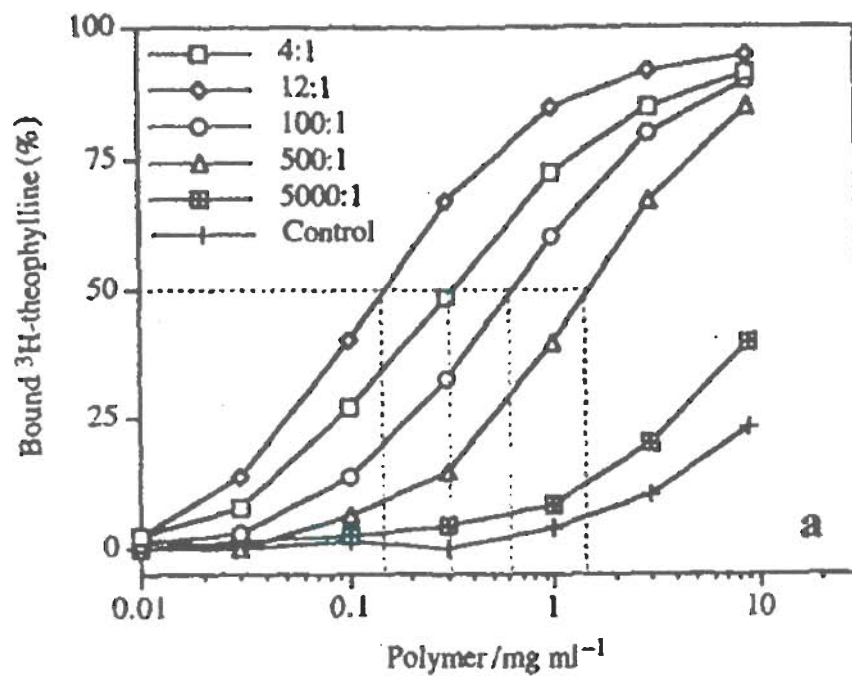


Table 2-8. Apparent dissociation constants (K_{Dapp}) and high affinity binding sites (Q_{Mapp}) for several different nicotine imprinted polymers. Adapted from Reference # 148

Ratio	K_{Dapp} (nM)	Q_{Mapp} (nmol/g)	Relative Yield (%)
4:1	10.0 ± 0.5	122.8 ± 0.8	0.007
12:1	9.4 ± 0.7	40.9 ± 2.2	0.039
100:1	8.1 ± 0.9	8.2 ± 0.6	0.063
500:1	14.7 ± 2.4	2.9 ± 0.4	0.120

Another intriguing study, examined the relationship between M/T ratios and chromatographic variables such as selectivity and sample loads.¹⁴⁹ Figure 2-15 shows the selectivity obtained on several polymers of varying monomer concentrations. In this study, the polymer containing the highest amount of monomer yielded the best overall selectivity.¹⁴⁹ This is plausible as nicotine possesses two interactive functional groups, therefore the addition of a slight excess of monomer would be expected to force the formation of the complex to completion. Another surprising effect was that polymer selectivity increased and then leveled off with increasing sample load for all polymer systems investigated as shown in Figure 2-16. The authors hypothesized that this may be caused by the existence of recognition sites specific for template-template complexes, which had formed in the pre-polymerization solution and were incorporated into the solid polymer.¹⁴⁹ This is in contradiction to other published results, which showed that polymer selectivity decreased as increasing sample loads were used.^{118,148,150}

Other studies have suggested that excessive monomer in the pre-polymerization solution does not result in increased chromatographic selectivity.^{128,151-153} Instead, several different studies in which the functional monomer, template, and poragen were different, demonstrated that there is an optimum ratio of monomer to template that will yield maximum enantioselectivity and that additional monomer beyond this optimum amount results in a decrease in the polymer's enantioselective ability. Yano et. al. reported that for their system employing a L-valine derivative as a functional monomer, maximum chromatographic selectivity was observed at a 2:1 M/T ratio and that additional increases resulted in decreasing chromatographic selectivity.¹⁵¹ Similarly, Zhou et.al. in their work

Figure 2-15. Chromatographic selectivity of several different nicotine imprinted polymers. Adapted from Reference #149

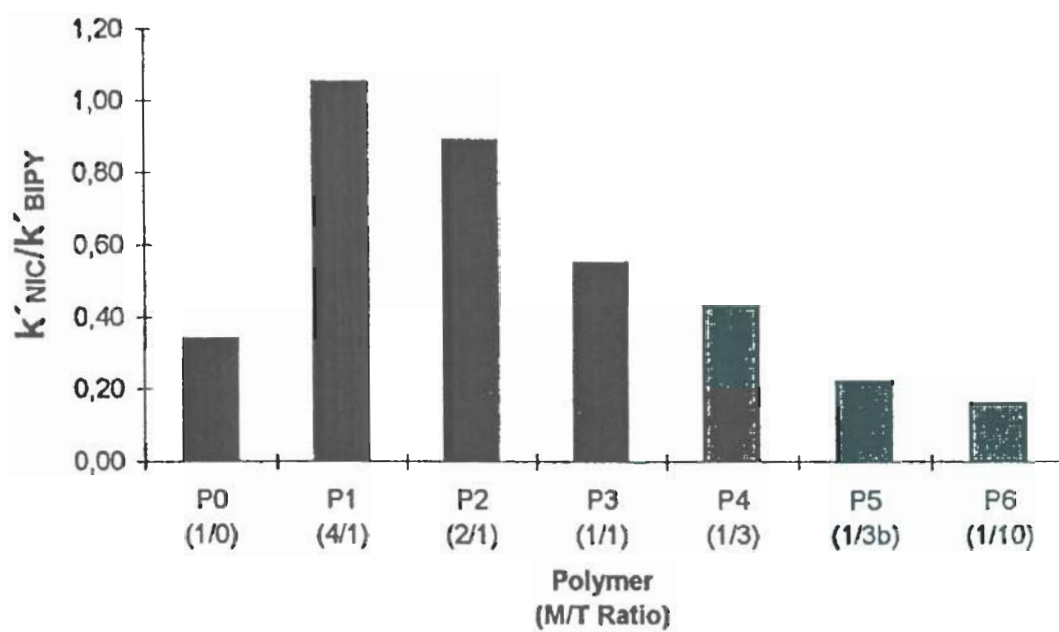
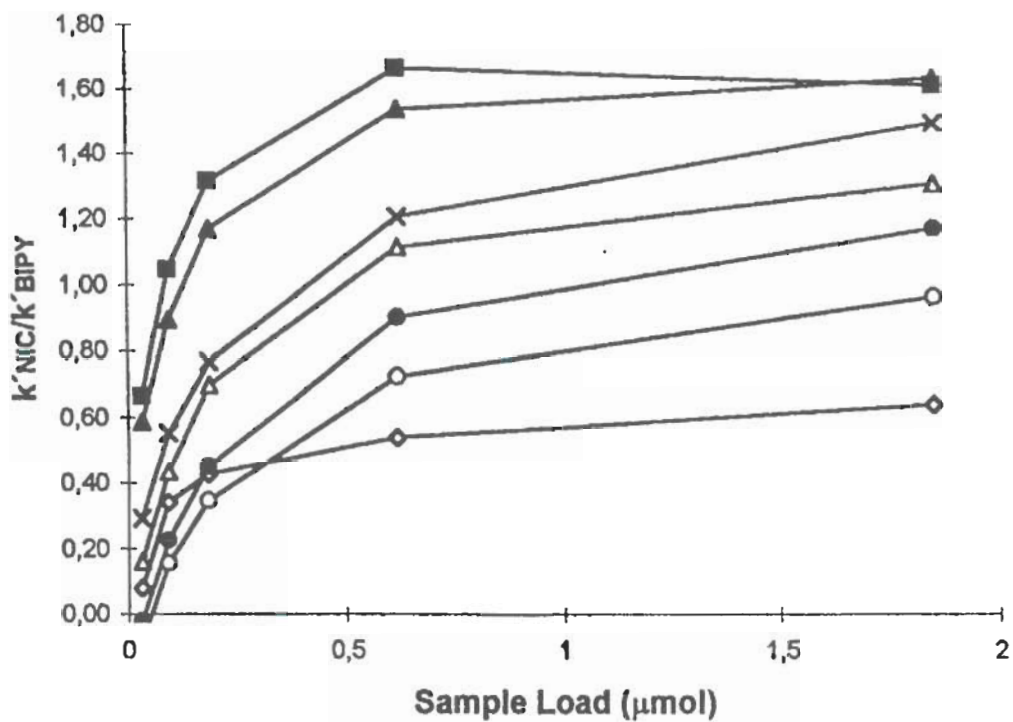


Figure 2-16. Effect of sample load on a nicotine imprinted polymer chromatographic selectivity. Adapted from Reference #149

1/0 M/T (\diamond) 4/1 M/T (\blacksquare) 2/1 M/T (\blacktriangle) 1/1 M/T (\times) 1/3 M/T (\triangle) 1/3b M/T (\bullet) 1/10 M/T (\circ)



describing the use of acrylamide as a functional monomer, reported that a 4:1 ratio yielded greater selective adsorption than compared to a 2:1 and a 8:1 polymer.¹²⁸ Finally, O'Brien et. al. reported that during the development of a MAA-Indinavir system, a 7:1 ratio gave maximum chromatographic selectivity.¹⁵³ Furthermore, an examination of the retention factors demonstrated that the excess monomer was being incorporated into the polymer as non-selective sites of interaction. Thus, while overall polymer selectivity didn't change, the resulting chromatograms for a higher M/T ratio polymer exhibited poorer peak shapes as well as increased analysis time.

Based on the above results, we felt that this particular aspect represented a significant obstacle in the design and implementation of imprinted polymers. Specifically, failure to properly understand the formation and stability of the multi-molecular complex will prevent accurate conclusions and observations between any two imprinted polymer systems. Therefore we believe that in order for valid conclusion to be drawn about the effects of changing monomer/template ratios further studies are warranted. In order to address this, a two part study was performed. The first part utilized different analysis methods, both spectroscopic and non-spectroscopic, not only to empirically determine the optimal monomer-template ratio necessary to obtain maximum polymer selectivity, but also to understand the formation mechanism of the monomer-template complex. Furthermore, these results will be compared to the selectivity of different polymers prepared with varying amounts of monomer. The second part of this work sought to examine the effects of changing monomer-template ratios on performance as an adsorbent for solid-phase extraction. Specifically, we sought to investigate the relationship between the ability of the polymer to form selective interactions and the flow

rate at which the extraction was occurring. This was investigated by performing several different characterizations studies on basic SPE parameters. It was believed that these studies would help provide significant understanding as to the underlying chemical phenomena that govern SPE performance. Overall, it is our belief that the above studies will not only provide a more complete understanding of the conditions necessary to generate a successful imprint but will also lead to more efficient design and synthesis processes for MIP materials.

Chapter 3. Rational Design of an Imprinted Polymer Selective for Cinchonidine

Introduction

The formation of the monomer-template complex prior to polymerization is governed by multiple equilibria. Since the majority of templates (T) possess multiple sites of interaction, each additional equivalent of monomer (M) will result in the formation of new higher ordered multi-molecular complexes in equilibrium with the previous multi-molecular complex, thus the potential for multiple complexes to exist prior to polymerization is possible. Consider a theoretical system in which a template (T) possesses two sites of interaction for MAA (M).¹⁵⁴



If the formation of the two hydrogen bonds is considered to be independent of each other as well as identical in strength, then their respective equilibrium constants can be considered to be identical.¹⁵⁴

$$K_1 = [TM]/[T][M] \quad [3-3]$$

$$K_2 = [MTM]/[TM][M] \quad [3-4]$$

$$[MTM] = K_1 K_2 [T][M]^2 \quad [3-5]$$

Thus at conditions with excess monomer present, the pre-polymerization solution should contain the excess monomer and the highest ordered multi-molecular complex.

Conversely, if the system does not contain enough monomer, then the resulting polymer will contain significant amounts of the lower ordered multi-molecular complex. This will increase the surface heterogeneity as a larger percentage of sites will be non- or slightly selective in nature.¹⁵⁴ In practice, the formation of the hydrogen bonds between monomer

and template are neither independent of each other, nor are they of the same strength. Thus, the overall process to form a complete and stable multi-molecular complex, while dependant primarily upon the overall monomer concentration, must account for the strength of the hydrogen bonds created as well as the influence of each hydrogen bond on the formation on the other hydrogen bonds (binding site independence).

As discussed earlier, this monomer-template ratio directly impacts the resulting polymer performance. The failure to add enough monomer results in an increase in surface heterogeneity, while too much monomer may lead to a decrease in chromatographic selectivity.¹⁵³ Therefore, it is necessary prior to polymerization to ascertain both the relative strengths of the hydrogen bonds present and their effect on other hydrogen bond formation, in addition to determining the optimal amount of monomer needed to ensure a fully formed complex. Surprisingly, given the importance of this parameter, very little work has been done to develop methodology that allows for the characterization and optimization of the monomer-template complex. Rather, the majority of work performed focused on synthesizing multiple polymers, each containing different amounts of monomer and evaluating their selectivity to find the optimal monomer concentration, a very time consuming process.

All of the published work performed on the optimization of the monomer-template complex has employed a spectroscopic technique as the method of analysis. ¹H NMR has been used successfully to study multi-molecular complexes as well as to assess the imprinting potential of different functional monomers. Sellergren et. al. used ¹H NMR to study a phenylalanine anilide (PheNHPh)-methacrylic acid system.¹⁵⁵ The authors observed that the line widths would broaden significantly as more MAA was

added, ultimately reaching a maximum value before decreasing. As illustrated in the top portion of Figure 3-1, three distinctive maxima are observed for both the cis and methyl protons of MAA. The valleys between each maxima represent the formation of a separate multi-molecular complexes. In the bottom portion of Figure 3-1, the exchangeable protons of PheNHPH demonstrate the formation of three multi-molecular complexes, while the amide proton spectra do not show the formation of any multi-molecular spectra. Based on these results, it was determined that the highest ordered complex would be formed upon the addition of three molar equivalents of MAA.¹⁵⁵ When the selectivity was calculated chromatographically for polymers prepared with increasing MAA equivalents, it was found that the NMR data did not correlate to polymer selectivity beyond the addition of one MAA equivalent.¹⁵⁵ In a second study performed by Spivak et. al., ¹H NMR was used to assess if a functional monomer, possessing a carboxylic acid, would interact strongly with 9-ethyladenine.¹²¹ The compound 9-ethyladenine was titrated with butyric acid and an association constant was determined. This allowed the authors to determine that Methacrylic acid would be a good choice as a functional monomer in creating an imprinted polymer specific for 9-ethyladenine.¹²¹

Ultraviolet-visible spectroscopy has also been utilized for several systems. Andersson and Nicholls measured the absorbance shift of several templates in the presence of increasing amount of monomer.¹⁵⁶ In Figure 3-2, a clear bathochromic shift is observed between 240 and 256 nm upon saturation with monomer. This shift is the result of the hydrogen bonded monomers surrounding the template, effectively increasing its solvation and lowering the $\pi \rightarrow \pi^*$ transition energy.¹⁵⁷ By monitoring the magnitude

Figure 3-1. Effect of increasing monomer concentration on ^1H NMR line width.
 a). Line widths of cis (\square) and methyl (\blacksquare) protons of MAA.
 b). Line widths of exchangeable (\bullet) and amide (\times) protons of PheNHPh.
 (Adapted from Reference #155)

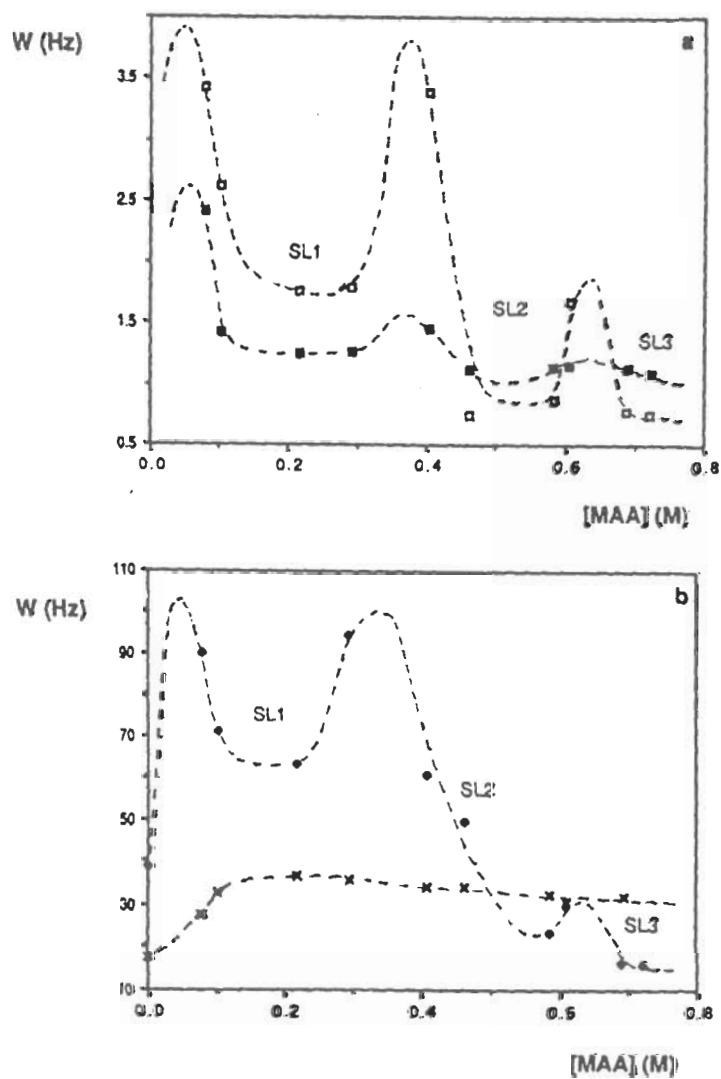
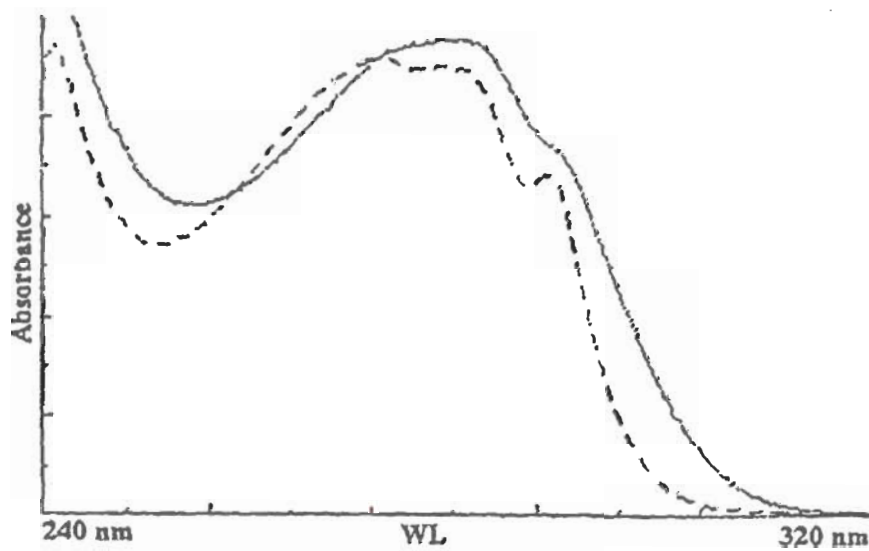


Figure 3-2. Effect of increasing monomer concentration on the ultraviolet-visible spectra of a dipeptide. Adapted from Reference #156

----- prior to addition of monomer
——— after addition of monomer.



of this shift, the authors were able to generate a saturation curve for each template from which a binding model was derived. This model allowed them to predict the optimal concentration of monomer needed to ensure complete complex formation. However, it was noted that for some templates, the peak spectra overlapped with MAA, obscuring any shifts in wavelength.¹⁵⁶ Recently, Mullet et. al. were able to confirm the presence of a 2-aminopyridine-MAA complex.¹⁵⁸ By calculating the change in absorbance upon addition of monomer, a scatchard plot was created and used to calculate an overall binding constant. While they observed some correlation between the calculated binding constant and experimentally determined binding constant for the 2-aminopyridine system, attempts to utilize the procedure for structurally similar compounds failed due to spectral overlap of MAA and template bands.¹⁵⁸

Infrared spectroscopy has also been used to understand the formation of monomer-template complex. Duffy et. al. studied a dodecyl thiamine template-diacrylamino pyridine monomer system.¹⁵⁹ IR spectra were obtained for solutions containing just monomer and template and then for a solution containing both compounds. A comparison of the three spectra revealed two IR bands not present in either the monomer or template solutions, but only appearing in the mixture solution. Consequently, these bands were interpreted as evidence of hydrogen bonding occurring between the monomer and template. Based on this observation, a binding constant was calculated by monitoring the intensity of these bands as the concentration of monomer was increased.¹⁵⁹ In another study, Katz et. al also studied a phenylalanine anilide-methacrylic acid system by ¹H NMR and FTIR.¹⁶⁰ This was accomplished by examining the shifts occurring in the characteristic stretches for the various functional groups. In

contrast to the work reported by Spivak et. al., the authors concluded that only a 1:1 molecular complex was formed, based on the fact that no more observable shifts in the IR spectrum occurred with the addition of additional monomer.¹⁶⁰

Recently, IR spectroscopy was utilized to optimize an imprinted polymer for Indinavir, shown in Fig. 3-3, an HIV protease inhibitor.¹⁵³ By determining the free amount of MAA in solution at various ratios, the authors were able to construct a Scatchard plot that allowed for the determination of the optimal amount of MAA needed to generate maximum selectivity. This predicted ratio correlated well with the order of selectivity for polymers prepared using various monomer-template ratios.¹⁵³

These results are significant compared to the above studies for several reasons. The previous studies discussed above were done utilizing fairly simple templates with one or two chiral centers, contrasted to Indinavir, which possess five chiral centers and a variety of functional groups. The presence of multiple functional groups increases the complexity of the imprinting process as it is possible that some functional groups will not interact with a given monomer. An examination of the Scatchard plot, Figure 3-4, yields significant qualitative information about the strength and independence of the hydrogen bonds. The authors observed that there was one very strong interaction between the template and monomer, with the other interactions being very weak in nature. This is supportive of the proposed enantioselective mechanism in which a strong leading interaction occurs between the template and polymer binding sites followed by the formation of weaker stabilizing interactions. Additionally, the authors noted that each successive addition of monomer resulted in a decreased ability of MAA to interact with

Figure 3-3. Structure of Indinavir. Adapted from Reference #153
Numbers denote chiral centers.

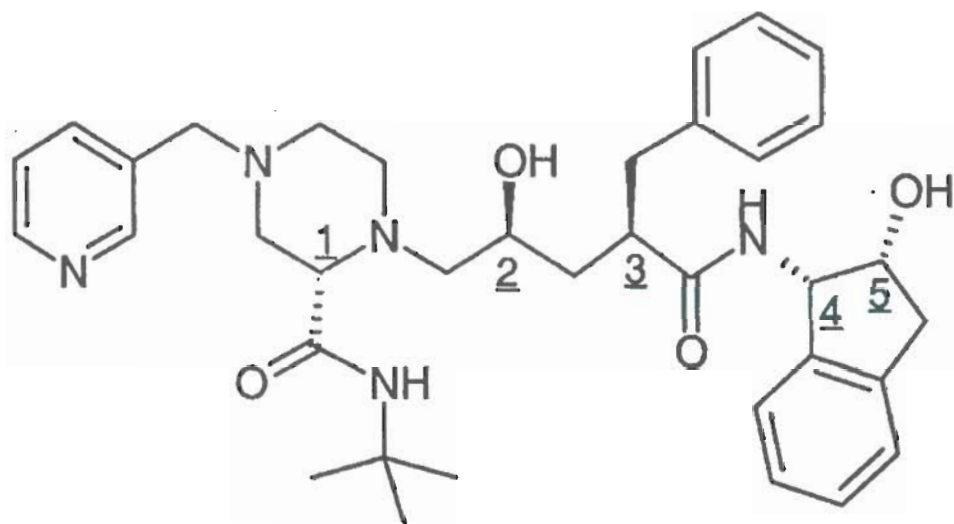
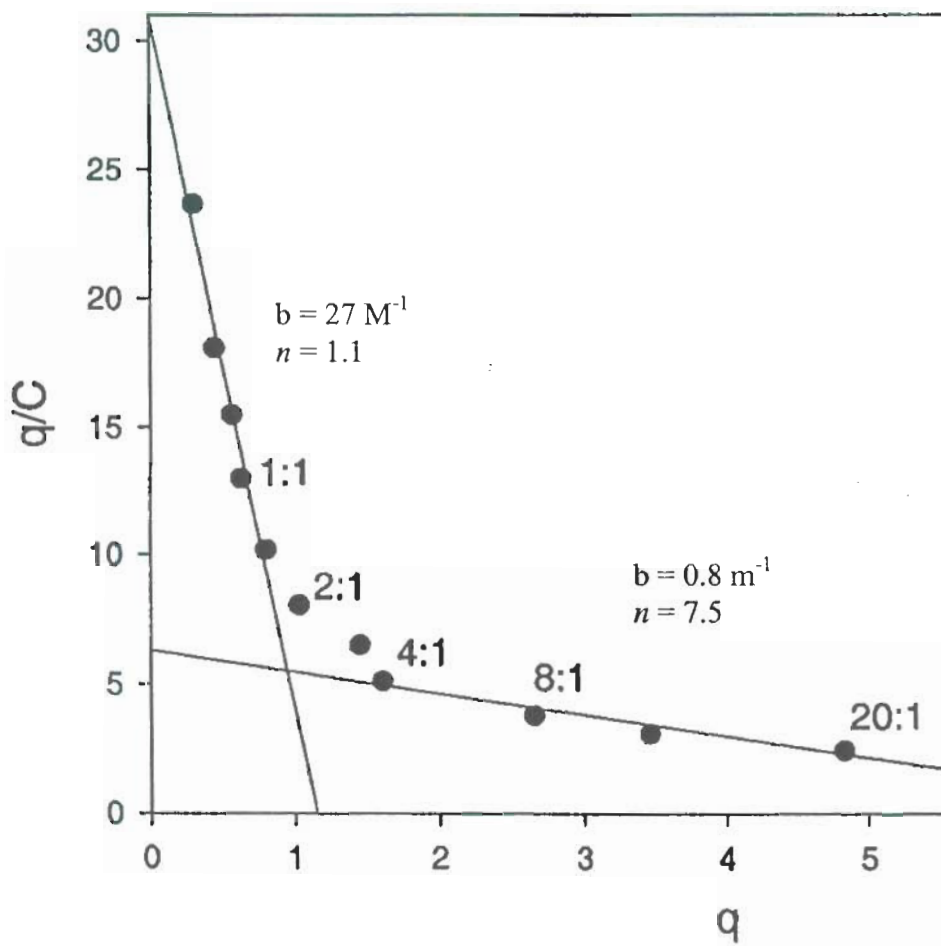


Figure 3-4. Scatchard plot for an Indinavir-MAA system. Adapted from Reference #153.



the template, indicative of negative cooperativity. Lastly, this study was the first to directly correlate polymer selectivity to a predicted concentration of monomer present prior to polymerization. The authors, upon further examination, divided the scatchard plot into two linear portions, representing the regions of strong and weak interactions.¹⁵³ By fitting a trend line through the weak portion of the plot, the number of binding sites on Indinavir was calculated to be 7, which the authors expressed as the optimal ratio of MAA needed to achieve a successful imprint.¹⁵³ Finally, the authors prepared several polymers with different monomer-template ratios, shown in Table 3-1, and evaluated their selectivity by HPLC. The results clearly illustrate the effect of monomer concentration on polymer performance. A comparison between the 2:1 and 7:1 polymer reveals a large jump in the retention factor for Indinavir compared to a minimal increase for its enantiomer. This gain in retention factor reflects the increase in the number of specific sites formed within the polymer matrix caused by the formation of a complete monomer-template complex. Conversely, the addition of excessive monomer did not yield any chromatographic advantage. While Indinavir and its enantiomer both exhibited increases in capacity factor on a 21:1 M/T polymer as compared to the 7:1 polymer, the overall polymer selectivity did not change.¹⁵³

Overall, the above method represents a significant improvement in the design and synthesis process of imprinted polymers. However, there are two concerns that this method poses. One, since this technique is spectroscopy based, the possibility of spectral overlap between the MAA stretches and that of a different template are a very real possibility. Additionally, instrument sensitivity is an issue as well. As stated before, the authors noted that the technique was not sensitive enough to observe very weak

Table 3-1. Selectivity of an Indinavir imprinted polymers prepared with different amounts of MAA. Adapted from Reference #153

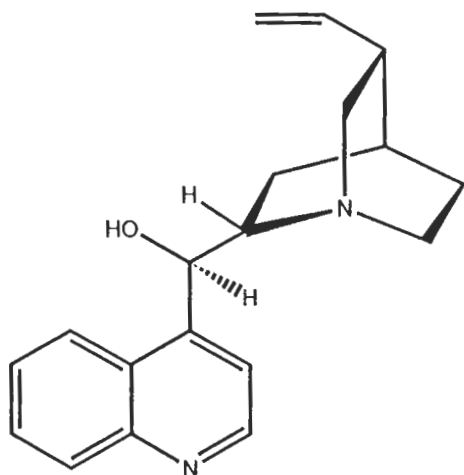
MAA Polymer	1:1 ^a	2:1 ^a	2:1 ^b	7:1 ^b	7:1 ^c	21:1 ^c
$k'_{\text{enantiomer}}$	0.21	3.4	0.4	0.97	0.39	1.9
$k'_{\text{Indinavir}}$	0.71	10.7	0.7	14.4	3.3	15.4
α	3.4	3.1	1.8	14.8	8.5	8.1

- a). Mobile Phase Composition: 1% Acetic Acid in Chloroform
b). Mobile Phase Composition: 2% Acetic Acid in Chloroform
c). Mobile Phase Composition: 3% Acetic Acid in Chloroform

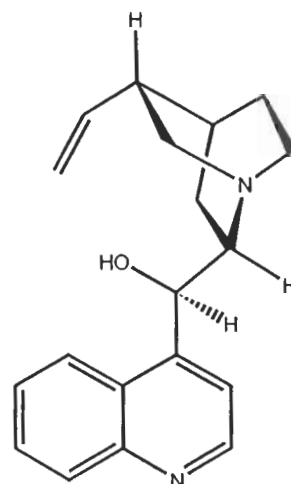
interactions,¹⁵³ however, in situations of very strong hydrogen bonding, where a majority of the monomer is interacting with the template, the possibility of undetectable levels of monomer in solution is very likely. The second concern is that this method has been only evaluated on one MIP system. It is unclear if this technique would allow for the characterization and most importantly, the optimization of the monomer-template complex for other polymer systems.

The goal of this research was to examine this technique on a different system and compare the predicted results with the results determined chromatographically. The system chosen for this experiment utilizes cinchonidine as the template. Cinchonidine is member of the *cinchona* alkaloid family, several of which are shown in Figure 3-5. They are found in the bark of a tree in South America, and are commonly used in the treatment of malaria. A prior published method reported that a cinchonidine based imprinted polymer demonstrated a selectivity of 31 versus its diastereomer, shown in Table 3-2, as well as significant selectivity with other closely related alkaloids.²⁰ Thus any changes in the system should result in observable changes in selectivity. These compounds are highly soluble in organic solvents,¹⁶¹ an advantage as the effects of organic solvents on imprinted polymers is well documented. It is believed that this system will provide an excellent case for evaluating this method.

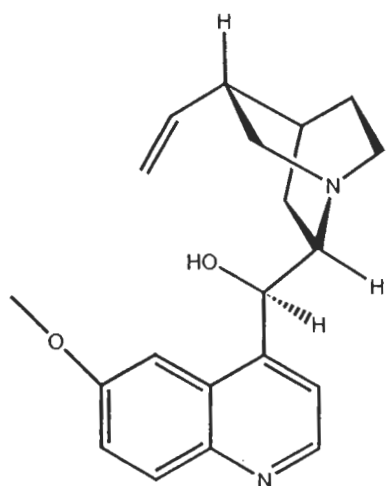
Figure 3-5. Structures of several *cinchona* alkaloids.



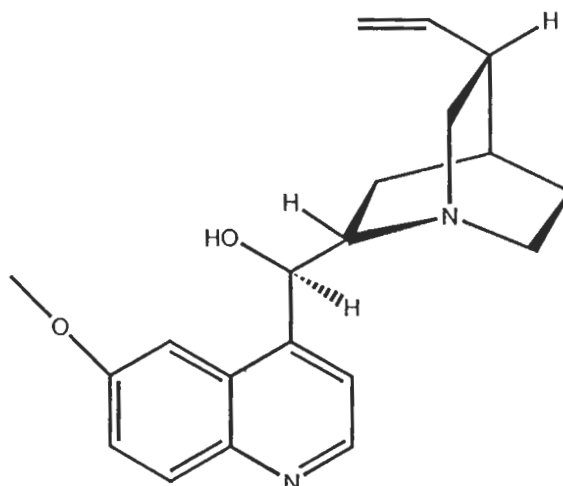
(-) Cinchonidine



(+) Cinchonine



Quinine



Quinidine

Table 3-2. Reported retention factors for various *cinchona* alkaloids on three different alkaloid imprinted polymers. Adapted from Reference #20

Column	(-) cinchonidine		(+) cinchonine		Non-imprinted	
Analyte	k'	α	k'	α	k'	α
(-)cinchonidine	34.24		1.46		0.29	
		31.70		23.05		1.17
(+) cinchonine	1.08		33.65		0.34	
quinine	5.35		0.97		0.34	
		3.45		4.85		2.0
quinidine	1.55		4.70		0.17	
quinoline	0.19	-	0.15	-	0.08	-

Experimental

Reagents

Methacrylic acid (MAA), ethylene glycol dimethacrylate (EGDMA), 4-vinyl pyridine (4-VP), methyl methacrylate (MMA), and 2,2'-azobisisobutyronitrile (AIBN) were obtained from Aldrich Chemical Company (Milwaukee, WI). Cinchonidine and Cinchonine were obtained from Spectrum Chemicals (New Brunswick, NJ), while Quinine and Quinidine were obtained from Fluka (Milwaukee, WI). Indinavir free base was supplied by Merck Research Laboratories (Rahway, NJ). All solvents were HPLC grade with acetonitrile and methanol obtained from Aldrich (Milwaukee, WI), chloroform (optimo grade) obtained from Fisher (Milwaukee, WI), and acetic acid obtained from Pharmco (Brookfield, CT). Nitrogen gas was obtained from AGL Industries (Clifton, NJ).

Instrumentation

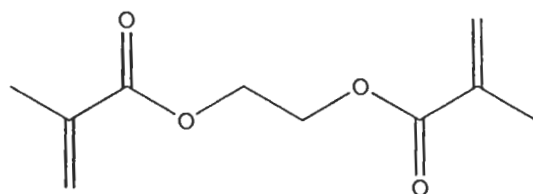
The HPLC system consisted of either a Perkin Elmer (San Jose, CA) ISS 200 system with Diode Array Detector using Turbochrom Software or an Agilent (Palo Alto, CA) 1100 system with Chemstation software. Polymer synthesis was performed in a Haak A80 (Germany) water bath. Columns were packed with an Isco (Lincoln, NE) 250 syringe pump (Lincoln, NB). IR studies were done using a Nicolet Nexus 870 FTIR with an attenuated total reflectance attachment. ITC experiments were performed on a Calorimetry Sciences Corporation 420 ITC (American Fork, UT) with data analysis performed with Origin Software (OriginLab Corp., Northhampton, MA).

Polymer Synthesis, Column and Sample Preparation

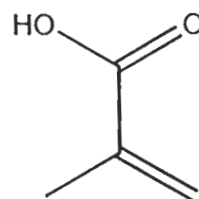
Eight polymers (4 sets of two) were prepared, adapted from a previous method for a 1:1, 3:1, 4:1, and 6:1 M/T ratio.²⁰ In a 25 mL borosilicate glass scintillation vial, cinchonidine (1.9 mMol), MAA (1.9, 5.7, 7.6, 11.3 mMol respectively), EGDMA (53 mMol), and AIBN initiator (4.3 mMol) were placed into optimo chloroform (128.3 mMol). Structures of materials are shown in Figure 3-6. The vial was sparged with nitrogen gas for 25 minutes in a 4 °C water bath before being capped and placed under UV light for 17½ hours. Finally, the hood window was closed and covered over with newspaper, followed by extinguishing the laboratory lights.

The resulting polymers were taken out and roughly ground with an electric coffee grinder followed by grinding with a mortar and pestle. The ground polymer was sieved between 38 and 25 µm sieves. Approximately 1 gram of particles was collected from the 25 µm sieve, slurried in acetonitrile and packed into 10 x 0.46 cm stainless steel HPLC columns. Figure 3-7 is a schematic of the packing system employed. A high speed/high pressure syringe pump was operated at a constant pressure of 5000 psi, and used acetonitrile as the driving solvent. An empty stainless steel preparatory HPLC column was attached to the standard HPLC column to form the column assembly. The slurried polymer was poured into the assembly and the remaining volume filled with acetonitrile. The assembly was then capped, attached to the syringe pump and the pump turned on. The resulting columns were washed with a mixture of methanol/acetic acid (7:3) until a stable baseline was achieved.

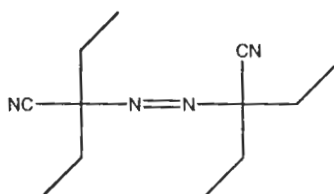
Figure 3-6. Structures of materials used in polymer synthesis.



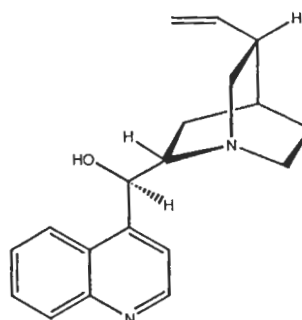
Ethylene Glycol Dimethacrylate



Methacrylic Acid

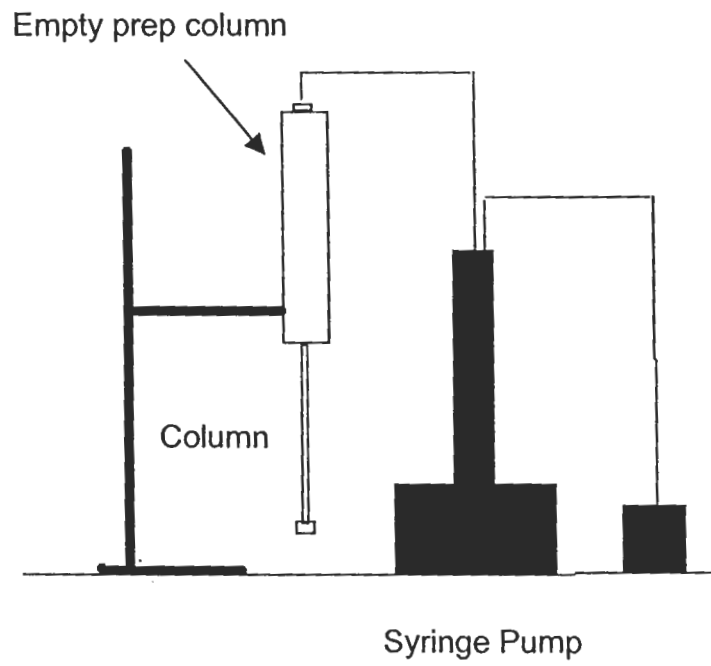


2,2-Azobisisobutyronitrile



(-) cinchonidine

Figure 3-7. Schematic of column packing system.

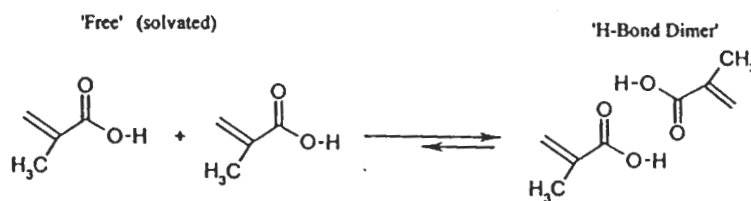


Standard samples were prepared by dissolving each component in a mixture of optimo chloroform/acetic acid (95:5) to achieve a concentration of 1.0 mg/mL. A 10 μ L sample was injected resulting in 10 μ g of each component being introduced onto the column. A mixture containing each component (1.0 mg/mL) was prepared to test column selectivity and utilized a 10 μ L injection as well.

ATR-IR Studies

Binding Studies

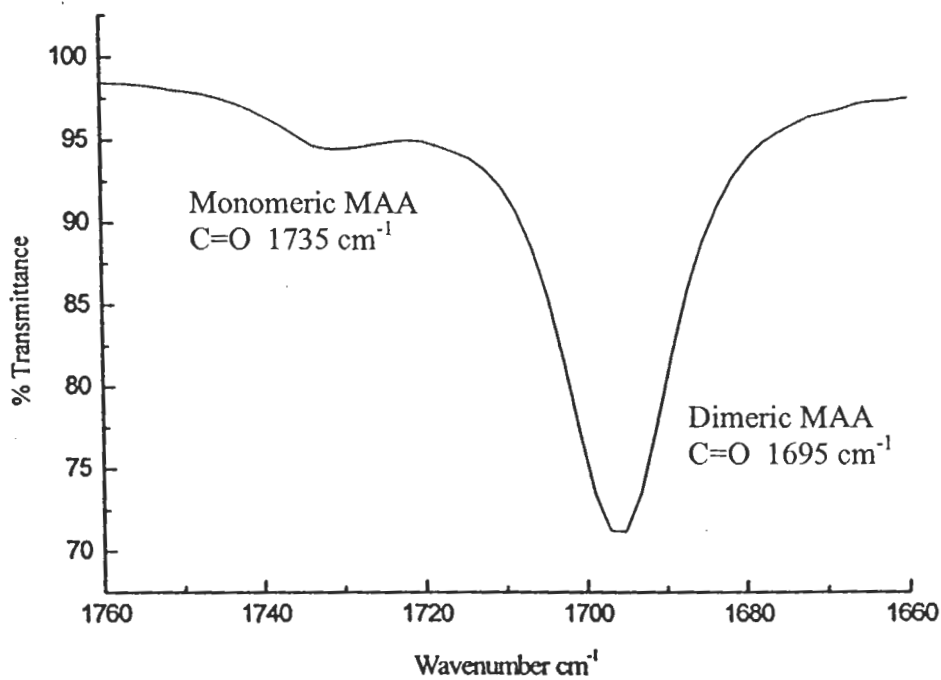
In non-polar solvents, at concentrations greater than 0.01 M, carboxylic acids will predominately exist as hydrogen-bonded dimers, although this dimer form is in equilibrium with the solvated or 'free' monomeric form.¹⁵³



Upon introduction of cinchonidine, the monomeric MAA will interact with the cinchonidine, causing the equilibrium to shift away from the dimer as it compensates for the loss of the monomer.

The IR spectrum of a 0.1 M solution of MAA in chloroform, Figure 3-8, clearly show the two solution forms of MAA, with the dimer having a carbonyl stretch of 1695 cm^{-1} and the monomer having a carbonyl stretch of 1735 cm^{-1} . Furthermore, O'Brien et. al. noted that the dimer stretch in the presence of Indinavir, decreased, thus it is possible to calculate the effective loss of MAA from solution due to hydrogen bonding with the

Figure 3-8. ATR-FTIR spectra of methacrylic acid. Adapted from Reference #153



template.¹¹⁸ This is accomplished by measuring the dimer stretch intensity of several concentrations of MAA in chloroform to generate a calibration curve:^{118, 153}

$$I = RC \quad [3-6]$$

Where:

I = intensity of dimer stretch at 1695 cm⁻¹.

R = slope of calibration curve

C = concentration of “free” MAA in solution.

Finally, the intensities of several MAA-template solutions are measured and the decrease in MAA due to hydrogen bonding, [MAA_{cinchonidine bound}] is calculated:

$$I/R = C \quad [3-7]$$

$$C = [\text{MAA}_{\text{added}}] - [\text{MAA}_{\text{cinchonidine bound}}] \quad [3-8]$$

$$[\text{MAA}_{\text{cinchonidine bound}}] = q/V \quad [3-9]$$

where I, R, and C are described above and,

q = effective amount of MAA bound to cinchonidine.

V = the volume of the solution

[MAA_{added}] = total concentration of MAA added to solution

Binding Studies: Sample Preparation

Standard solutions of MAA were prepared by preparing a stock solution of MAA in chloroform (10.0 mL of MAA to 50.0 mL with Chloroform). Appropriate volumes were pipeted and diluted to 10.0 mL with chloroform to give a range of concentrations from 0.012 M to 2.36 M. Several different monomer-template ratios were prepared by placing 0.201 g of cinchonidine into a 2.0 mL vial along with 1.0 mL of an appropriate standard MAA solution. Table 3-3 lists the range of ratios analyzed. All samples were

analyzed by ATR-FTIR using 200 scans with 1 cm^{-1} resolution and the peak height of the 1695 cm^{-1} stretch recorded.

Isothermal Titration Calorimetry

A standard solution of MAA (6.5 M) was prepared by diluting 5.51 mL MAA to 10.0 mL with chloroform. A standard solution of MMA (6.5 M) was prepared by dissolving 6.97 mL into 10.0 mL of chloroform. A standard solution of 4-VP (6.5 M) was prepared by dissolving 5.85 mL into 10.0 mL of chloroform. A standard solution of cinchonidine (0.10 M) was prepared by dissolving 0.294 g into 10.0 mL chloroform. A standard solution (0.01 M) of Indinavir was prepared by dissolving 0.061 g into 10.0 mL of chloroform. Prior to analysis, 1.0 mL of each standard solution, except for Indinavir, was diluted to 10.0 mL to give concentrations of 0.65 M and 0.01 M respectively. The ITC sample and reference cells (1300 μL each) were filled with the 0.01 M template solution and the injection syringe was filled with the 0.65 M monomer solution. The instrument was equilibrated to $4.0\text{ }^\circ\text{C}$. before the titration began and was held constant throughout the course of the experiment.

Results and Discussion

ATR-IR Studies: Evaluation of IR method

Cinchonidine possess three key structural features. First, the fused aromatic ring system containing a nitrogen heteroatom, will be expected to yield characteristic stretches for both aromatic C=C bonds around $1500\text{-}1600\text{ cm}^{-1}$ as well as for the C-N bond at $1200\text{-}1360\text{ cm}^{-1}$. The alcohol present in the middle of the molecule will yield stretches for the C-O bond $1050\text{-}1300\text{ cm}^{-1}$. Lastly, it possesses a tertiary amine within a bridged carbon

Table 3-3. Monomer-template ratios used for ATR-FTIR binding studies.

M/T Ratio	MAA (M)	Cinchonidine (M)
.35:1	0.236	0.682
.52:1	0.354	0.682
.7:1	0.472	0.682
.8:1	0.531	0.682
1:1	0.708	0.682
3.5:1	2.360	0.682
4.3:1	2.950	0.682
5.2:1	3.540	0.682
10:1	7.080	0.682

skeleton that would be expected to yield stretches for another C-N bond.¹⁶² Based on this it is anticipated that there would be no spectral overlap with the MAA dimer and monomer carbonyl stretches. Figure 3-9 is a FTIR spectrum of a 0.1 M solution of cinchonidine in chloroform. Examination of this spectrum reveals that cinchonidine has no major spectral peaks present between 1600 and 1800 cm^{-1} and based on this it was hypothesized that ATR-FTIR binding studies would yield successful quantitative data.

Figure 3-10 represents the overlay of several ATR-FTIR spectra obtained for the standard MAA solutions. The decrease in both the dimer and monomer stretches are visible and it is readily apparent that good sensitivity is possible as we were able to achieve detection as low as 0.012 M MAA, which is approximately 2% of the template concentration used in this study. The peak intensity of the dimer stretch was recorded and then plotted against the concentration of the MAA solution to generate a calibration curve, shown in Figure 3-11. The calibration curve is linear, as expressed by a correlation coefficient of 0.9942, and is characterized by a slope of 0.9169.

The second part of this experiment attempted to characterize the hydrogen bond created during the formation of the cinchonidine-MAA complex as well as to calculate the optimal amount of MAA needed to generate maximum selectivity. Figure 3-12 represents ATR-FTIR spectra obtained for several solutions containing cinchonidine and MAA. It was surprising to observe that no detectable amount of 'free' MAA was achieved until almost equal molar concentrations of cinchonidine and MAA were achieved. This lack of 'free' MAA indicated that first interaction occurring with cinchonidine is exceptionally strong, since the disappearance of the carboxylic acid stretch suggests near stoichiometric binding with cinchonidine. Further attempts were

Figure 3-9. FTIR spectra of cinchonidine.

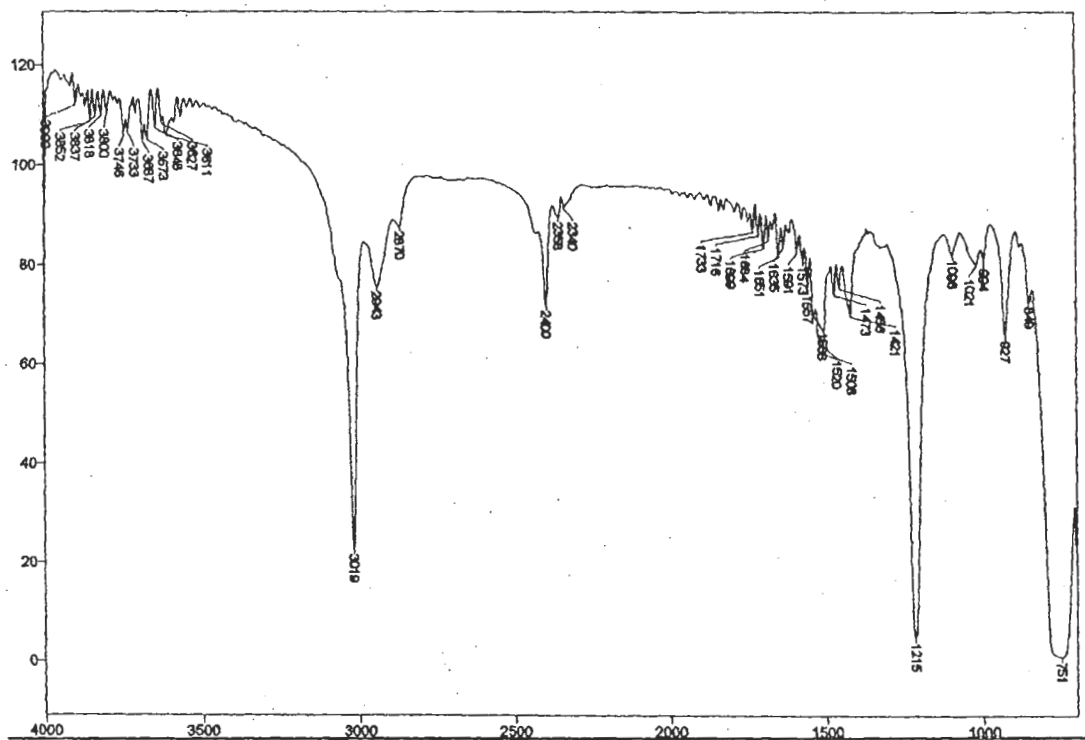


Figure 3-10. Several ATR-FTIR spectra of methacrylic acid solutions.

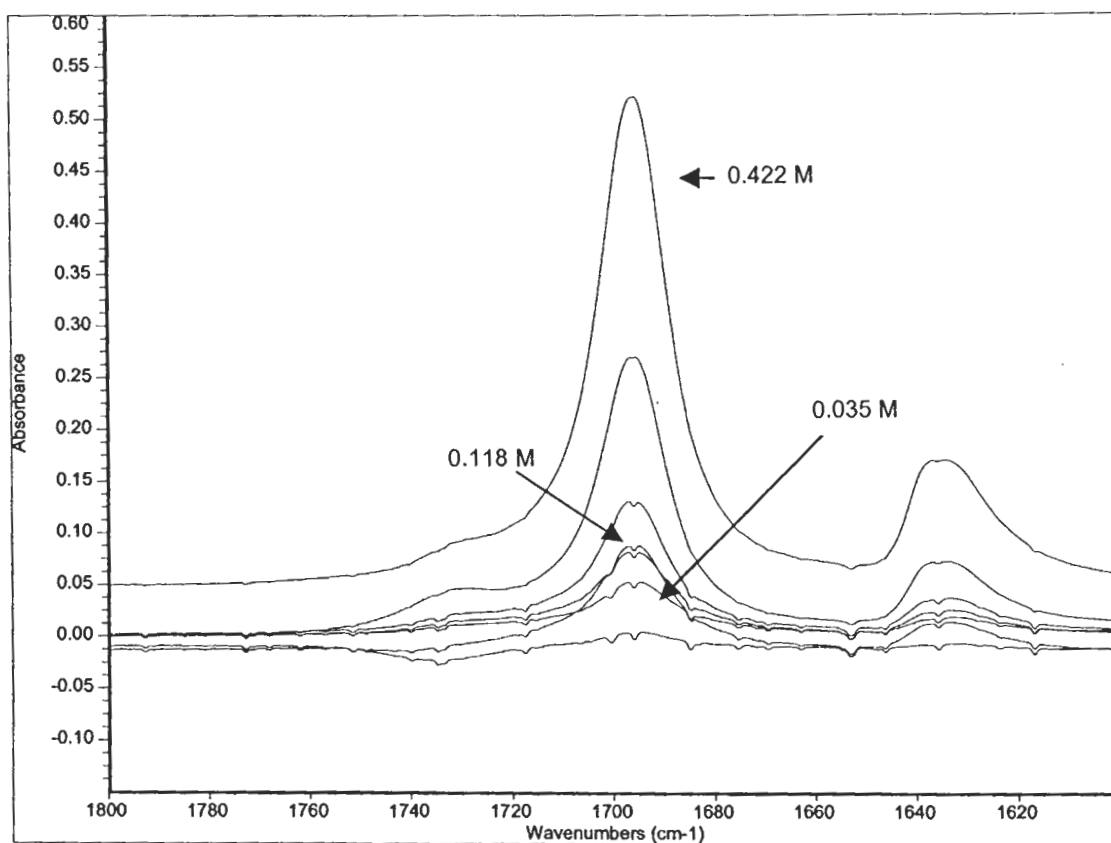


Figure 3-11. Calibration curve constructed by plotting peak intensity versus concentration.

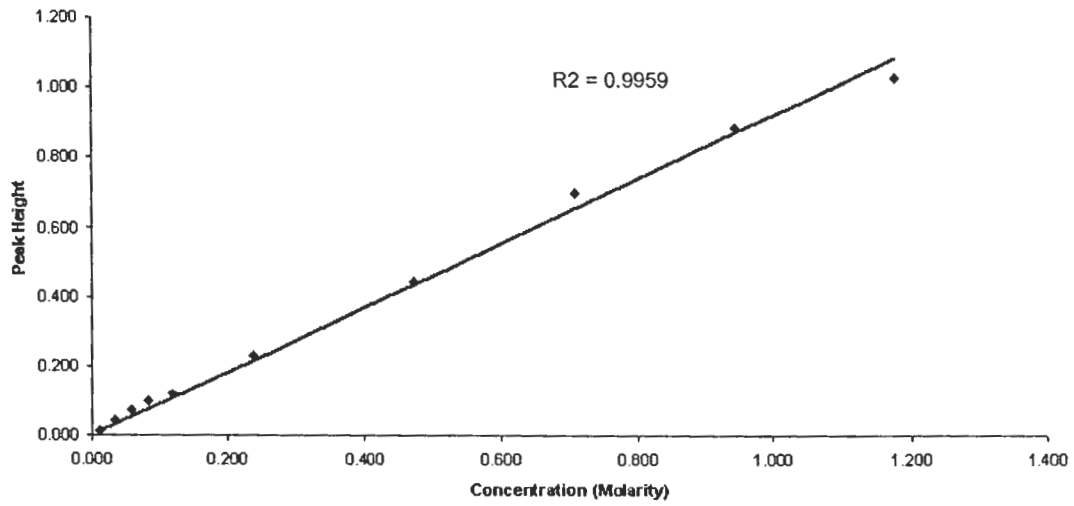
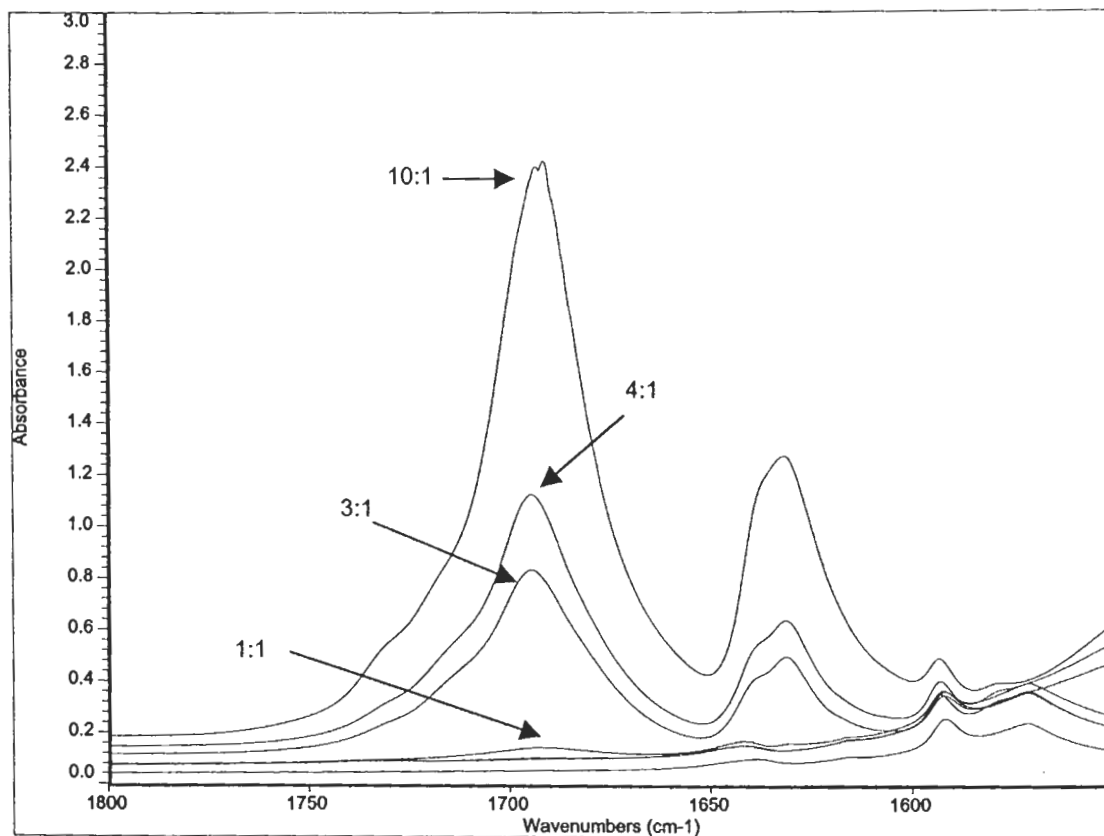


Figure 3-12. ATR-FTIR spectra of several cinchonidine-MAA solutions.



tried in an effort to increase the concentration of 'free' MAA above the method's limit of detection, however, these attempts were not successful and as a result, the amount of 'free' MAA cannot be determined experimentally until the molar ratio of MAA to cinchonidine reaches 0.8:1. It was concluded that one very strong hydrogen bond exists between MAA and cinchonidine. It is reasoned that the functional group on cinchonidine responsible for this interaction is the tertiary amine which is expected to act as strong H bond acceptor.

In the case of complex formation, MAA can be considered a ligand capable of forming multiple hydrogen bonds with cinchonidine. In general, if each binding site on the template is considered independent and identical, then all the equilibrium constants governing the binding of one MAA ligand, will be equivalent. Statistically, this can be represented as:¹¹⁸

$$q = (bnC)/(1+bC) \quad [3-10]$$

where:

q = amount of MAA bound to cinchonidine.

b = equilibrium constant for the binding process.

n = number of binding sites on cinchonidine.

C = concentration of 'free' MAA remaining after q moles become bound.

Traditionally, this equation has been rearranged into the following expression, commonly known as a Scatchard plot:¹¹⁸

$$q/C = -bq + bn \quad [3-11]$$

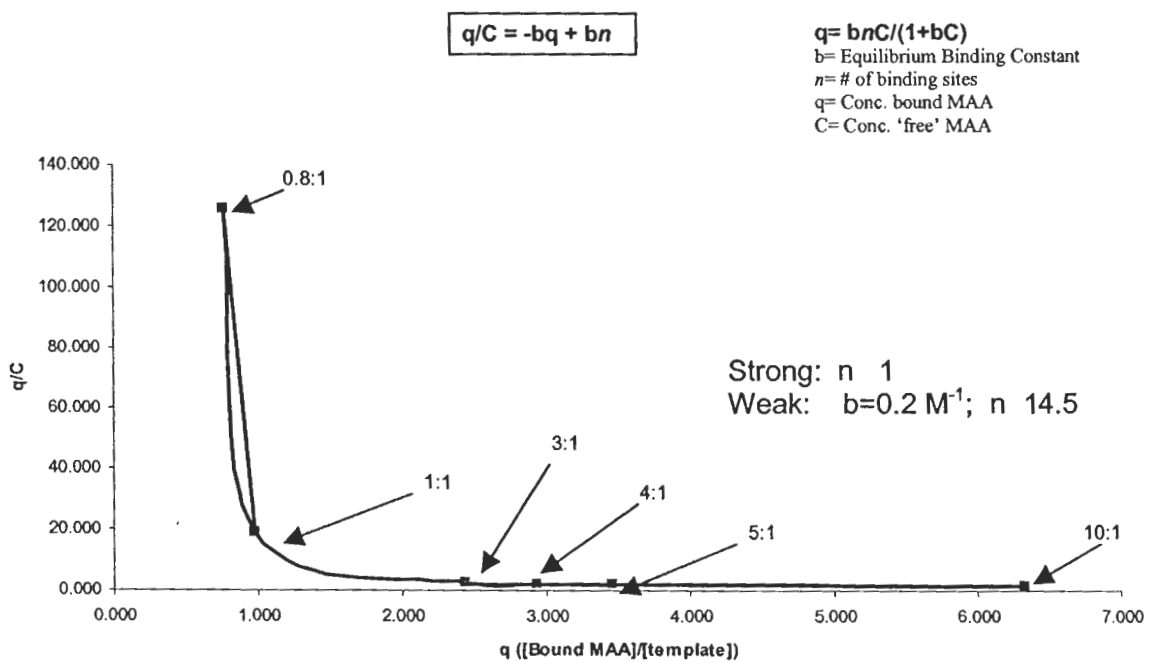
If the template's binding sites are identical and independent, then the scatchard plot will be linear with a slope of $-b$ and an abscissa of n .¹¹⁸

If the Scatchard plot is curved, this indicates that the binding sites are not identical and or independent. Non-independent binding sites exist when the binding of a ligand to one site affects the binding of another ligand to another site. If b increases with the additional ligand equivalents, then this is considered to be “positive cooperativity” and the plot will be concave downward. If b decreases with increasing ligand equivalents, then this is considered to be “negative cooperativity” and the plot is concave upwards.¹¹⁸

When the ATR-FTIR data is cast as a Scatchard plot, as shown in Figure 3-13, the strong interaction observed in the ATR-FTIR spectra is clearly exhibited. The very sharp concave upward curve signifies that the sites of interaction on cinchonidine are not identical. Thus, the equilibrium constants for the formation of the cinchonidine-MAA complex are not equivalent. The decreasing slope, b , signifies that the cinchonidine binding sites are not independent of one another and given the magnitude that that b decreases, it is obvious that significant negative cooperativity among the binding sites is being expressed.

The large drop of q/C from 0.8:1 to 1:1 clearly illustrates that the majority of MAA is engaged in a very strong hydrogen bond, leaving no detectable amounts of ‘free’ MAA in solution. As additional equivalents of MAA are added a smaller drop in q/C is observed until eventually leveling off. This indicates that there are additional interactions occurring beyond the addition of one mole equivalent MAA. More than one MAA molecule is interacting with one mole cinchonidine, albeit very weakly, indicating that higher order multi-molecular complexes are being formed.

Figure 3-13. Scatchard plot constructed for a cinchonidine-MAA system.



An attempt was made to use the Scatchard plot to determine n for the complex, which represents the optimum amount of MAA for this system. The plot was divided into two approximate linear portions and an attempt was made to determine the binding constants and number of binding sites determined for each. For the strong portion representing 0.8 to 1 mol equivalents, only two points were successfully determined, however the general slope of this portion indicates a large binding constant, due to the sharp decrease in q/C from 0.8 to 1 mol equivalents added. The second portion, from 3 to 10 mol equivalents, which is expected to be heterogeneous, can be assessed as the weaker interactions will possess similar strengths. Analysis of this portion ($R^2=0.93$, $y=-0.1874x + 2.7123$) yields a binding constant of 0.2 M^{-1} , which is reasonable given that the interactions expected at these monomer concentrations are anticipated to be weak in nature. However, the number of binding sites was determined to be approximately 14.5, a value that is large, given that cinchonidine possesses only three functional groups that are likely to engage in appreciable hydrogen bonding. This would suggest that MAA is forming a multi-layered complex with cinchonidine, which may not be desirable for molecular imprinting.

Based on these results it was determined that for this particular system, the IR technique described above, while providing insightful qualitative information concerning the strengths of the hydrogen bonds, could not readily determine the optimal ratio for a cinchonidine-MAA system. It was observed that the ATR-IR instrument does not possess adequate sensitivity to detect very low concentrations of MAA, a situation that occurs in the presence of strong non-covalent interactions. More importantly, this technique cannot accurately determine the endpoint for the weak interactions occurring directly with the template and when any multi-layering begins. It is possible to examine

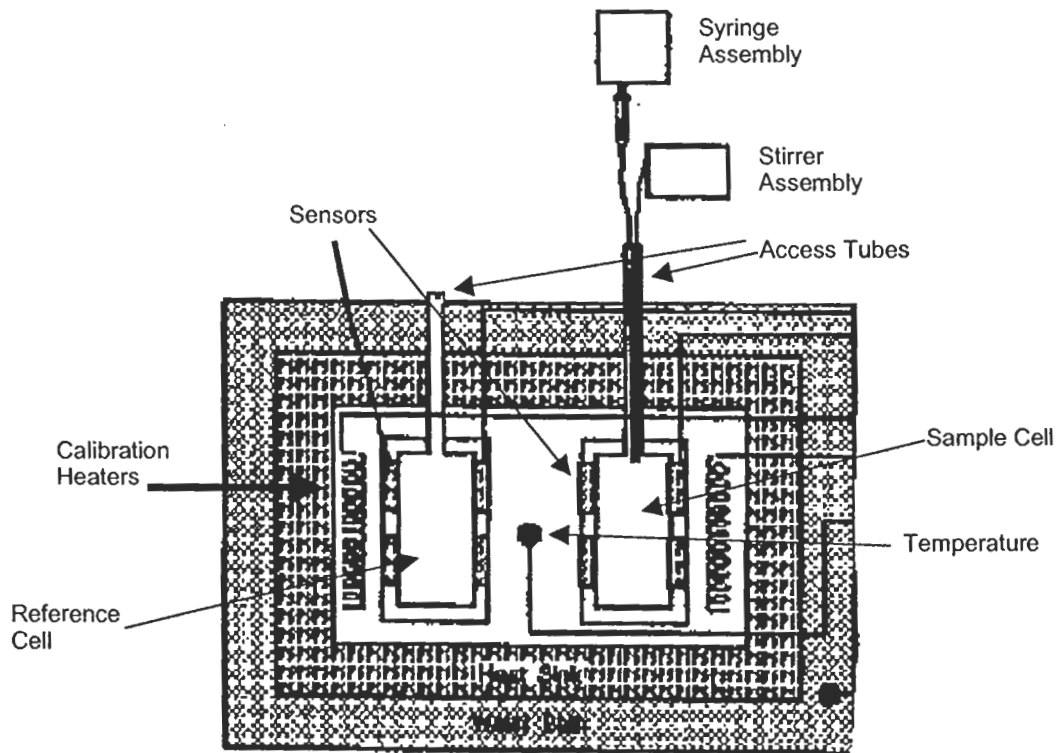
the various functional groups spectra for several different MAA concentrations and observe shifts resulting from hydrogen bonding, however, the shifts associated with weaker interactions may be difficult to observe. While this technique may be applicable to other polymer systems, it stands to reason that other molecules possessing similar functional groups or structures will likely encounter the same situation. Therefore it is necessary to develop techniques that do not require assumptions to be made concerning the strength of hydrogen bonds in order to fit data to a line.

Isothermal Titration Calorimetry: Cinchonidine-MAA System

Isothermal Titration Calorimetry (ITC) is a microcalorimetry technique that is commonly utilized in biochemistry to study the energy of DNA-drug or protein-protein interactions. ITC simply measures stepwise changes in the energy of a system, thus there is no need to isolate a spectral peak to observe and quantify these changes. Furthermore, ITC instruments typically have minimum detectable heat values in the μcal range,¹⁶² thereby ensuring adequate sensitivity for measuring weak hydrogen bonding interactions. With these advantages, it was proposed that ITC would be a good method for optimizing monomer-template interactions for the formation of MIP's. In this study, we used ITC to predict the ideal monomer - template stoichiometry for the preparation of a MIP for cinchonidine.

Figure 3-14 is a schematic of the system utilized for this experiment. In this setup, the reference and sample cell are filled with a solution containing cinchonidine at a known concentration. The injection syringe is loaded with the MAA solution and the instrument is equilibrated to the correct temperature. This particular instrument utilizes a

Figure 3-14. Schematic of Isothermal Titration Calorimetry Instrument. (Adapted from Reference 163)

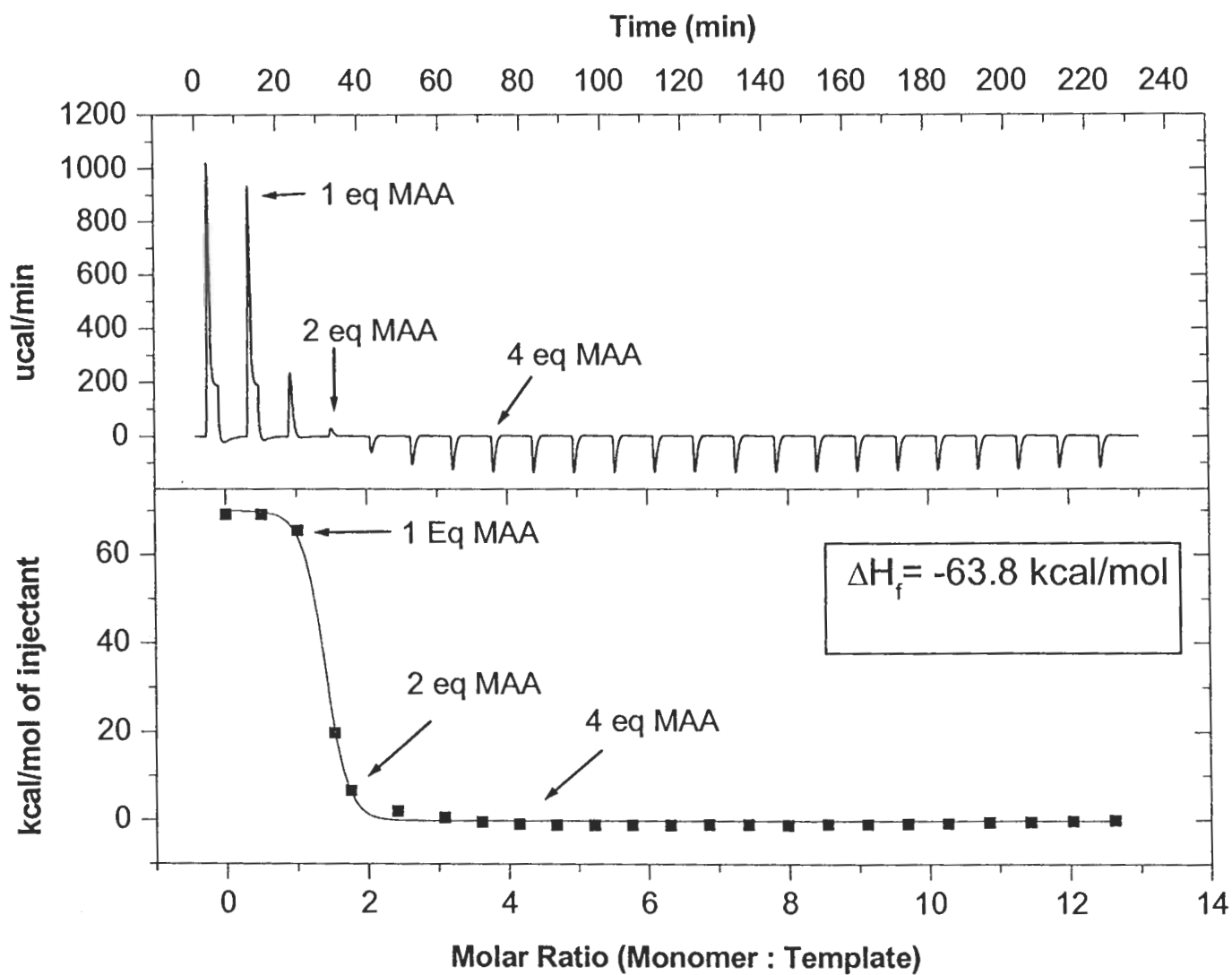


power compensation system for measuring heat release or intake. Upon addition of MAA into the sample cell, the sample cell temperature will either increase (exothermic) or decrease (endothermic) in relation to the reference cell. The microprocessor measures this change and calculates the amount of energy it needs to either add or subtract from the reference cell in order to regain equilibrium. Thus ITC plots showing positive peaks represent exothermic processes, while plots with negative peaks are indicative of endothermic processes.

Figures 3-15 and 16, with the experimental conditions listed, represent the titration of cinchonidine with $\frac{1}{2}$ and $\frac{1}{4}$ incremental mole equivalents of MAA respectively. For these experiments, the template and MAA were separately dissolved in chloroform at the specified concentrations. The top portion of each figure is a plot of heat released for each increment of MAA added versus time. The bottom portion of each figure gives the amount of energy released per mole of MAA added. From this, the ΔH_f for the cinchonidine-MAA complex was calculated. The values obtained for each titration are shown.

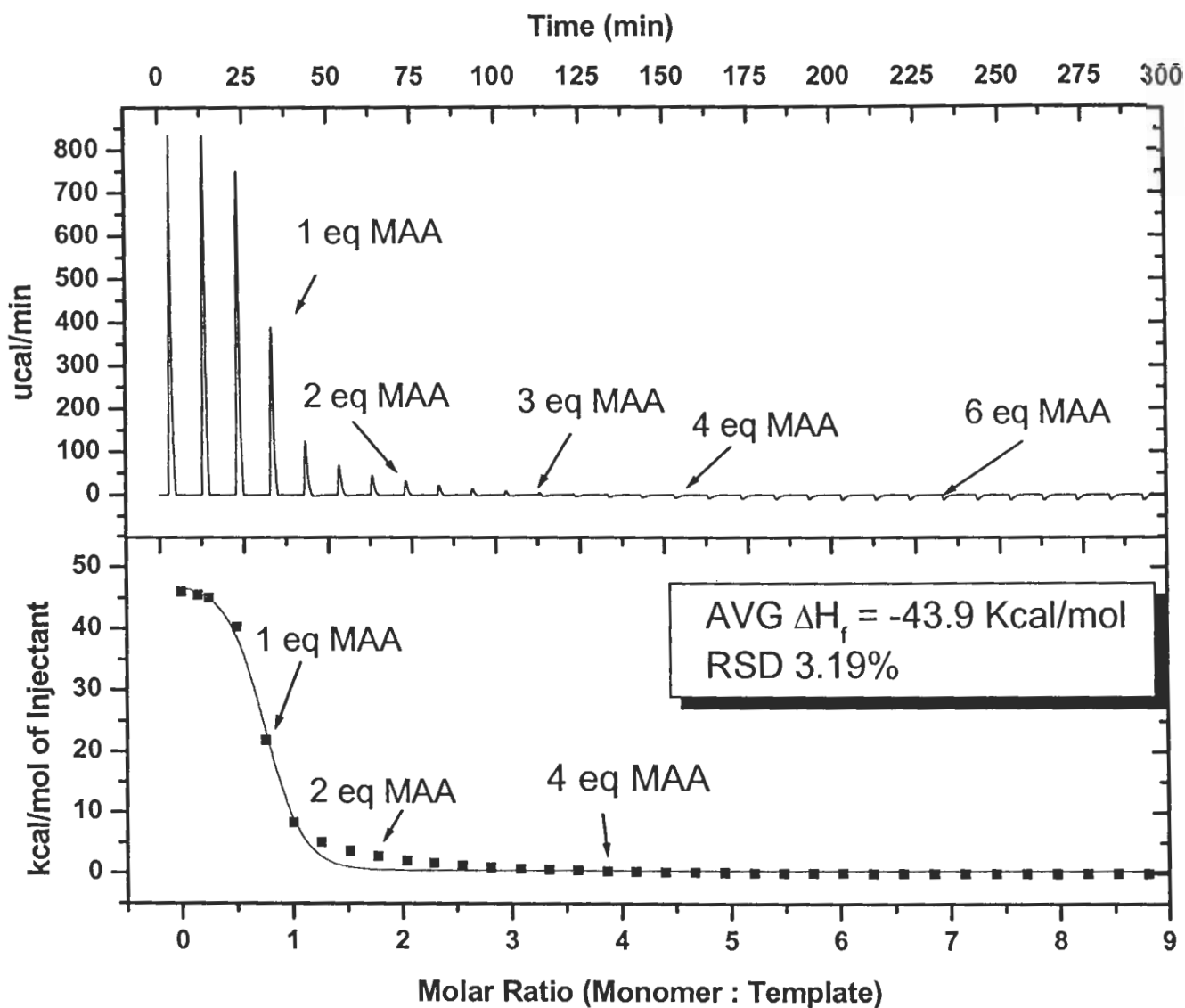
For both titrations, the data plots begin with large positive peaks that gradually get smaller and eventually become negative. This indicates that large exothermic processes are occurring initially and gradually becoming smaller until they cease to occur. This is reasonable as hydrogen bonding is an exothermic process, so it would be expected that as cinchonidine becomes saturated with MAA, the strengths of the hydrogen bonds formed would gradually become smaller. Also, this indicates that the total energy needed to break the MAA dimer and reform hydrogen bonds with cinchonidine is a favorable process.

Figure 3-15. ITC plot for titration with 1/2 MAA mole equivalents.



Temp: 4.0 °C 10 μ L injections [Template]=0.01 M [Monomer]= 0.65 M

Figure 3-16. ITC plot for a titration with ¼ MAA mole equivalents.



Temp: 4.0 ° C 5 μ L injections [Template]=0.01 M [Monomer]= 0.65 M

Additionally, it was observed that a large amount of heat is released up through the addition of the first mole equivalent of MAA, indicating the presence of one very strong interaction between the template and the monomer, which agrees with the IR data. Upon addition of further equivalents of MAA, the amount of energy released was small, indicating relatively weak interactions of cinchonidine with the additional MAA. The point at which the addition of MAA produced no further binding with the template was determined, by measuring when the slope became zero, to be four mole equivalents. Based on these data, it was hypothesized that the optimum monomer-template ratio for the formation of a MIP for cinchonidine was 4:1.

Polymer Selectivity

To correlate the observed binding interaction of MAA and cinchonidine to the selectivity of MIP's prepared for cinchonidine, four polymers were prepared using 1, 2, 4, and 6 mole equivalents of MAA relative to the template. The selectivity of these polymers was then compared by using them as HPLC stationary phases to separate cinchonidine from its isomer, cinchonine. The polymer synthesis and preparation of the HPLC columns were similar to those described previously.²⁰ The results for each polymer are presented in Table 3-4. Figures 3-17 through 3-20 are representative chromatograms for the 1:1, 3:1, 4:1, and 6:1 polymers respectively.

The 1:1 polymer was prepared in order to evaluate the influence of the strong hydrogen bond, occurring between MAA and the tertiary amine, on selectivity. Since only one equivalent was added, the MAA should only associate with the functional group responsible for the strong interaction. The results in Table 4 reveal the polymer demonstrates a minimal selectivity of 1.2, which could only be determined by injecting

Table 3-4. Selectivity of cinchonidine imprinted polymers containing various equivalents of MAA. For all separations, a mobile phase of 5 % acetic acid in chloroform was utilized with a flow rate of 0.5 mL/min. Retention factor (k') determined by $(t_r - t_0)/t_0$ and selectivity (α) calculated by $k'_{\text{cinchonidine}}/k'_{\text{cinchonine}}$.

MAA Polymer	1 ^a	3	4	6
avg. k' Cinchonine	0.41	1.21	1.51	3.30
avg. k' Cinchonidine	0.50	16.38	37.38	54.90
Avg. α	1.21	13.59	24.38	16.00
α RSD %	3.83	8.13	16.27	27.20

a). Selectivity determined by individually injecting 10 μg of each component.

Figure 3-17. Representative chromatogram obtained using a 1:1 MAA-Cinchonidine polymer. Mobile phase is 5% acetic acid in chloroform with a flow rate of 0.5 mL/min. Approximately 10 μ g of each component was injected individually with acetone as void volume marker.

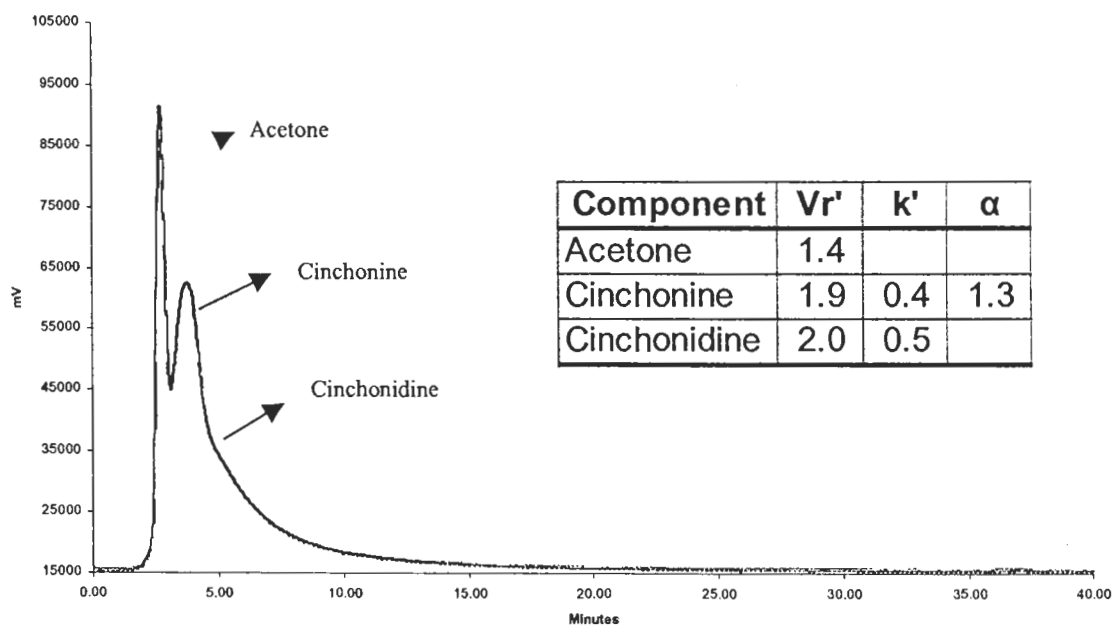


Figure 3-18. Representative chromatogram obtained using a 3:1 MAA-Cinchonidine polymer. Mobile phase is 5% acetic acid in chloroform with a flow rate of 0.5 mL/min. A 10 μ L injection of a mixture was used resulting in the introduction of 10 μ g of each component onto the column with acetone used as a void volume marker.

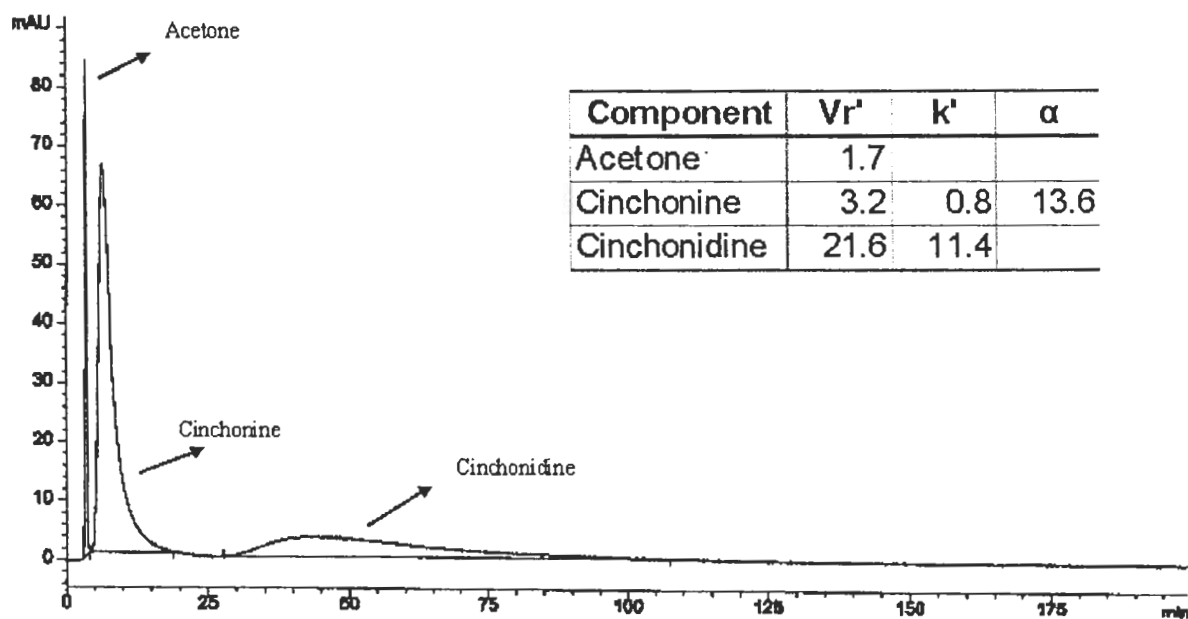


Figure 3-19. Representative chromatogram obtained using a 4:1 MAA-Cinchonidine polymer. Mobile phase is 5% acetic acid in chloroform with a flow rate of 0.5 mL/min. A 10 μ L injection of a mixture was used resulting in the introduction of 10 μ g of each component onto the column with acetone used as a void volume marker.

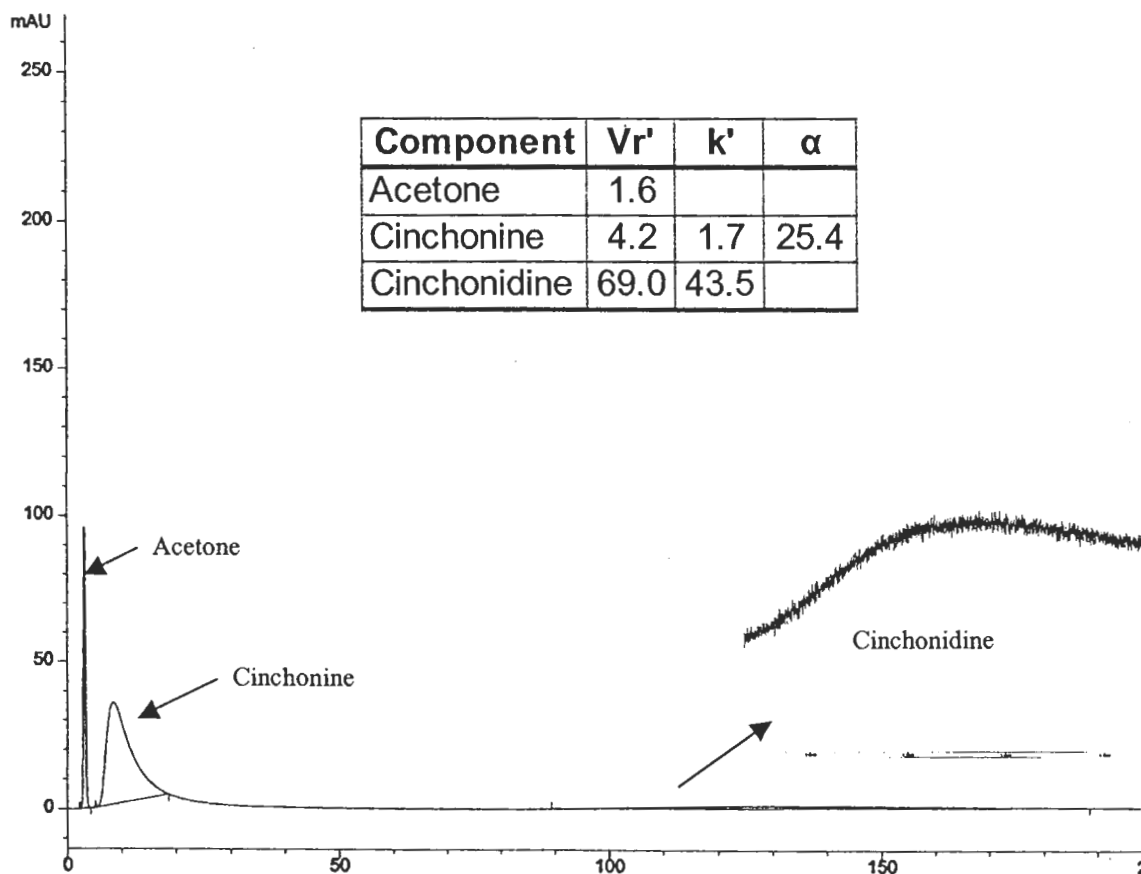
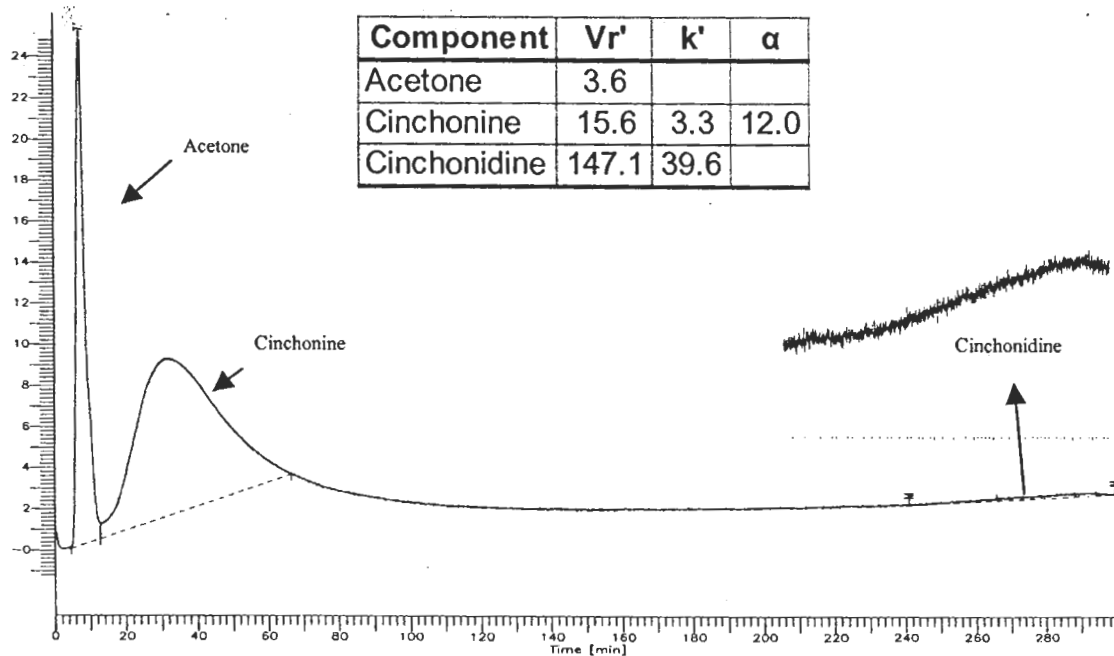


Figure 3-20. Representative chromatogram obtained using a 3:1 MAA-Cinchonidine polymer. Mobile phase is 5% acetic acid in chloroform with a flow rate of 0.5 mL/min. A 10 μ L injection of a mixture was used resulting in the introduction of 10 μ g of each component onto the column with acetone used as a void volume marker.



each component separately. This is reasonable, even though the ITC data suggests that the first MAA-template interaction is the strongest interaction. This is perhaps due to the fact that both isomers possess the same functional groups, so both would be expected to have a similarly strong interaction with the polymer.

The 3:1 ratio was selected because cinchonidine possesses three functional groups capable of hydrogen bonding and all should be actively engaged with the MAA. The results demonstrate that the polymer possesses very good selectivity as shown by the value of 13.6. A comparison between the retention factors for 1:1 and 3:1 shows that the retention factor for cinchonine increased only minimally from 0.41 to 1.21, while the retention factor for cinchonidine increased by an order of magnitude going from 0.50 to 16.38. This may be explained by the differences in orientation of the three hydrogen-bonding functional groups on each isomer. Since the MAA groups are incorporated in the polymer in a manner that is complementary to cinchonidine, strong, selective re-binding of cinchonidine relative to its isomer occurs with this polymer.

The 4:1 polymer was prepared in order to assess the significance of the fourth interaction on polymer selectivity. As discussed above, cinchonidine possesses only three functional groups capable of hydrogen bonding with MAA. However, the ITC results clearly indicate that binding, while very weak relative to the firsts strong interaction, was occurring up through the addition of four equivalents of MAA. The results, when compared to the 3:1 polymer, show that this interaction, while weak in nature, is an important stabilizing interaction within the polymer binding sites. Upon addition of the extra equivalent of MAA, the retention factor for cinchonine changes negligibly, increasing from 1.21 to 1.51, while the retention factor for cinchonidine

doubles from 16.38 to 37.38. This translates into an increase in polymer selectivity from 13.59 to 24.38. Most importantly though, is that this observation agrees with the optimal ratio predicted by ITC. This is intriguing, since the template only has 3 hydrogen bonding functional groups. Nevertheless, it is evident that the fourth equivalent gives the complex a stabilizing interaction that results in a polymer with greater selectivity.

Finally, an examination of the 6:1 polymer illustrates that excess monomer is not beneficial since its selectivity is markedly less than that of the 4:1 polymer. In this instance, the excess monomer in solution has been incorporated into the solid polymer, generating non-specific sites of interaction as shown by comparing retention factors to that of the 4:1 polymer. The retention factors on the 6:1 polymer are 49 for Cinchonidine and 3.6 for Cinchonine, versus 33.6 and 1.4 respectively on the 4:1 polymer. While both retention factors increased, indicating greater interaction with the polymer, the selectivity exhibits a decrease from 24.38 down to 16.

Isothermal Titration Calorimetry: Indinavir-MAA system

Given the successful correlation between the ITC and chromatographic results, it was proposed that the Indinavir-MAA system should be examined with ITC. This would allow ITC to be evaluated on a separate system that utilizes a sophisticated template molecule and if the result correlated with the polymer selectivity, then it would be strong evidence that ITC could be used as a universal technique for the design of imprinted polymers.

The first part of this experiment evaluated ITC's ability to measure the binding between three different monomers and the template molecule. These results were then

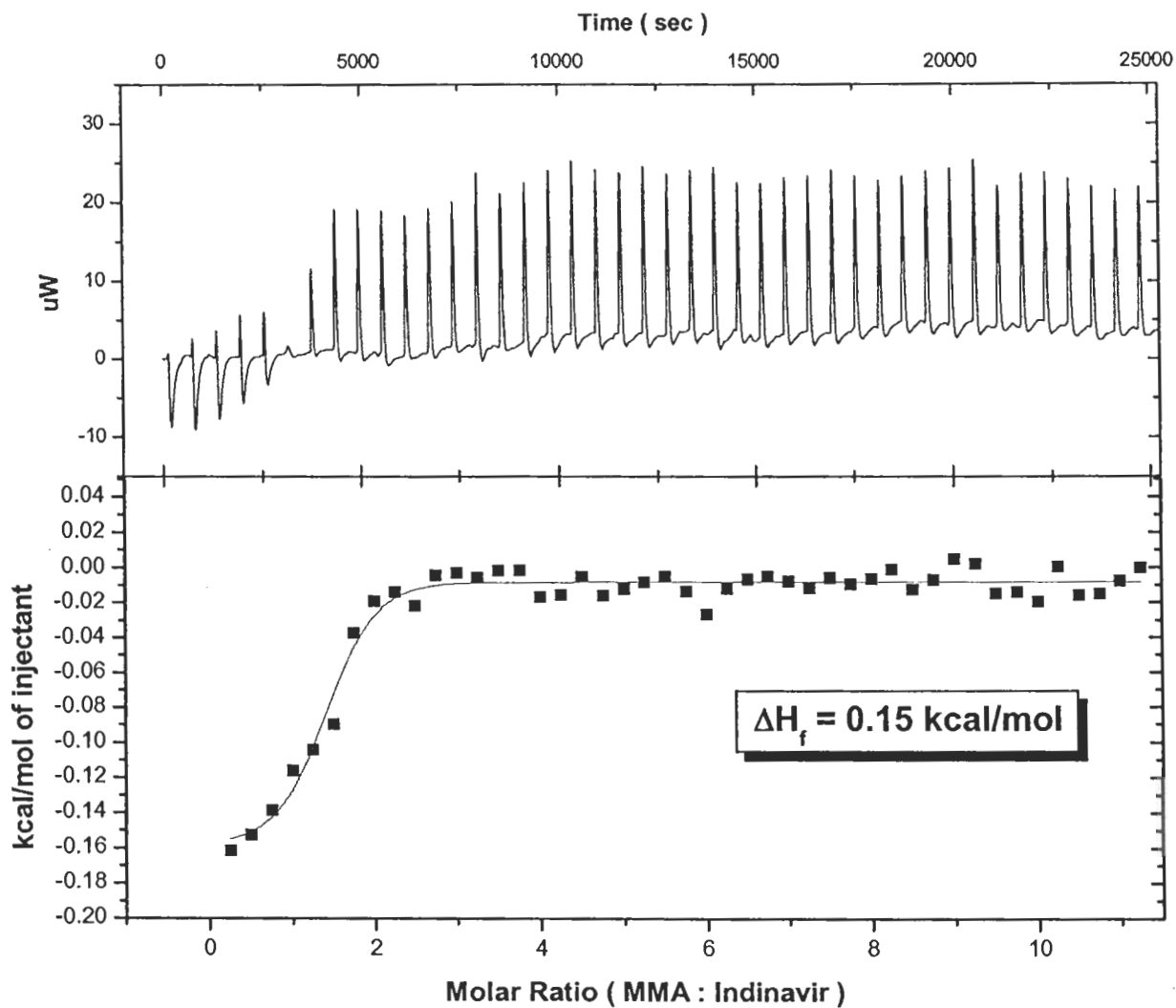
correlated with prior published results.¹¹⁸ Figures 3-21, 3-22, 3-23 are the results for the titration of Indinavir with MMA, 4-VP, and MAA respectively.

For the titration of Indinavir with MMA and 4-VP, the overall results show that neither of these monomers experiences significant interactions with Indinavir. In the case of MMA, the binding of MMA to Indinavir is an endothermic process as illustrated by the negative peaks at the start of the titration and gradually becoming positive as the titration increases. Thus the $\Delta H_f = 0.15$ kcal/mol is a positive value. This, as well as the low ΔH_f , suggests that the formation of a MMA-Indinavir complex is energetically unfavorable and that the complex is not formed, resulting in a polymer with poor selectivity as previously shown.¹⁵³

The titration of Indinavir with 4-VP, reveals that some interactions are occurring, albeit very weakly. The positive peaks illustrate that the overall process is exothermic, thus the formation of the complex is energetically favorable. However, the $\Delta H_f = -0.13$ kcal/mol suggests that any interactions are energetically small. This is reasonable, given the structure of Indinavir, which does not possess any functional groups that should be capable of interacting strongly with a basic monomer. It is noted that the endpoint for this titration was around 9 equivalents of monomer, which suggests that the monomer is either forming a multi-layered complex or is associating with itself to give a multi-molecular assembly in solution. This agrees with the polymers formed with VP, which show measurable, but very small selectivity.¹⁵³

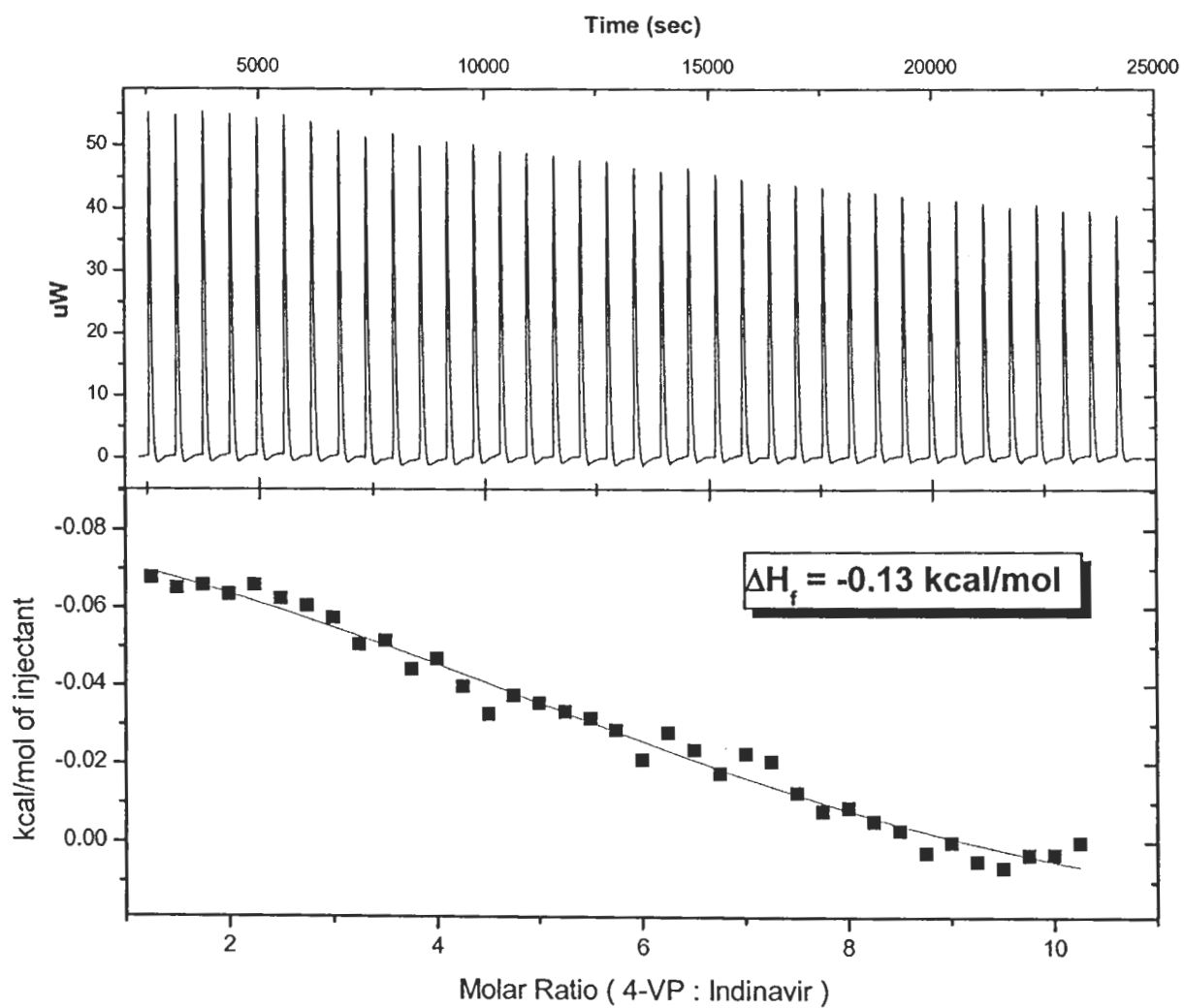
For the titration of Indinavir with MAA, better results are obtained than with the other monomers. A larger exothermic process is observed as indicated by the large

Figure 3-21. Titration of Indinavir with 1/4 mol equivalents of MMA.



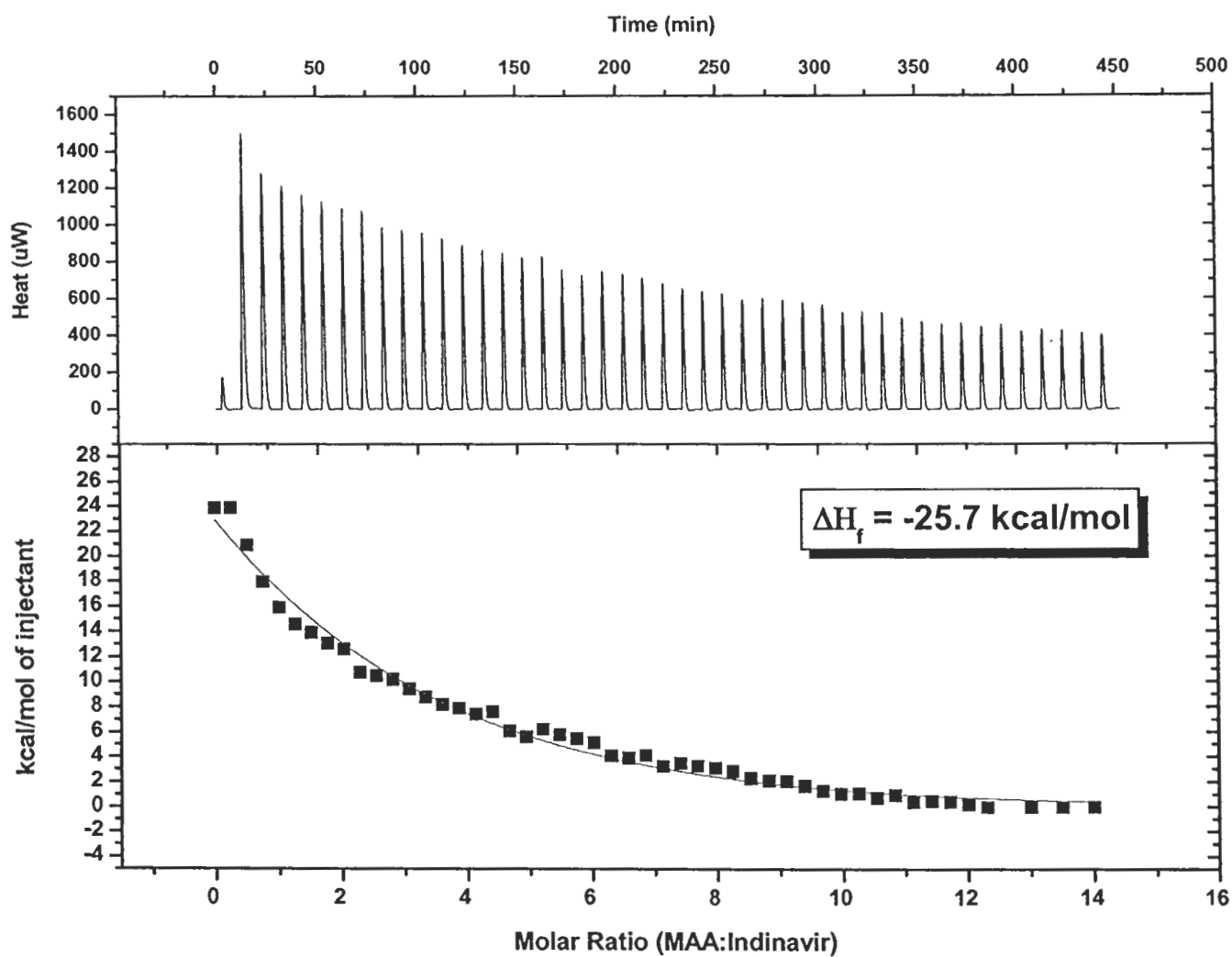
Temp: 4.0 °C 5 μ L injections [Template]=0.01 M [Monomer]= 0.65 M

Figure 3-22. Titration of Indinavir with ¼ mol equivalents of 4-VP.



Temp: 4.0 ° C 5 μ L injections [Template]=0.01 M [Monomer]= 0.65 M

Figure 3-23. Titration of Indinavir with 1/4 mol equivalents of MAA.



Temp: 4.0 °C 5 μL injections [Template]=0.01 M [Monomer]= 0.65 M

positive peaks, indicating that the process of forming the template-monomer complex is energetically favorable. A $\Delta H_f = -25.7$ kcal/mol indicates that MAA is significantly interacting with Indinavir and that the complex being formed is fairly stable. It is interesting to note that the endpoint value was determined to be approximately 10 mol equivalents of MAA. Prior work utilizing the ATR-IR method suggested that 7 mol equivalents was necessary to achieve optimum selectivity as it was observed that all functional groups on Indinavir were engaged in hydrogen bonding, however it was noted that additional interactions were occurring up to 21 equivalents.¹⁵³ As demonstrated with the cinchonidine-MAA system, weak energetic interactions can result in a significant gain in selectivity as these interactions serve to stabilize the template molecule within the polymer binding cavity. Therefore, further chromatographic analysis will be needed to assess the influence of these weak interactions on polymer selectivity.

Table 3-5 compares the ΔH_f obtained for each monomer with the chromatographic selectivity obtained in prior work. It is shown that a good correlation between the ITC and chromatographic results exists. Both MMA and 4-VP polymers exhibited very poor selectivity, 1.0 and 1.1 respectively, between Indinavir and its enantiomer, while the polymer prepared with MAA displayed a selectivity of 6.0 between Indinavir and its enantiomer. This suggests that ITC can not only be used to selectively optimize the functional monomer for an imprinted polymer system, but also can determine the optimal amount of monomer needed in a single experiment. Thus this technique would represent a significant improvement in the design and synthesis process of imprinted polymers.

Table 3-5. ITC results for Indinavir compared to prior chromatographic results.

Monomer	ΔH_f (kcal/mol)	$k_{\text{enantiomer}}$	$k_{\text{Indinavir}}$	Selectivity^a
Methyl Methacrylate	0.15	0.8	0.8	1.0
4-Vinyl Pyridine	-0.13	1.5	1.6	1.1
Methacrylic Acid	-25.7	4.6	27.8	6.0

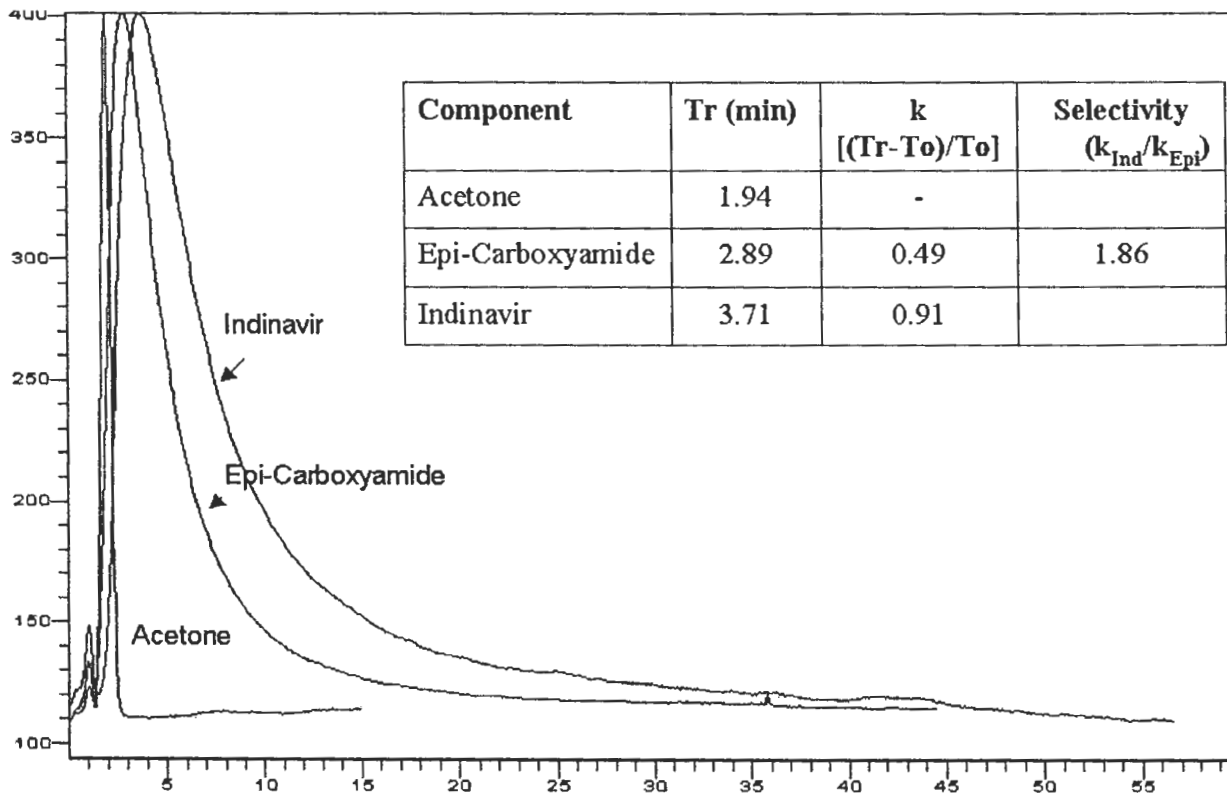
a). Adapted from Reference # 153

Chromatographic Evaluation of Indinavir

In order to assess the influence of the weak interactions, three new Indinavir polymers, with 7, 10, and 15 equivalents of MAA were prepared using a prior published method.¹⁵³ The resulting polymers were ground, washed and packed into HPLC columns for chromatographic analysis using methods described previously. Figure 3-24 is a representative chromatogram for the 7:1 polymer. As with the cinchonidine imprinted polymer, acetone was used a column volume marker and the selectivity was determined using the epi-carboxamide isomer of Indinavir and Indinavir. Analysis of the chromatographic data reveals that all components are not significantly retained as evident by the low retention factors, 0.49 and 0.91 for epi-carboxamide and Indinavir respectively, resulting in a observed selectivity of 1.86. Prior published literature reported retention factors of 0.6 and 3.3 for epi-carboxamide and Indinavir respectively, which results in a selectivity of 5.5.¹⁵³ Further analysis of the 10:1 polymer revealed the same results, which suggests that during the synthesis process the formation of the monomer-template complex was disrupted.

A possible explanation for these results may be due to Indinavir high affinity for water. Analysis of the chloroform, MAA, and EGDMA by Karl Fischer titration, revealed that water had accumulated within the solvents, around 300 µg/mL. A calculation revealed that during synthesis, the template:water mol ratio was approximately 4:1, indicating that significant amounts of water were present while the polymerization reaction was occurring. The presence of high amounts of water would serve to disrupt any interaction between Indinavir and MAA preventing the formation of a stable monomer-template complex. This would translate into very poor selectivity for

Figure 3-24. Chromatographic results for a 7:1 MAA:Indinavir polymer.
 Mobile phase is 3% acetic acid in chloroform (v/v) with a flow rate of 1.0 mL/min.
 Detection is at 260 nm with 50 μ g of each component injected.



the resulting polymer as the polymer would be expected to possess only weak and non-specific sites of interaction.

Conclusions

A cinchonidine-MAA system was utilized to test and validate an IR spectroscopy method for the characterization of the pre-polymerization solution. Previously research had suggested that ATR-FTIR spectroscopy could be used to rapidly evaluate molecular imprinted polymer systems utilizing MAA as the functional monomer and to determine the optimal amount of MAA needed to generate maximum selectivity, while minimizing the formation of non-specific sites of interaction. Our results showed that ATR-FTIR spectroscopy is not sensitive enough to detect low levels of MAA that result from strong interactions with the template molecule. Additionally, an attempt was made to determine the correct MAA-cinchonidine stoichiometry, however, this method was not sensitive enough to determine the endpoint at which MAA and cinchonidine were interacting to form a mono-layer or a multi-layer, within the weak binding region of the scatchard plot.

ITC, a microcalorimetry technique primarily used in biochemistry, was proposed as a possible alternative to conventional spectroscopic techniques. The results from these experiments revealed that formation of the cinchonidine-MAA complex has a ΔH_f of -40 kcal/mol. Furthermore, the ITC data suggested that the optimal ratio of MAA to cinchonidine was 4:1.

This predicted ratio was evaluated by preparing a series of polymers containing different amounts of MAA and chromatographically determining their selectivity. The selectivity values obtained for the 4:1 polymer ($\alpha = 24.4$) was significantly higher than

that of the polymer prepared with three equivalents ($\alpha = 13.6$), equaling the number of functional groups, of MAA. Additionally it was noted that adding higher amounts of MAA did not improve polymer selectivity as the polymer prepared with six equivalents of MAA demonstrated a selectivity of 16.0, even though both compounds demonstrated larger capacity factors. This reconfirms the idea that excess monomer is incorporated into the solid polymer as non-specific binding sites.

Finally, ITC was used to re-evaluate an Indinavir-MAA polymer system that had been previously studied. The ITC results for several different titrations of Indinavir with other monomers, correlated directly with the observed selectivity for polymers prepared with the respective monomers. It was also shown that the ITC detected three possible weak interactions that were occurring between MAA and Indinavir, which were not observed using ATR-FTIR. However, further chromatographic analysis will be needed to assess the impact of these interactions on polymer selectivity as it is believed that significant amounts of water present during polymer synthesis resulted in the disruption of hydrogen bonding between MAA and Indinavir.

Chapter 4. Investigation of Molecular Imprinted Polymer-Solid Phase Extraction

Introduction

Developed in the early 1970's as a sample pretreatment process for the analysis of pollutants in water, solid phase extraction (SPE) has become a popular choice for use in sample pretreatment for liquid and gas chromatography. Solid phase extraction is defined as the process by which an analyte in a liquid mobile phase will become retained by a solid adsorbent that is packed into a short cartridge. Figure 4-1 shows the basic components to a SPE cartridge.¹⁶⁴

SPE may be considered a four-step process, which is outlined in Figure 4-2. The first step is the conditioning of the adsorbent by passing a small volume of solvent through the cartridge prior to the application of the sample solution.¹⁶⁴ This serves to maximize the surface contact between the liquid and solid phases, ensuring good mass transfer of the analyte. The second step is the application of the sample solution to the cartridge. Analytes, as well as impurities, will become adsorbed onto the stationary phase, effectively becoming trapped inside the cartridge.¹⁶⁴ The third step involves washing the cartridge with a small volume of solvent that will cause the impurities trapped within the cartridge to elute, leaving behind only the analyte.¹⁶⁴ Finally, the fourth step, elution, is performed. Here, a solvent that is compatible for use in the desired instrumental method, is passed through the cartridge and elutes the analyte of interest. Thus in order to achieve high preconcentration factors, the elution solvent volume should be as small as possible.¹⁶⁴

While predominately used, by chromatographers as HPLC stationary phases for chiral separations, molecular imprinted polymers have become popular choices as stationary phases for

Figure 4-1. Schematic of a solid phase extraction cartridge. A typical cartridge will usually contain 300, 600, or 900 mg of sorbent with an average particle size of 40-50 μm . Adapted from Reference # 164

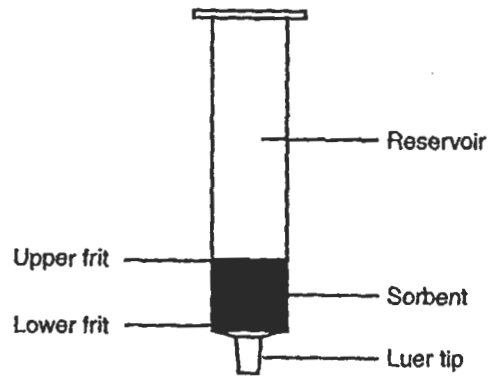
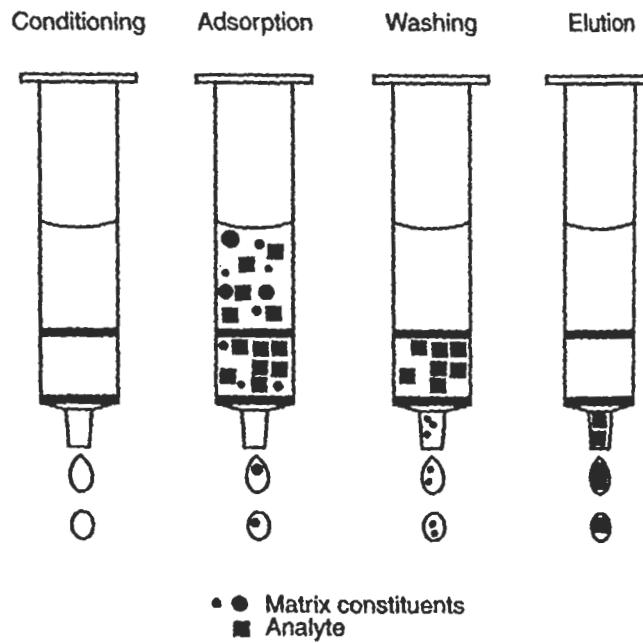


Figure 4-2. Illustration of the four basic steps in solid phase extraction. Adapted from Reference #164



SPE. As previously shown in Table 1-11, MIPs have been used to extract many different analytes from a variety of matrixes. This increase in usage is in part because SPE is not greatly affected by the broad peaks that are a major problem with MIP-HPLC. Additionally, MIPs offer a couple of advantages over conventional SPE phases. First, the pre-determined selectivity allows for the potential of a highly efficient sample clean up, particularly from complex matrices, such as biological fluids.⁸³ Second, it was reported that greater sensitivity could be achieved because straightforward extraction from large sample volumes would be possible.¹⁵

However, several fundamental questions concerning MIP-SPE remain unanswered. Specifically, we are concerned about understanding the relationship between MIP selectivity and SPE cartridge efficiency and the resulting impact on practical MIP-SPE method development. Failure to understand this basic relationship and its impact on overall performance, will lead to erroneous interpretation and conclusions of MIP-SPE experiments. The relationship between selectivity and efficiency comes from basic chromatographic theory. In column chromatography, there are two basic concepts that are actively governing the separation process, retention and band broadening. For this discussion, an SPE cartridge can be considered analogous to a liquid chromatography column.

In liquid chromatography, the analyte is injected onto the stationary phase and moved through the column by pumping a liquid mobile phase through the column. At some point, the analyte will emerge from the column as a peak. The volume at which the highest detector response occurs is denoted as the retention volume (V_r).¹⁶⁴ Commonly, a non-retained marker is also injected at the same time, and its retention volume is reflective of the column dead volume (V_0).¹⁶⁵ Historically, the parameter most commonly associated with the description of analyte

retention is the 'capacity factor' or 'retention factor', k . The retention factor is related to the retention volume by the relationship:

$$k = (V_r - V_o) / V_o \quad (4-1)^{165}$$

or

$$V_r = V_o(1 + k) \quad (4-2)^{164}$$

The shape of the peak as it emerges from the column is controlled by the efficiency of the column. Efficiency is a measure of the analyte band broadening as it moves through column and is dependent upon various physical parameters such as particle size, column length, and flow rate. High band broadening translates into low efficiency, or a broad peak, while low band broadening translates into higher efficiency, or a sharp peak.¹⁵⁶ Efficiency can be expressed as the number of theoretical plates (N) within the column and can be calculated from the chromatogram using the relationship:

$$N = 16 (t_r / w_b)^2 \quad (4-3)^{165}$$

Where, t_r is the retention time and w_b is the width at the base of the peak. Since the number of plates is dependant on column length, the term plate height or height equivalent to a theoretical plate (h) is more commonly used to describe column efficiency and is calculated by dividing the column length by the number of theoretical plates.¹⁶⁶

The term resolution (R) is used to describe the overall separation process between two components and is used to indicate the degree that two components are separated. Two components are considered completely separated, or resolved, if the resolution is greater than 1. This term incorporates both the influence of retention and efficiency and is described below:

$$R = (\sqrt{N}/2) [(k_2 - k_1) / (k_2 + k_1 + 2)] \quad (4-4)^{165}$$

With these basic relationships in mind, we can now try to understand these affects on MIP-SPE. First, consider how the cartridge efficiency will impact the extraction process. The Van Deemter equation is well recognized for describing the band broadening process by relating height equivalent to a theoretical plate (h) to mobile phase velocity.¹⁶⁶ It consists of three terms: multiple path of an analyte through the column packing (eddy diffusion), molecular diffusion (longitudinal band broadening), and effects of mass transfer between phases.¹⁶⁵ Its general form is written as

$$H = A + B/u + Cu \quad (4-5)^{166}$$

or

$$H = 2\lambda d_p + 2(\gamma D_m)/u + (\omega d_p^2/D_m)u \quad (4-6)^{165}$$

Where

λ = coefficient dependent on the particle sized distribution

d_p = average particle diameter

γ = factor which is related to the diffusion restriction by column packing

D_m = analyte diffusion coefficient in the mobile phase

ω = coefficient determined by the pore size distribution, shape, and particle size distribution

u = mobile phase velocity

As shown, the A term represents the influence that the particle diameter and particle size distribution have on efficiency. Within the cartridge, there are channels between the particles, thus each analyte molecule can take a different path as it travels through the column. By using smaller diameter particles, coupled with a narrow distribution range in size, this will translate into more even spacing between particles, reducing the magnitude of λ and d_p and consequently

lowering the overall plate height.^{157,165} However, for use with MIP materials, this term will play a significant role in reducing efficiency. As stated before, the common method for preparing MIPs for use in chromatography is by grinding and sieving. This method creates irregular shaped particles whose size distribution is large (25-38 μm) compared to traditional silica phases, resulting in a large value for d_p as well as for λ . Also, there is poor control over the ability to pack SPE cartridges, which will ensure uneven packing of the particles and further increase λ . Overall this will translate in very uneven spacing between particles, resulting in significant differences in column path length. Therefore it is reasonable to conclude that this term will significantly impact the cartridge efficiency.

The B term or longitudinal diffusion refers to the diffusion that the analyte will undergo along the column axis. This term is impacted primarily on the diffusion coefficient of the analyte in the mobile phase (D_m) and the mobile phase velocity.¹⁶⁵ For standard HPLC phases, molecular diffusion is approximately five orders of magnitude lower than that in the gas phase, thus D_m can be considered negligible for conventional flow rates. For an MIP-SPE cartridge, it would be expected that this would be true as well. The very short cartridge length coupled with the speed at which the mobile phase is pulled through the cartridge should not allow molecular diffusion to be a dominate force in the band broadening process.

The C term or kinetics of mass transfer refers to the process by which the analyte will diffuse from the mobile phase and interact with the stationary phase, either through adsorption onto the surface or diffusion inside the particle pores.¹⁶⁵ For MIP-SPE it is expected that ω and the particle diameter will play a significant role. As stated before, the MIP-SPE cartridge will be expected to have irregular shaped particles along with a large distribution in size. Thus it will be

expected to have a larger ω value compared to other SPE stationary phases, and consequently a larger overall plate height.

Thus it is expected that the overall efficiency of the extraction cartridge will be very poor, resulting in significant decreases in the amount of time as well as the surface area with which an analyte will have time to interact. Therefore resolution must be achieved by very high selectivity, through strong interactions between the analyte and polymer phase. As shown earlier, large retention factors are possible for MIP based systems. However, these retention factors are the result of a precise steric and chemical fit within the polymer binding sites, rather than general non-specific interactions. Additionally, it was also demonstrated that kinetics of these interactions are much slower than other non-specific interactions as demonstrated by the very broad peaks observed in HPLC. Therefore, it is logical to assume that with such a poor efficiency, there may not be enough time in SPE, for the selective interactions to occur. Thus a theoretical limit must exist as to the specificity of the MIP interactions. If the interactions are very selective it will take longer for them to fully occur and therefore can't overcome the poor efficiency. On the other hand less selective interactions may occur fast enough that the poor efficiency may be overcome.

As demonstrated in the prior set of experiments, less selective interactions will result in decreased enantioselectivity between other structurally related compounds. It is to be expected that the sample matrix will contain other similar components, such as metabolic products, and that their presence would cause a competition for binding sites. If the quality of the available binding sites is reduced, a greater competition between analytes for the binding sites will occur, further reducing the ability to generate a selective interaction.

The goal of these experiments was to evaluate an MIP-SPE method for *cinchona* alkaloids on several different polymers, each of which possesses different degrees of selective interactions, in an attempt to understand the relationship between the efficiency and selectivity. As demonstrated in the prior sets of experiments, by changing the amount of monomer within the polymer system in relation to the amount of the template, several polymers were made that possessed poor enantio-recognition (1:1) as well as very good enantio-recognition (4:1). By using these polymers, for which the retention factors of different components are known, a much better understanding of the fundamental processes occurring during the extraction may be better understood.

Experimental

Reagents

Methacrylic acid (MAA), ethylene glycol dimethacrylate (EGDMA), and 2,2'-azobisisobutyronitrile (AIBN), sodium dihydrogen phosphate, phosphoric acid (85%), and sodium perchlorate were obtained from Aldrich (Milwaukee, WI). Cinchonidine and Cinchonine were obtained from Spectrum Chemicals (New Brunswick, NJ), while Quinine and Quinidine were obtained from Fluka (Milwaukee, WI). All solvents were HPLC grade with Acetonitrile and Methanol obtained from Aldrich (Milwaukee, WI), chloroform (optimo grade) obtained from Fisher (Milwaukee, WI), and acetic acid obtained from Pharmco (Brookfield, CT). Purified water was obtained using a Millipore filtration system.

Instrumentation

Gas Chromatography

All gas chromatography experiments were carried out using an Agilent (Palo Alto) 5890 Series II Gas Chromatography equipped with an Agilent 7673A auto sampler and an Agilent 5972 mass selective detector. Data analysis was done using Chemstation software (Agilent, Palo Alto, CA).

The following instrument parameters were used:

1. Inlet Temperature: 280°C
2. Transfer Line Temperature: 250°C
3. Temperature Program: 200°C with a rate of 20°C/min until a final temperature of 280°C was reached. The temperature was then held for two minutes.
4. Detection Mode: Detector was operated in single ion monitoring (SIM) mode at a m/z ratio of 136.
5. Injection Volume: An injection volume of 1µL was used.

HPLC Analysis

The HPLC system consisted of either a Perkin Elmer (San Jose, CA) ISS 200 system with Diode Array Detector using Turbochrom Software or an Agilent (Palo Alto, CA) 1100 system with Chemstation software and utilized a phenomenex 5µm C18 (4.6 mm x 150 mm) column (Torrence, CA) as the stationary phase. The mobile phase was an 85% aqueous phosphate buffer (10 mM sodium dihydrogen phosphate) with 25 mMol of sodium perchlorate dissolved in it. Phosphoric acid was used to adjust the pH to 2.4. The organic modifier was 15% HPLC grade acetonitrile. The mobile phase was pumped at a flow rate of 1.0 mL/min and the diode array detector set to 280 nm.

Polymer Synthesis

Polymers were prepared according to the procedures described elsewhere.

Molecular Imprinted Polymer-Solid Phase Extraction

Preparation of MIP-SPE Cartridges

Prior to extraction, approximately 0.7 g of polymer particles, with a size of 25-38 μM , was slurried packed into a stainless steel HPLC column and washed on an HPLC system using the following method:

1. 5 hrs of 7:3 Methanol/Acetic Acid (1 mL/min)
2. 5 hrs of 7:3 Acetonitrile/Acetic Acid (1 mL/min)
3. 5 hrs of 7:3 Chloroform/Acetic Acid (1 mL/min)
4. Methanol until constant baseline (1 mL/min)

After washing, the particles were removed from the column and dried under vacuum.

Approximately 0.5 g of material was then slurried in Acetonitrile and packed at -20 psi into an empty solid phase extraction tube containing an inert frit. After the solvent had been suctioned away another inert disk was placed on top of the polymer and then compressed evenly using a glass stirring bar to form the final cartridge.

Breakthrough Volume

As previously discussed, in column chromatography, the analyte is injected onto the stationary phase and moved through the column by pumping a liquid mobile phase through the column. At some point, the analyte will emerge from the column as a peak possessing a Gaussian distribution shape. The volume at which elution occurs is denoted as the retention volume (V_r) and is related to the retention factor by the relationship

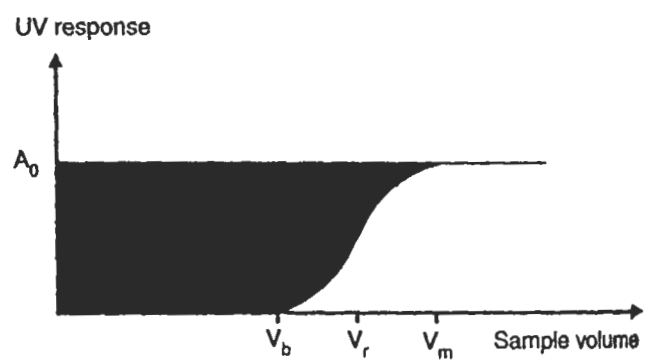
$$V_r = V_o(1 + k) \quad (4-2)^{164}$$

where V_o is the volume of liquid within the system from the injector to the detector.

In the case of SPE, the sample solution itself is the mobile phase and upon elution from the column will exhibit a peak shape similar to that in column chromatography. However, rather than achieving a maximum followed by a constant decrease, as is the case with column chromatography, more sample solution will continue to flow into the cartridge until the amount of analyte entering the column is equal to the amount of analyte eluting from the column. This process is illustrated in Figure 4-3.¹⁶⁷ The point at which the analyte first elutes from the packed column is called the breakthrough volume. (V_b) Larger breakthrough volumes will allow for greater sample volumes to be applied to the cartridge.¹⁶⁷ The shape of this of this peak is dependent upon the efficiency, or number of theoretical plates (N), that are generated by the stationary phase. If N is large, then the peak will be sharper, which is advantageous for SPE because the breakthrough volume will occur later.¹⁶⁴ However, most conventional SPE phases do not generate high numbers of theoretical plates due to the inefficient packing process and larger sized particles. Therefore in order to develop a strong extraction for a particular analyte such that it has a large breakthrough volume, a large retention factor is necessary.¹⁶⁴

For an imprinted polymer, the retention factor is dependent upon the quality of the imprinted sites and the selective recognition that they have for a particular analyte. This should translate into increased breakthrough volumes for the imprinted analyte, while other analytes should have smaller breakthrough volumes. However, with MIP based phases, the interactions are not general interactions, such as hydrophobic interactions, but rather are based on the precise steric fit of an analyte into the binding cavities. These hindered interactions may not occur kinetically fast enough relative to the flow rate of extraction. Thus by measuring the

Figure 4-3. Theoretical breakthrough volume curve for a SPE cartridge. Adapted from Reference # 164



breakthrough volumes for different analytes on several selective polymers, an estimation as to the relationship between efficiency and retention can be made.

Breakthrough Volume: Sample Preparation

Standard solutions of cinchonidine and cinchonine were prepared by dissolving 0.01 g into 10 ml of chloroform to yield a stock solution of 1000 $\mu\text{g/mL}$. Volumetric pipets were used to prepared 10 ml standards from the stock solution so that a range from 1-500 $\mu\text{g/mL}$. For breakthrough volume determinations, 0.05 g of analyte was dissolved into 100 mL of chloroform to yield a final concentration of 500 $\mu\text{g/mL}$. A 2.0 mL portion was passed through the column using only gravity to generate a flow. This fraction was collected in a clean test tube, placed in a sample vial, and analyzed using GC/MS. This was repeated for each analyte four times.

Batch Binding Studies

Batch binding experiments were performed by placing 0.150 g of either a blank imprinted polymer or a 4:1 imprinted polymer into a 4.5 mL vial with 4.0 mL of a chloroform solution, with a known analyte concentration, to yield the initial amount of template at the start. A stir bar was added to the vial, followed by tightly capping it and allowed to stir for 30 minutes. After stirring, the vial was uncapped and secured using a clamp and a 1.0 mL volumetric pipet was slowly inserted into the vial. After 10 minutes, a 1.0 mL aliquot was pulled out and placed into a clean vial and evaporated to dryness, using a heating block. 1.0 mL of a suitable solvent was then added to the vial to reconstitute the sample and the vial was capped and placed in a sonicator for 10 min. After sonication the sample was transferred with a clean glass pipet to an auto sampler vial and analyzed by HPLC.

Results and Discussion

Molecular Imprinted Polymer-Solid Phase Extraction

Cartridge Inertness

Prior to packing the MIP material, the components of the extraction cartridges were fitted together and analyzed to ensure that they were inert and that non-specific adsorption was not occurring. Separate samples of cinchonidine and cinchonine, 2 mg/mL, in chloroform were prepared and extracted according to the procedure above. The peak areas were recorded and compared to the peak area of a control (2 mg/mL) sample. The results indicated that nearly all of the analyte passes through the cartridge, indicating that the components are not exhibiting any interactions with the analytes.

Breakthrough Volume Curves

As discussed previously, HPLC was used to determine the retention factor for cinchonidine, cinchonine, quinine, and quinidine on a 4:1 imprinted polymer and these are listed in Table 4-1. Based on this it would be expected that cinchonidine should possess a higher breakthrough volume than its diastereomer cinchonine. This is due to the fact that the retention factor for cinchonidine (37.38) is significantly larger than that of cinchonine (1.51), indicating that cinchonidine has significant interactions with the stationary phase. Based on equation 4-2, it is expected that cinchonidine should exhibit a larger breakthrough volume compared to cinchonine.

Breakthrough volume curves were generated by plotting the concentration of analyte present versus the total volume of sample passed through the cartridge. Figures 4-4 and 4-5 are representative breakthrough volume curves for cinchonidine and cinchonine respectively. Based

Table 4-1. Retention factors obtained on a 4:1 methacrylic acid/cinchonidine imprinted polymer.

Analyte	Retention Factor
Cinchonidine	37.38
Cinchonine	1.51
Quinine	6.47
Quinidine	0.62

Figure 4-4. Initial breakthrough volume curve for cinchonidine.

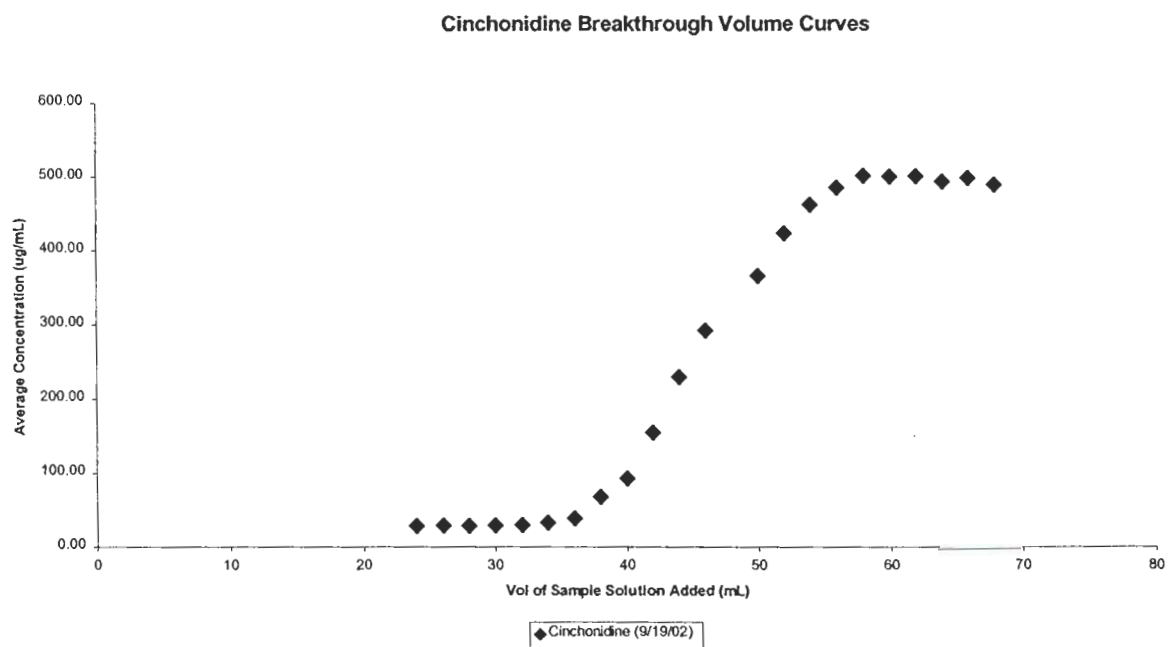
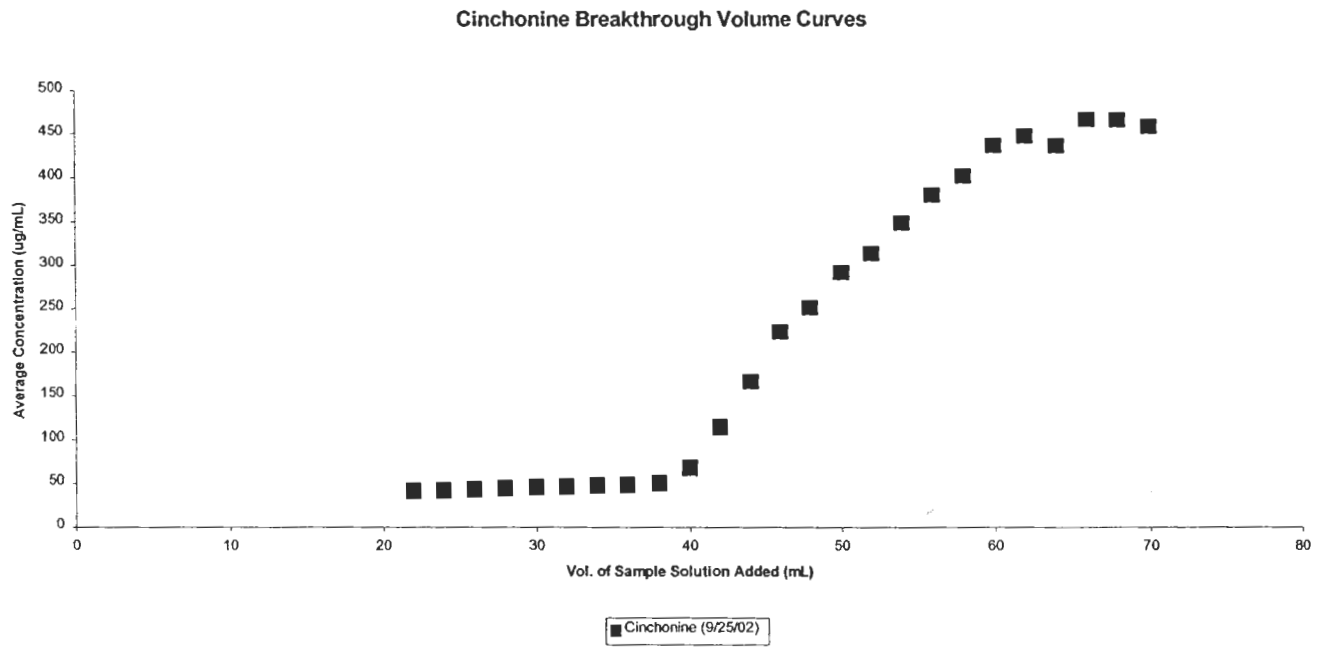


Figure 4-5. Initial breakthrough volume curve for cinchonine.



on initial examination, it appeared that cinchonine has a larger breakthrough volume, 22 mL, than that of cinchonidine, 20 mL, which would be opposite the anticipated results. To evaluate this further, the experiment was repeated three more times and all of the results are displayed in Figures 4-6 and Figures 4-7, which show the breakthrough volume curves obtained for cinchonidine and cinchonine. Examination of the data suggests that cinchonine has a larger breakthrough volume than that of cinchonidine, although given the experimental error, both experimental breakthrough volumes can be considered identical indicating that it is interacting. This may be explained by two possible causes. The first cause may be attributed to the fact that chloroform is less polar than the functional groups on the polymer. This would cause both analytes to engage in non-specific adsorption interactions with the surface, thus retention is simply governed by the surface area exposed to the analyte. This could be corrected by the addition of a mobile phase competitor, such as acetic acid, which would help increase the polarity of the mobile phase, eliminating the non-specific adsorption. The second possible explanation is that the kinetics governing the formation of the interaction between cinchonidine and the polymer are too slow compared to the speed at which the extraction is occurring. As demonstrated in prior HPLC work, cinchonidine has significantly broad peaks, suggesting that these interactions may not be kinetically favorable for solid phase extraction.

Mobile Phase Competitor

By adding a weak competitor, such as acetic acid, in low percentages, it is possible to disrupt the non-specific interactions, such as surface adsorption, and allow the selective interactions to dominate the retention process. Additionally, the addition of a competitor may help to properly balance the relative polarities of the sample solvent and polymer, facilitating the

Figure 4-6. Complete set of breakthrough volume curves for cinchonidine.

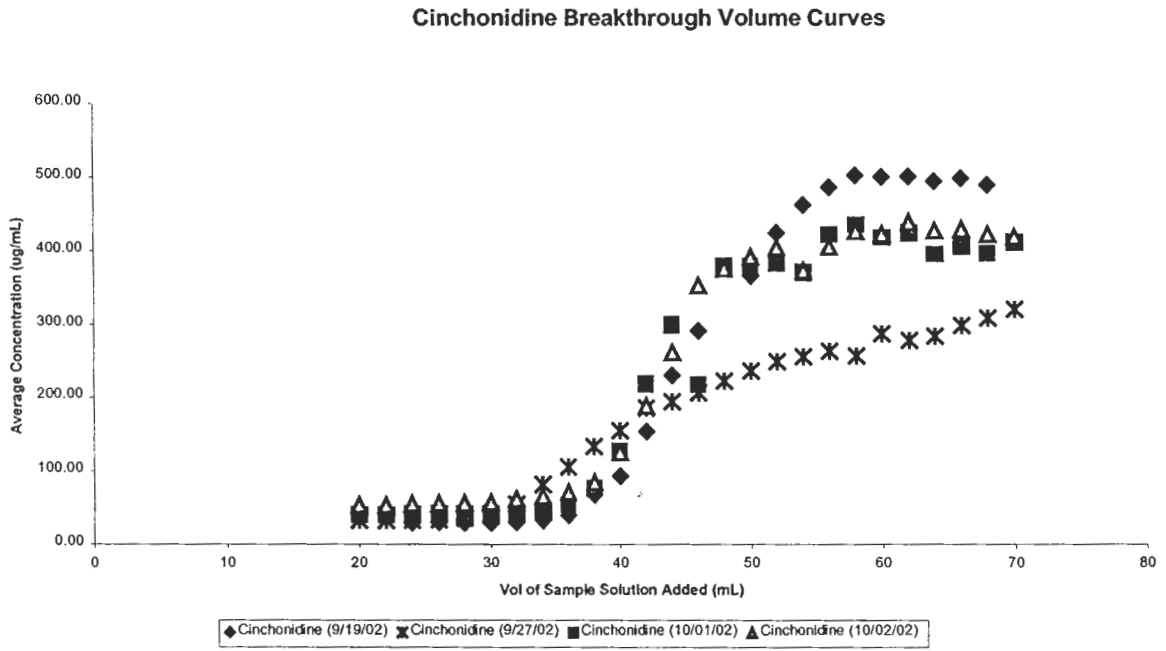
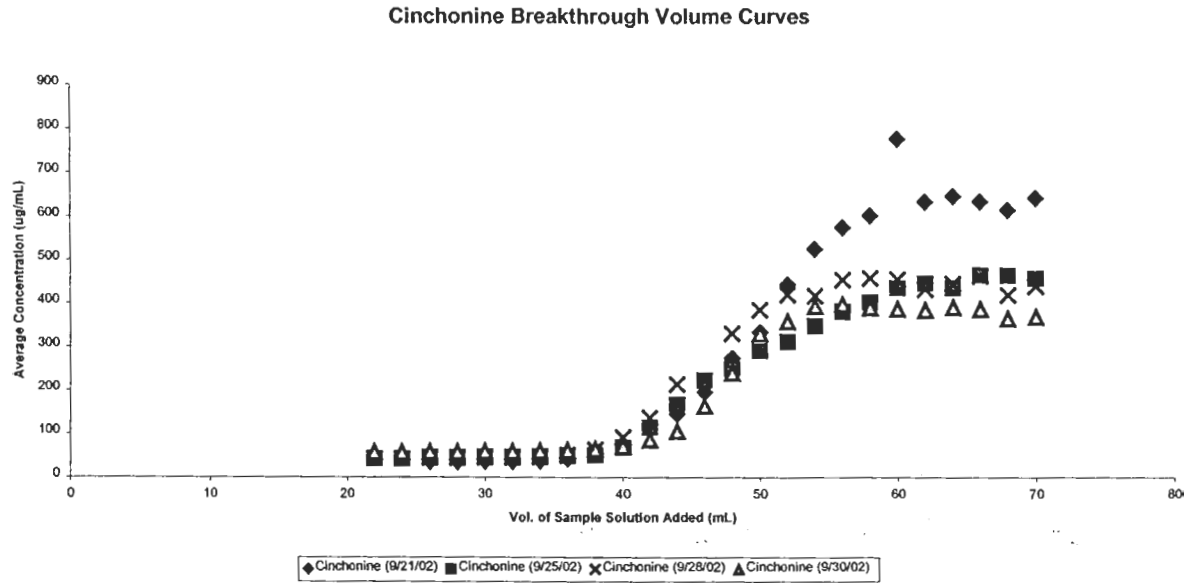


Figure 4-7. Complete set of breakthrough volume curves for cinchonine.



formation of selective interactions. Therefore, different percentages of acetic acid were studied, through batch binding analysis, as a possible solution to generating selective binding.

The results of these experiments, Table 4-2, show that the addition of a small amount of acetic acid to the sample solution does indeed allow for selective interactions to occur. A comparison between the recovery for the blank polymer and the recovery for the imprinted polymer, shows that there is a difference in analyte concentration especially with very low percentages. The largest difference occurred around 0.35% acetic acid, as the blank polymer exhibited a recovery of 61% while, the imprinted polymer yielded a recovery of 5%. Based on this it was determined that all further batch binding analysis would utilize a 0.35% Acetic Acid in chloroform solution. Analysis of solutions that contained no acetic acid, showed low recovery as well as significant non-specific interactions occurring with the polymer phase.

The next set of experiments was aimed at understanding the poor recovery of cinchonidine. Cinchonidine dissolves most easily in chloroform and in most alcohols such as methanol, ethanol, and isopropanol. The above experiments utilized a 50/50 methanol/water (v/v) solution, which should easily dissolve the low levels of cinchonidine. However, as the data shows, recovery of control samples are still very low and not very reproducible, two factors that must be corrected in order for further analysis to proceed.

Recovery Studies

Initial studies of elution solvents focused on methanol solutions that were spiked with glacial acetic acid and concentrated hydrochloric acid so that each acid represented 1% of the total volume. Recovery analysis was performed by placing a 1.0 mL sample solution, whose concentration was 72 µg/mL, into a vial and sealing it. Using a heating block, the sample was

Table 4-2. Results from acetic acid studies.

Sample	µg Recovered	% Recovered
0.20 % ACA (Control)	47.89	63.85
0.20 % ACA (Blank)	145.86	48.62
0.20 % ACA (Control)	46.58	62.11
0.20 % ACA (4:1)	20.88	6.96

Sample	µg Recovered	% Recovered
0.35 % ACA (Control)	44.68	59.57
0.35 % ACA (Blank)	183.43	61.14
0.35 % ACA (Control)	57.16	76.22
0.35 % ACA (4:1)	16.07	5.36

Sample	µg Recovered	% Recovered
0.50 % ACA (Control)	58.53	78.04
0.50 % ACA (Blank)	217.57	72.52
0.50 % ACA (Control)	58.98	78.64
0.50 % ACA (4:1)	156.78	52.26

Sample	µg Recovered	% Recovered
1.00 % ACA (Control)	56.71	75.61
1.00 % ACA (Blank)	213.37	71.12
1.00 % ACA (Control)	55.49	73.98
1.00 % ACA (4:1)	167.18	55.73

evaporated to dryness. In all cases recovery was very low, between 30-50%.

The next choice for a recovery solvent was tetrahydrofuran (THF). A 50/50 THF/Water mixture (v/v) and a 100% THF solution were used in an attempt to generate sufficient recovery of cinchonidine. The results in Table 4-3 reveal that 90% or better recovery is obtained, which was the desired minimum target for these studies. However, evaluation of the HPLC chromatograms revealed that a new component was now present. After determining that the peak was not the result of a contaminated solvent or compound, further studies were performed using varying percentages of THF as a diluent. As shown in Figure 4-8, a diluent using 20/80 THF/water (v/v) shows significant fronting indicating some secondary equilibria occurring on the column. Upon increasing the THF to 30%, the emergence of the second peak in front of the analyte is observed, as shown in Figure 4-9. Finally, upon increasing the THF to 50%, the two peaks are baseline resolved as shown in Figure 4-10. This effect, which is attributed to mismatched polarities between the diluent and mobile phase, significantly decreased sensitivity as the limit of detection increased an order of magnitude from 1 $\mu\text{g/mL}$ using methanol/water as a diluent to 10 $\mu\text{g/mL}$. Since, it was anticipated that future experiments would require the lowest possible detection limit, coupled with the fact that at least 50% THF was needed to get a 90% recovery, THF was eliminated as a possible elution solvent.

Finally, several different acetonitrile/water mixtures were examined, even though the solubility of cinchonidine is not large in acetonitrile. Two acetonitrile/water mixtures were tried along with pure acetonitrile as possible recovery solvents. Surprisingly, the problem of mismatched diluent:mobile phase polarities that was present for THF was also present for acetonitrile.

Table 4-3. Recoveries obtained using THF as the reconstitution solvent.

Top: Quantitation from first peak

Bottom: Quantitation from second peak

Sample	µg Recovered	Recovery %
50/50 THF/Water	88.12	91.79
50/50 THF/Water	88.11	91.78
100% THF	104.11	108.45
100% THF	107.89	112.38

Sample	µg Recovered	Recovery %
50/50 THF/Water	75.60	78.75
50/50 THF/Water	75.12	78.25
100% THF	41.59	43.32
100% THF	42.11	43.87

Figure 4-8. HPLC chromatogram obtained using a 20/80 THF/Water mix as the sample diluent.

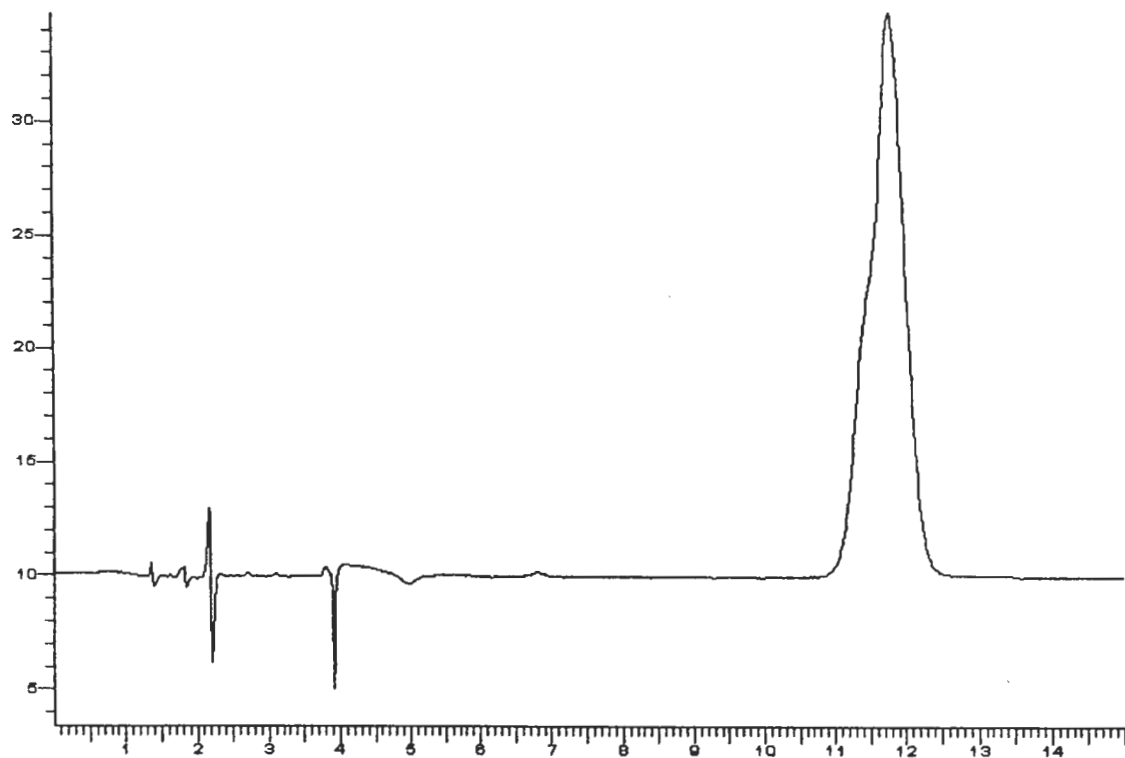


Figure 4-9. HPLC chromatogram obtained using a 30/70 THF/Water mix as the sample diluent.

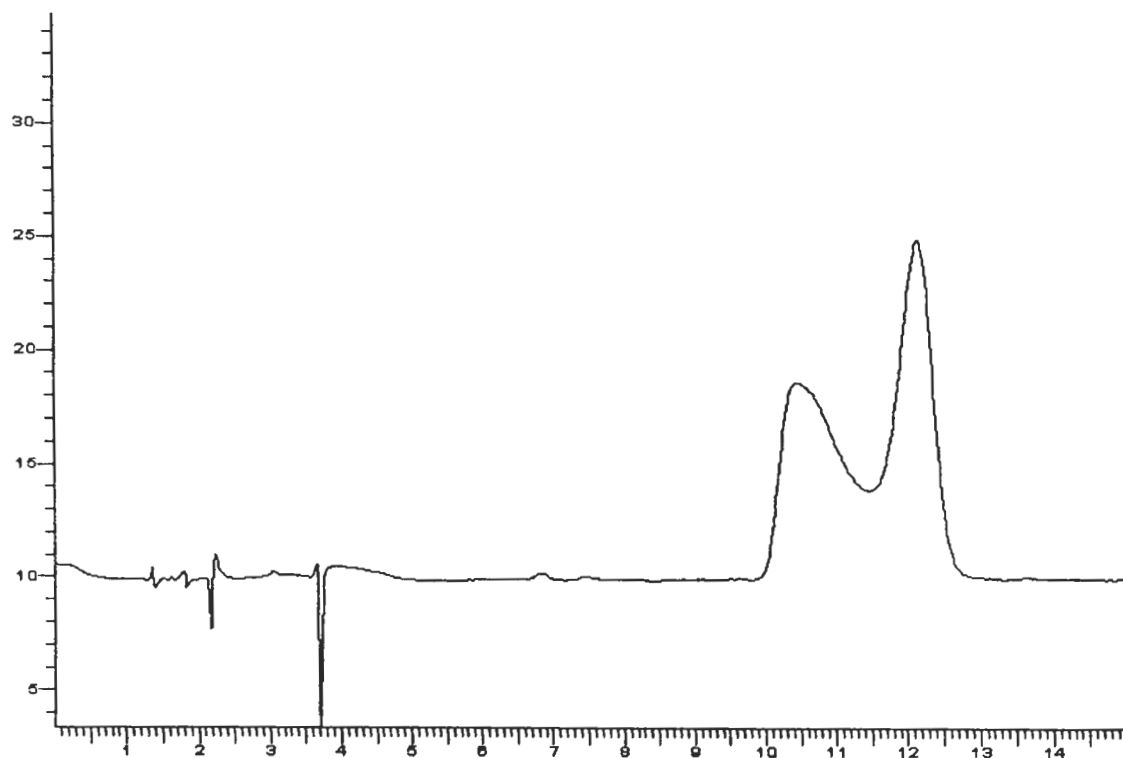
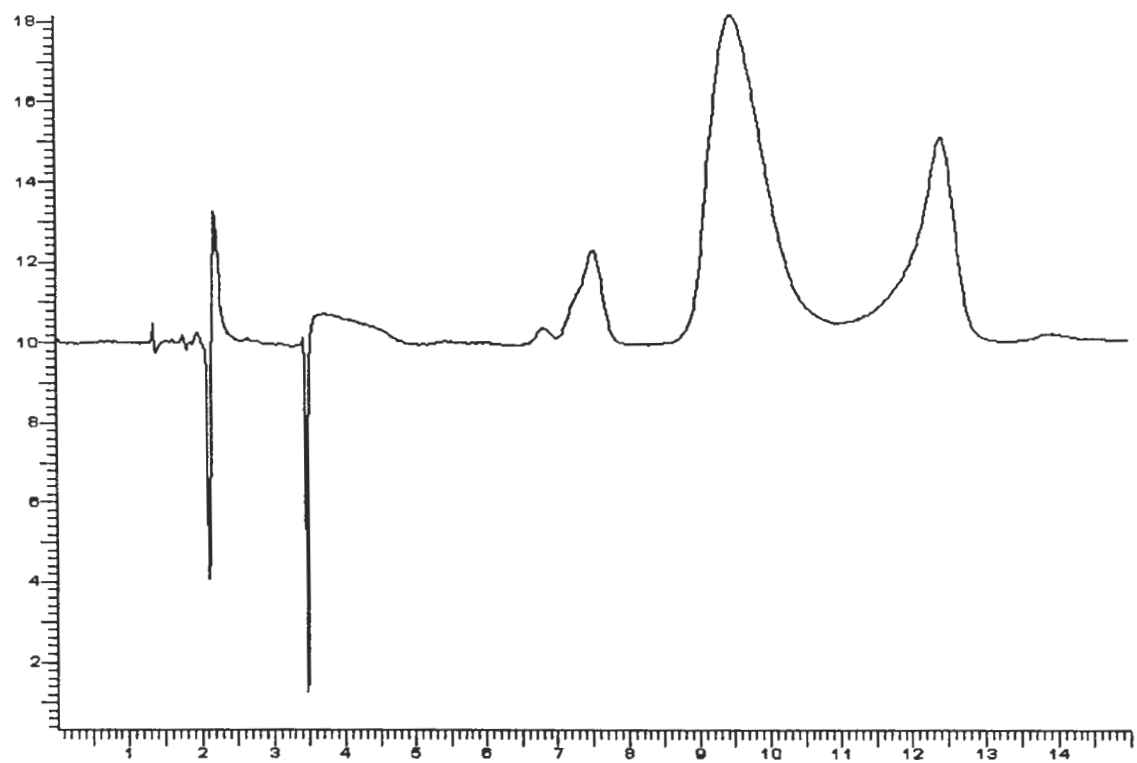


Figure 4-10. HPLC chromatogram obtained using a 50/50 THF/Water mix as the sample diluent.



However, this effect did not begin to appear until the diluent acetonitrile percentage reached 50%. An examination of recoveries for a 30/70 acetonitrile/water mixture (v/v), Table 4-4, revealed that this mixture was capable of recovering approximately 98 % of the cinchonidine from the standard sample. Additionally, no problems with solvent polarities (Figure 4-11) were observed when analyzed by HPLC and a limit of detection of 1 μ g/mL was achieved (S/N=6.5) for quantitative analysis. Therefore all further experiments will utilize a 30/70 acetonitrile/water mixture (v/v) as the recovery solvent.

Comparison between Blank and Imprinted

Upon optimizing solvent conditions for both binding and recovery, a set of batch binding experiments were performed on both the 4:1 and blank imprinted polymer to examine the extent of selective interactions. A series of solutions containing cinchonidine were prepared ranging from 125 μ g/mL to 750 μ g/mL and 4.0 mL of each solution was added to vials containing 0.15 g of the desired polymer, representing a range of 500 to 3000 μ g. As described previously, the amount of cinchonidine remaining in solution was quantitated and the amount bound to the polymer calculated. Table 4-5 shows the results achieved on the 4:1 imprinted polymer and the results achieved on the blank polymer. As shown, it appears that selective interactions are now occurring as demonstrated by the differences in the amount of cinchonidine bound to the imprinted polymer. A simple binding isotherm was constructed for each polymer by plotting amount of cinchonidine bound versus the amount of free cinchonidine and is shown in Figure 4-12. The blank polymer demonstrates a decreased ability to bind cinchonidine compared to the imprinted polymer. Additionally, the isotherm of the imprinted polymer shows that the maximum binding occurs around the addition of 3000 μ g, suggesting that the imprinted polymer

Table 4-4. Recovery results using acetonitrile and water.

Sample	µg Recovered	Recovery %
50/50 ACN/Water (88 µg)	91.91	104.45
50/50 ACN/Water (88 µg)	93.08	105.77
30/70 ACN/Water (80 µg)	77.63	97.04
30/70 ACN/Water (80 µg)	78.36	97.96

Figure 4-11. HPLC chromatogram obtained using a 30/70 ACN/Water mix as the sample diluent.

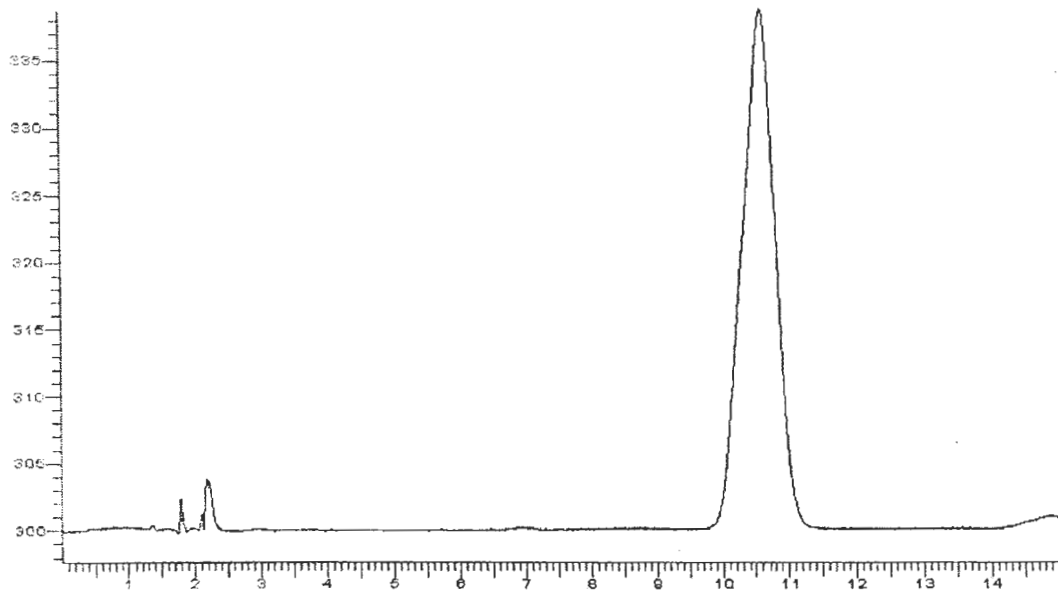


Table 4-5. Batch binding results obtained for several concentrations.

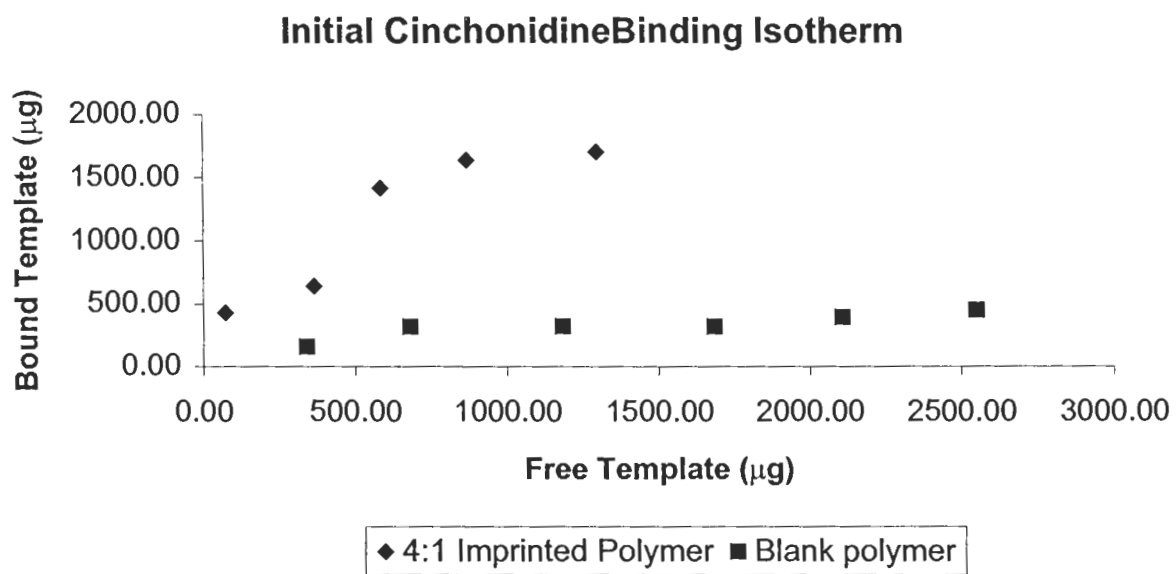
Top: Imprinted Polymer

Bottom: Blank Polymer

Sample	µg Recovered	µg Bound
500 µg	71.58	428.42
1000 µg	364.96	635.04
2000 µg	585.05	1414.95
2500 µg	866.55	1633.45
3000 µg	1297.67	1702.33

Sample	µg Recovered	µg Bound
500 µg	341.45	158.55
1000 µg	680.80	319.20
1500 µg	1182.10	317.90
2000 µg	1683.53	316.47
2500 µg	2108.58	391.42
3000 µg	2550.93	449.07

Figure 4-12. Initial cinchonidine binding isotherms generated for both a 4:1 imprinted and blank polymer.



has a maximum capacity of approximately 33 $\mu\text{mol/g}$ of polymer. Based on the above results, further batch binding experiments were performed under these optimal conditions and through scatchard plot analysis, an understanding as to the binding occurring within the polymer system was made.

Scatchard Plot Analysis

In order to properly construct the Scatchard Plot, a wider range of concentrations needed to be used. It was found that unbound template could be detected in solutions whose starting amount was 60 μg . Based on this, a series of ten solutions, resulting in a range of 60-3000 μg of cinchonidine in solution was used to evaluate the 4:1 and the blank polymer. A calibration curve from 1.0 $\mu\text{g/mL}$ to 3000 $\mu\text{g/mL}$ was prepared for cinchonidine and is shown in Figure 4-13.

A binding isotherm was constructed for each polymer and is shown in Figure 4-14. As observed in earlier studies, the 4:1 polymer demonstrates an increased ability to selectively bind cinchonidine compared to the blank polymer. It is observed that the imprinted polymer has a maximum binding capacity of approximately 25 $\mu\text{mol/g}$ polymer versus 7 $\mu\text{mol/g}$ polymer, for the blank polymer which suggests that selective interactions are occurring. The data was also cast as a Scatchard Plot, which is shown in Figure 4-15. For the 4:1 polymer two distinct classes of binding sites are present as shown by the downward curve of the plot. These two regions are reflective of the heterogeneous nature of the imprinted polymer cavities. The steep downward portion of the plot represents the selective sites of interactions that are present in the polymer, while the flat portion represents the weak and non-specific sites of interaction. However, for the blank polymer it appears that only one class of binding sites are present as indicated by the near

Figure 4-13. Calibration curve for cinchonidine.

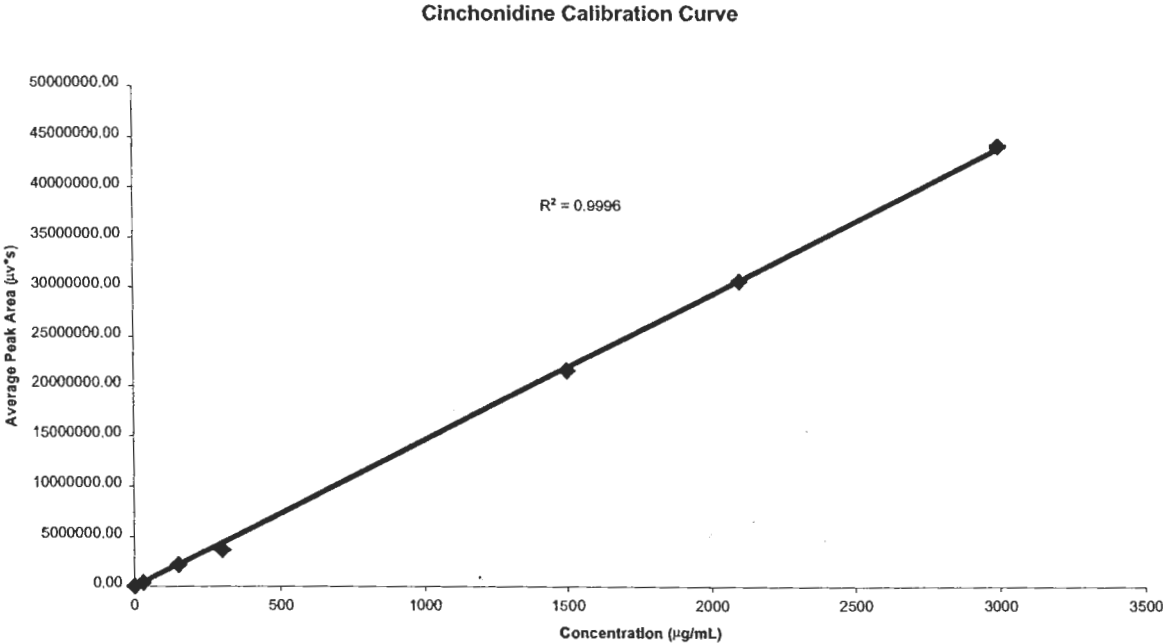


Figure 4-14. Cinchonidine binding isotherms for a 4:1 and a blank imprinted polymer.

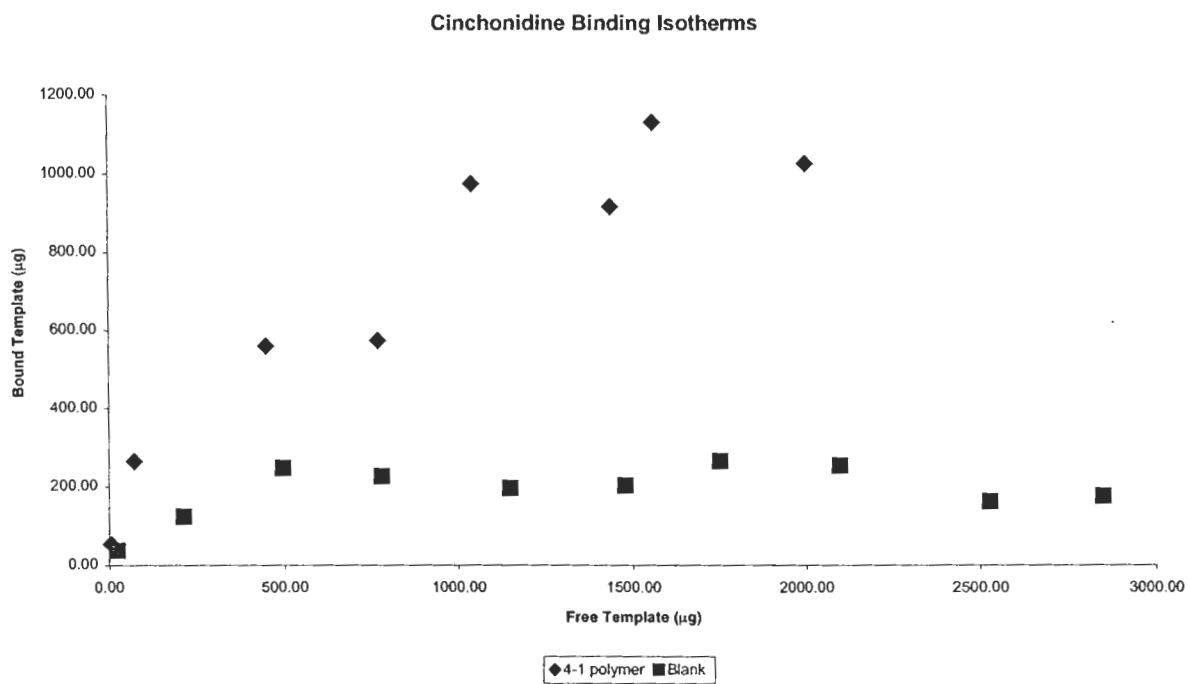
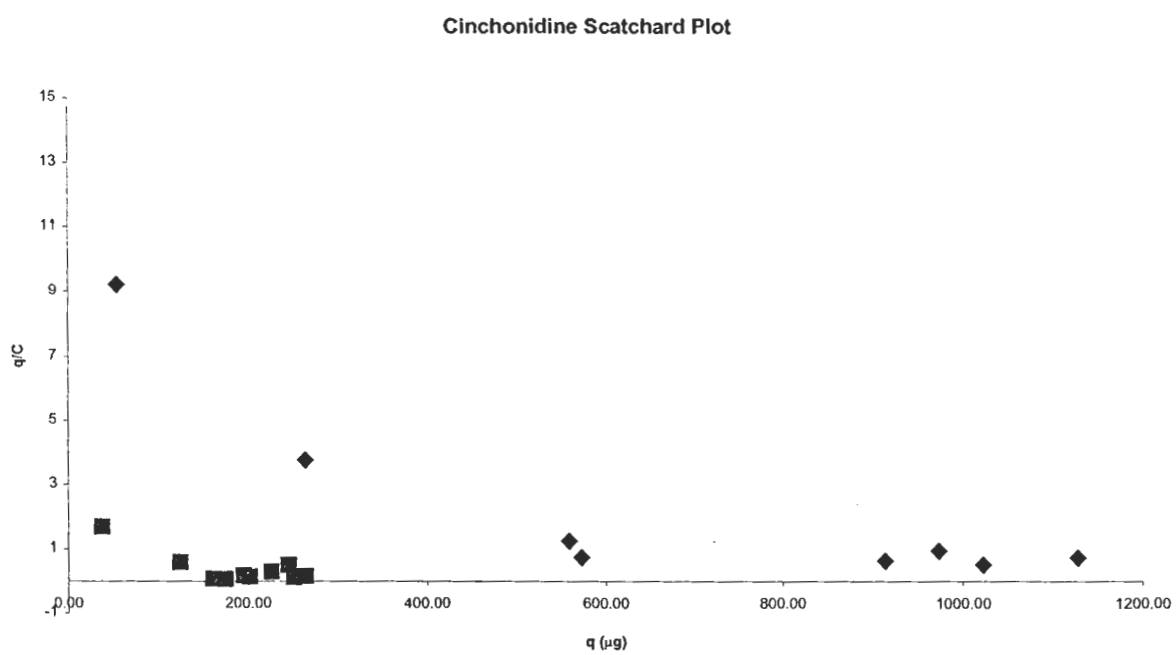


Figure 4-15. Scatchard plot analysis for cinchonidine binding.



linear curve. This is reasonable, as the blank polymer would be expected to only possess non-specific sites of interactions. Finally, each portion of the scatchard plot was analyzed and the binding constants as well as the number of selective sites were determined for both polymers and are presented in Table 4-6.

A comparison between the two binding constants for the 4:1 polymer shows that the selective interactions occurring in the strong region, $q = 4.42 \times 10^6 \text{ mol}^{-1}$, are approximately 200 times larger than those of the weak portion, $q = 2.36 \times 10^4 \text{ mol}^{-1}$, indicating that the polymer does possess strong, selective binding cavities. This is also supported by the fact that the binding constant is approximately 20 times larger than that of blank polymer, $q = 2.36 \times 10^5 \text{ mol}^{-1}$. The number of selective binding cavities was determined to be $13.9 \mu\text{mol/g}$ polymer, which is roughly 1% of the total number possible. The number of weak and non-specific sites was determined to be $222 \mu\text{mol/g}$ polymer, which is approximately 18.5% of the theoretical maximum. All together, the total number of binding sites present account for 20% of the theoretical maximum possible, which is consistent with other literature publications.

In order to further assess the selective nature of the imprinted polymer, the above studies were repeated with cinchonine, the diastereomer of cinchonidine. Cinchonine solutions, used in analysis as well as those for the calibration curve, were prepared over the same range as those used in the cinchonidine studies, with the cinchonine calibration curve shown in Figure 4-16.

Again, the data was cast as a simple binding isotherm, shown in Figure 4-17. It is observed that the imprinted polymer does demonstrate some interaction with cinchonine as shown by the difference in binding between the imprinted and blank polymers. It was calculated that the imprinted polymer had a binding capacity of approximately $20.4 \mu\text{mol/g}$ polymer versus $4.5 \mu\text{mol/g}$ polymer for the blank. This can be attributed to the imprinted polymer containing

Table 4-6. Scatchard plot analysis results for cinchonidine.

Strong Binding Region			
Polymer	b (mol⁻¹)	<i>n</i> (μmol/g)	Theoretical <i>n</i> (μmol/g)^a
4:1	4.42 x 10 ⁶	13.9	1200
Blank	Na	Na	Na

Weak Binding Region			
Polymer	b (mol⁻¹)	<i>n</i> (μmol/g)	Theoretical <i>n</i> (μmol/g)^a
4:1	2.36 x 10 ⁴	222	1200
Blank	2.36 x 10 ⁵	10.9	Na

- a. Represents the total number of binding sites possible based on the moles of MAA added to polymer system

Figure 4-16. Cinchonine calibration curve for binding analysis.

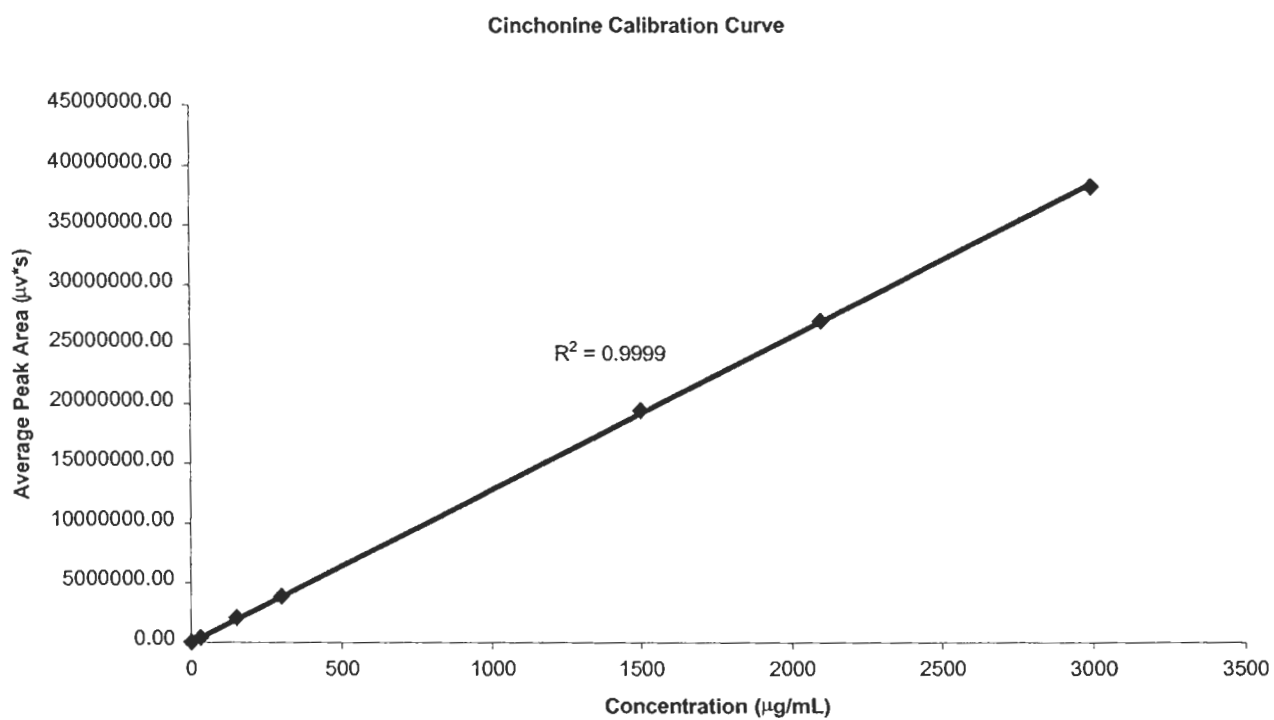
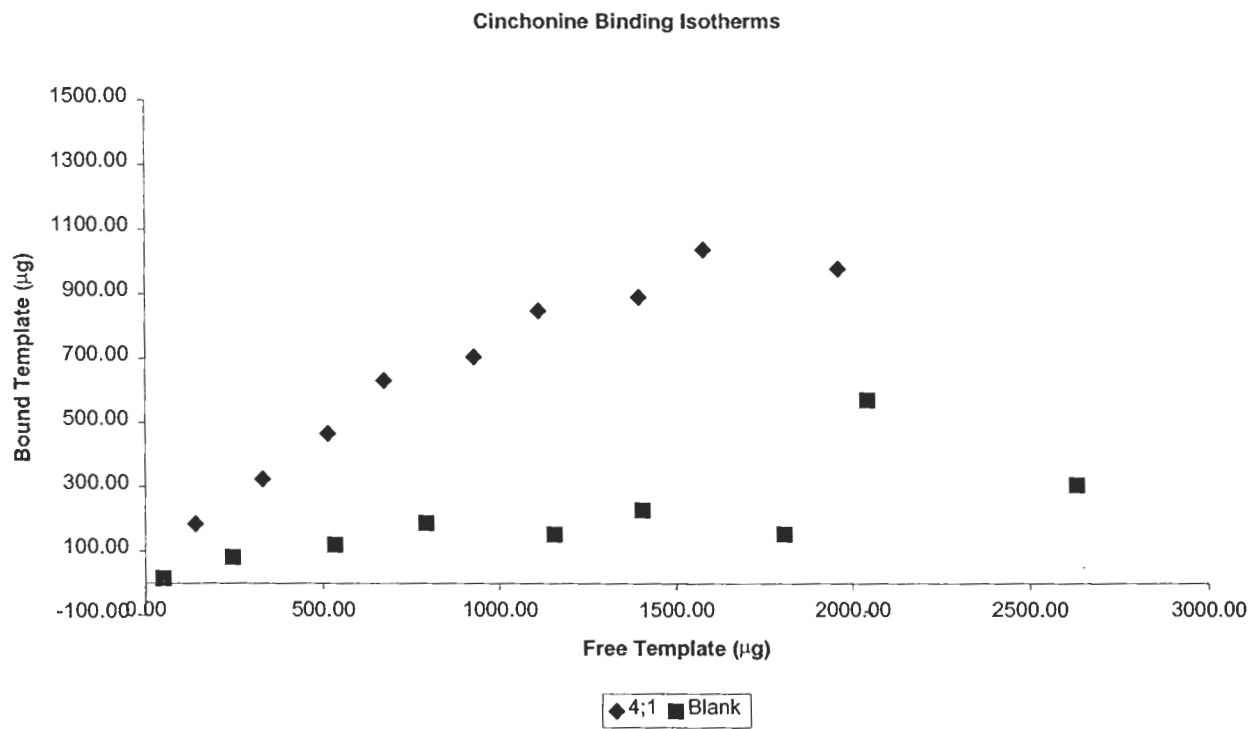


Figure 4-17. Cinchonine binding isotherms.



both weak sites of interactions as well as non-specific sites of interaction, where as the blank polymer would only possess non-specific sites of interaction. It is important to note that the imprinted polymer demonstrated a higher binding capacity for cinchonidine, 25 $\mu\text{mol/g}$ polymer compared to the binding capacity of cinchonine, 20.4 $\mu\text{mol/g}$ polymer, proving that the polymer does indeed possess binding sites selective only for cinchonidine.

Analysis of the scatchard plots prepared from the binding data, Figure 4-18, shows that for both polymers, only one class of binding sites are present for cinchonine further proving that selective interactions are occurring. Table 4-7 lists the binding constants and number of sites of interactions for both polymers. When compared to the data obtained from the cinchonidine studies, the binding constants are similar as the imprinted polymer had an observed binding constant of $2.06 \times 10^5 \text{ mol}^{-1}$ for cinchonine versus $2.36 \times 10^4 \text{ mol}^{-1}$ for cinchonidine. However, the number of weak interacting sites for the imprinted polymer is significantly different for cinchonidine than for cinchonine. Based on the cinchonine data, it was determined that the imprinted polymer possesses approximately 42.98 $\mu\text{mol/g}$ polymer of weak interacting sites, while using the cinchonidine data the number of weak interacting sites was calculated to be 222 $\mu\text{mol/g}$ polymer. This would seem reasonable as cinchonidine is the template molecule, so it would be expected that the majority of the weaker sites would more readily bind cinchonidine than cinchonine. Overall though, the data conclusively proves that a selective extraction is possible, provided that the experimental conditions are optimized to facilitate binding.

Figure 4-18. Scatchard plots for cinchonine binding.

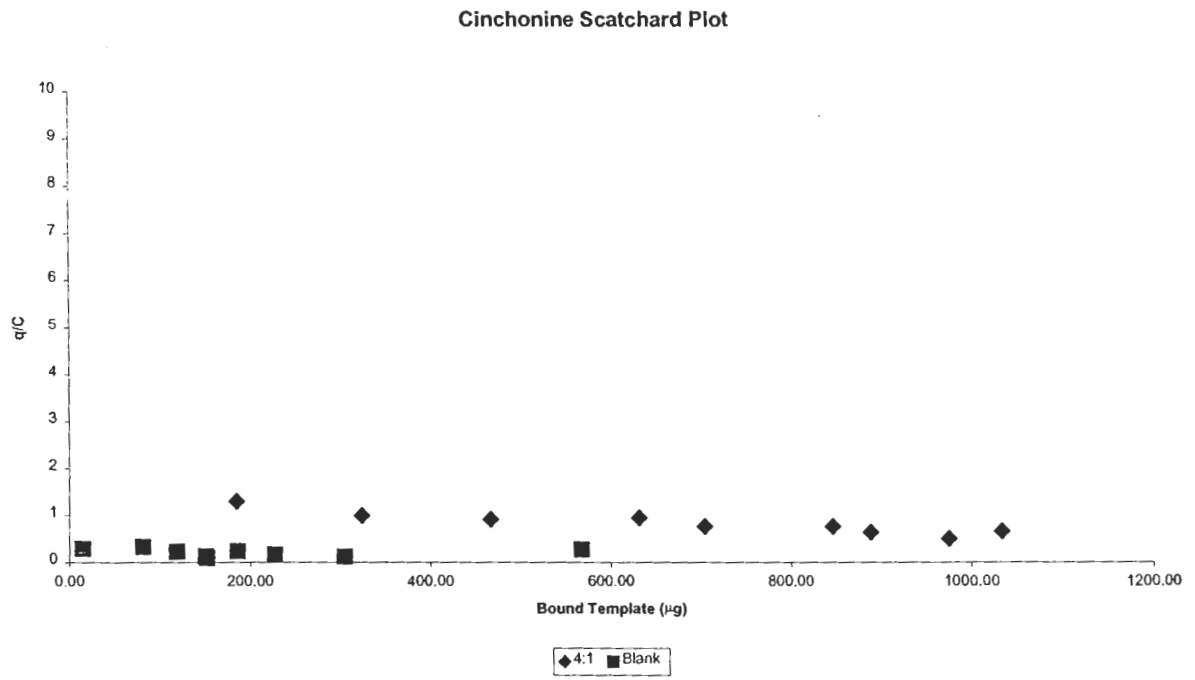


Table 4-7. Scatchard plot analysis results for cinchonine.

Strong Binding Region			
Polymer	b (mol⁻¹)	n (μmol/g)	Theoretical n (μmol/g)^a
4:1	Na	Na	1200
Blank	Na	Na	Na

Weak Binding Region			
Polymer	b (mol⁻¹)	n (μmol/g)	Theoretical n (μmol/g)^a
4:1	2.06 x 10 ³	42.98	1200
Blank	8.83 x 10 ³	158.51	Na

a). Represents the total number of binding sites possible based on the moles of MAA added to polymer system

Conclusion

A discussion concerning basic theoretical parameters relating to solid-phase extraction was presented. From this discussion, it was shown that there are two competing forces in generating a selective extraction, specifically cartridge efficiency and analyte retention. By using the Van Deetmer equation, it was shown that the MIP-SPE cartridge would have very low efficiency and that any selective extraction would have to be generated by high selective interactions.

Breakthrough volumes were determined for both cinchonidine and cinchonine on a cinchonidine imprinted polymer. It was predicted that cinchonidine would have the higher breakthrough volume, based on previously calculated retention factors. However, experimental results showed that cinchonine had a higher breakthrough volume, opposite of the predicted results. This raised the possibility that the kinetics of the interactions were too slow compared to the overall speed of extraction and that any retention was the result of non-specific interactions with the polymer.

In response to this, batch binding analysis was performed in order to remove any kinetic effects from the extraction process. Initial results suggested that the solvent conditions were not optimized to facilitate a selective extraction. In addition, it appeared that solvent conditions were not fully optimized to generate a large recovery. A mobile phase competitor, acetic acid, was investigated as a possible solution to the problems occurring during binding. Several solutions containing small percentages of acetic acid were examined and it was found that the addition of 0.35% acetic acid (v/v) resulted in noticeable differences in recoveries between a blank and imprinted polymer, providing the first evidence that selective interactions were occurring. Additionally, many different solvents were investigated for use in reconstitution. It was

discovered that both Tetrahydrofuran and acetonitrile in combination with water allowed for recoveries greater than 90%, however, the use of these mixtures in HPLC analysis caused for the diluent and mobile phase polarities to be mismatched, resulting in the analyte peak being split, the degree depending upon what percentage the solvent was mixed in with water. After careful analysis, it was discovered that a mixture of 30/70 acetonitrile/water gave close to 100% recovery as well as good chromatographic stability in the resulting quantitative analysis.

Finally, batch binding analysis using different amounts of cinchonidine as well as cinchonine was performed on both the blank and imprinted polymer. Scatchard plots were used to assess the binding occurring within each polymer and allowed for the determination of both the binding constant as well as the number of binding sites present. Analysis of the scatchard plots for both cinchonidine and cinchonine conclusively prove that selective extractions are possible. This was demonstrated as the cinchonidine scatchard plot revealed the presence of two distinct classes of binding sites, while the cinchonine plot showed the presence of only one class of binding sites. It was found that the imprinted polymer possesses 13.9 $\mu\text{mol/g}$ polymer of these selective sites, which have a binding constant of $4.42 \times 10^6 \text{ mol}^{-1}$. Overall, these results show that selective interactions are occurring, which will allow for a selective extraction, assuming the extraction conditions are correctly optimized.

Chapter 5. Overall Conclusions

The origins of molecular imprinting were discussed and two general types of imprinting were presented. Covalent imprinting uses covalent bonds between the monomer and the template to provide a stable monomer-template complex, which results in a small distribution of binding sites. However, this technique is limited by the kinetics that are associated with the formation of different covalent bonds, thus only certain molecules may be imprinted. Non-covalent imprinting utilizes intra-molecular interactions, such as hydrogen bonding, to create the monomer-template complex. This allows for many different types of molecules to be used as templates, however, the resulting polymer will possess a large distribution of binding sites. Lastly, several different applications were examined and the impact and future potential of imprinted polymers was discussed.

A cinchonidine-MAA system was utilized to test and validate an IR spectroscopy method for the characterization of the prepolymerization solution. Previously research had suggested that ATR-FTIR spectroscopy could be used to rapidly evaluate a molecular imprinted polymer systems utilizing MAA as the functional monomer and to determine the optimal amount of MAA needed to generate maximum selectivity, while minimizing the formation of non-specific sites of interaction. Our results showed that ATR-FTIR spectroscopy is not sensitive enough to detect low levels of MAA that result from strong interactions with the template molecule or discern very weak bonding interactions that have a dramatic effect on polymer selectivity. As shown with the ATR-FTIR spectra, detectable amounts of MAA were not observed below equal mole equivalents, indicating that a strong interaction was occurring between the template and monomer. It was

reasoned that this interaction was occurring between the tertiary amine of cinchonidine and the MAA in solution. Additionally, a scatchard plot was used to evaluate the binding occurring within the system. Analysis of the weak binding region revealed that 15 equivalents of monomer were needed to ensure optimal complex formation. This suggested that the IR method could not accurately determine the endpoint at which direct template-monomer binding had ended.

ITC, a microcalorimetry technique primarily used in biochemistry, was proposed as a possible alternative to conventional spectroscopic techniques. The results from these experiments revealed that formation of the cinchonidine-MAA complex has a ΔH_f of -43.9 kcal/mol (RSD=3.19%), which indicates that the formation of the monomer-template complex is energetically favorable. The data also showed that the presence of two strong hydrogen-bonding interactions that accounted for the majority of energy released. It was suggested that the tertiary amine and aromatic amine were responsible for these interactions, based on their basicity. Furthermore, the ITC data suggested that the optimal ratio of MAA to cinchonidine was 4:1, as there were two weak interactions that were observed during the titration. This was surprising given that the template possesses only three functional groups capable of engaging in hydrogen bonding.

This predicted ratio was evaluated by preparing a series of polymers containing different amounts of MAA and chromatographically determining their selectivity. The selectivity values obtained for the 4:1 polymer ($\alpha = 24.4$) was significantly higher than that of the polymer prepared with three equivalents ($\alpha = 13.6$), equaling the number of functional groups, of MAA. This is significant as this additional interaction, while energetically small, provides a significant contribution to the enantioselective recognition

mechanism. Thus we have demonstrated conclusively the importance of determining the correct amount monomer for an imprinted polymer system as very small interactions play a significant role in the resulting polymer selectivity. Additionally it was noted that adding higher amounts of MAA did not improve polymer selectivity as the polymer prepared with six equivalents of MAA demonstrated a selectivity of 16.0, even though both compounds demonstrated larger capacity factors. This reconfirms the idea that excess monomer is incorporated into the solid polymer as non-specific binding sites.

Finally, ITC was used to re-evaluate an Indinavir-MAA polymer system that had been previously studied. The ITC results for several different titrations of Indinavir with other monomers, correlated directly with the observed selectivity for polymers prepared with the respective monomers. It was also shown that the ITC detected three additional weak interactions that were occurring between MAA and Indinavir, which were not observed using ATR-FTIR. Given the results from the cinchonidine-MAA system, further chromatographic analysis will be needed to assess their impact. However, a new set of polymers that had been prepared, demonstrated minimal selectivity between Indinavir and one of its isomers. It is believed that significant amounts of water present during polymer synthesis resulted in the disruption of hydrogen bonding between MAA and Indinavir.

A discussion concerning basic theoretical parameters relating to solid-phase extraction was presented. From this discussion, it was shown that there are two competing forces in generating a selective extraction, specifically cartridge efficiency and analyte retention. By using the Van Deetmer equation, it was shown that the MIP-SPE

cartridge would have very low efficiency and that any selective extraction would have to be generated by high retention factors.

Breakthrough volumes were determined for both cinchonidine and cinchonine on a cinchonidine-imprinted polymer. It was predicted that cinchonidine would have the higher breakthrough volume, based on previously calculated retention factors. However, experimental results showed that cinchonine had a higher breakthrough volume, opposite of the predicted results. This raised the possibility that the kinetics of the interactions were too slow compared to the overall speed of extraction and that any retention was the result of non-specific interactions with the polymer.

In response to this, batch-binding analysis was performed in order to remove any effects due to the extraction flow rate. Initial results suggested that the solvent conditions were not optimized to facilitate a selective extraction. In addition, it appeared that solvent conditions were not fully optimized to generate a large recovery. A mobile phase competitor, acetic acid, was investigated as a possible solution to the problems occurring during binding. Several solutions containing small percentages of acetic acid were examined and it was found that the addition of 0.35% acetic acid (v/v) resulted in noticeable differences in recoveries between a blank and imprinted polymer, providing the first evidence that selective interactions were occurring. Additionally, many different solvents were investigated for use in reconstitution. It was discovered that both tetrahydrofuran and acetonitrile in combination with water allowed for recoveries greater than 90%, however, the use of these mixtures in HPLC analysis caused for the diluent and mobile phase polarities to be mismatched, resulting in the analyte peak being split, the degree depending upon what percentage the solvent was mixed in with water. After

careful analysis, it was discovered that a mixture of 30/70 acetonitrile/water gave close to 100% recovery as well as good chromatographic stability in the resulting quantitative analysis.

Finally, batch binding analysis using different amounts of cinchonidine as well as cinchonine were performed on both the blank and imprinted polymer. Scatchard plots were used to assess the binding occurring within each polymer and allowed for the determination of both the binding constant as well as the number of binding sites present. Analysis of the scatchard plots for both cinchonidine and cinchonine conclusively prove that selective extractions are possible. This was demonstrated as the cinchonidine scatchard plot revealed the presence of two distinct classes of binding sites, while the cinchonine plot showed the presence of only one class of binding sites. It was found that the imprinted polymer possesses 13.9 $\mu\text{mol/g}$ polymer of these selective sites, which have a binding constant of $4.42 \times 10^6 \text{ mol}^{-1}$. Overall, these results show that selective interactions are occurring, which will allow for a selective extraction, assuming the extraction conditions are correctly optimized.

The use of MIP materials in analytical methods has brought forth new and exciting developments. However, several challenges still remain unfulfilled in fully understanding the importance of these materials. The work presented in this dissertation provides a significant contribution in the design of imprinted polymers as we have shown microcalorimetry to be a valuable technique for understanding the formation of the monomer-template complex. It is our hope that this work provides guidance to other researchers and helps facilitate a greater understanding of these materials.

Literature Cited

1. Spivak, D. A., Shea, K.J. *Anal. Chim. Acta.* **2001**, *435*, 65-74.
2. Dickey F. H., *J. Phys. Chemistry*, **1955**, *59*, 695-707.
3. Curtis, R., Colombo, U., *J. Am. Chem. Soc.*, **1952**, *74*, 3961.
4. Sellergren, B., *Trends. Anal. Chem.*, **1997**, *16*, 310-320.
5. Andersson, L., I., Mosbach, K., *J. Chromatogr.*, **1990**, *516*, 313-322.
6. Wulff, G., *Angew. Chem. Int. Ed. Eng.*, **1995**, *34*, 1812-1832.
7. Wulff, G., Kemmerer, R., Vietmeier, J., Poll, H., G., *Nouveau J. DeChemie*, **1982**, *12*, 681-687.
8. Wulff, G., Schauhoff, S., *J. Org. Chem.*, **1991**, *56*, 395-400.
9. Kugimiya, A., Matsui, J., Takeuchi, T., Yano, K., Muguruma, H., Elgersma, A., V., Karube, I., *Anal. Lett.*, **1995**, *28*, 2317-2323.
10. Shea, K. J., Dougherty, T., *J. Am. Chem. Soc.*, **1986**, *108*, 1091-1109.
11. Shea, K. J., Sasaki, D.Y., *J. Am. Chem. Soc.*, **1989**, *111*, 3442-3444.
12. Wulff, G., Heide, B., Helfmeier, G., *J. Am. Chem. Soc.* **1986**, *108*, 1089-1091.
13. Wulff, G., Sarhan, A., Zabrocki, K., *Tetrahedron Lett.*, **1973**, *44* , 4329-4332.
14. Sarhan, A., Wulff, G., *Makromol Chem.*, **1982**, *183*, 85-92.
15. Andersson, L.I., *J. Chromatogr. B.*, **2000**, *745*, 3-13.
16. Sellergren, B., *Makromol Chem.*, **1989**, *190*, 2703-2711.
17. Kempe, M., Mosbach, K., *J. Chromatogr. A*, **1995**, *694*, 3-13.
18. Shea, K.J., Spivak, D.A., Sellergren, B., *J. Am. Chem. Soc.*, **1993**, *115*, 3368-3369.
19. Ramström, O., Nicholls, I.A., Mosbach, K., *Tetrahedron: Asymmetry*, **1994**, *5*, 649-656.

20. Matsui, J., Nicholls, I.A., Takeuchi, T., *Tetrahedron: Asymmetry*, **1996**, *7*, 1357-1361.
21. Piletsky, S.A., Alcock, S., Turner, A.P.F., *Trends in Biotechnology*, **2001**, *19*, 9-12.
22. Mosbach, K., Haupt, K., *Tibtech.*, **1998**, *16*, 468-475.
23. Piletsky, S.A., Piletska, E.V., Bossi, A., Karim, K., Lowe, P., Turner, A.P.F., *Biosensors and Bioelectronics*, **2001**, *16*, 701-707.
24. Andersson, L.I., *Anal. Chem.*, **1996**, *68*, 111-117.
25. Lulka, M.F., Iqbal, S.S., Chambers, J. P., Valdes, E. R., Thompson, R. G., Goode, M. T., Valdes, J.J., *Material Science and Engineering C*, **2001**, *11*, 101-105.
26. Suárez-Rodríguez, J. L., Díaz-García, M.A., *Biosensors and Bioelectronics*, **2001**, *16*, 955-961.
27. Haupt, K., *Reactive and Functional Polymers*, **1999**, *41*, 125-131.
28. Ye, L., Cormack, P.A.G., Mosbach, K., *Anal. Commun.*, **1997**, *34*
29. Haupt, K., Mayes, A.G., Mosbach, K., *Anal. Chem.*, **1998**, *70*, 3936-3939.
30. Takeuchi, T., Dobashi, A., Kimura, K., *Anal. Chem.*, **2000**, *72*, 2418-2422.
31. Rathbone, D.L., Ge, Y., *Anal. Chim. Acta*, **2001**, *435*, 129-136.
32. Scheller, F.W., Wollenberger, U., Warsinke, A., Lisdat, F., *Current Opinion in Biotechnology*, **2001**, *12*, 35-40.
33. Takeuchi, T., Haginaka, J., *J. Chromatogr. B.*, **1999**, *728*, 1-20.
34. Dickert, F.L., Hayden, O., *Trends in Analytical Chemistry*, **1999**, *18*, 192-198.
35. Tan, Y., Yin, J., Liang, C., Peng, H., Nie, L., Yao, S., *Bioelectrochemistry*, **2001**, *53*, 141-148.

36. Liang, C., Peng, H., Zhou, A., Nie, L., Yao, S., *Anal. Chem. Acta*, **2000**, *415*, 135-141.
37. Piletsky, S.A., Piletskaya, E.V., Elgersma, A.V., Yano, E. K., Karube, I., *Biosensors and Bioelectronics*, **1995**, *10*, 959-964.
38. Kriz, D., Mosbach, K., *Anal. Chim. Acta*, **1995**, *300*, 71-75.
39. Kriz, D., Ramström, O., Svensson, A., Mosbach, K., *Anal. Chem.*, **1995**, *67*, 2142-2144.
40. Kriz, D., Kempe, M., Mosbach, K., *Sensors and Actuators B*, **1996**, *33*, 178-181.
41. McNiven, S., Kato, M., Levi, R., Yano, K., Karube, I., *Anal. Chim. Acta*, **1998**, *365*, 69-74.
42. Turkewitsch, P., Wandelt, B., Darling, G., Powell, W.S., *Anal. Chem.*, **1998**, *70*, 2025-2030.
43. Suárez-Rodríguez, J.L., Díaz-García, M.A., *Anal. Chem. Acta*, **2000**, *405*, 67-76.
44. Dickert, F.L., Lieberzeit, P., Totrschanoff, M., *Sensors and Actuators B*, **2000**, *65*, 186-189.
45. Ji, H.S., McNiven, S., Lee, K.H., Saito, T., Ikebukuro, K., Karube, I., *Biosensors and Bioelectronics*, **2000**, *15*, 403-409.
46. Dickert, F.L., Halikias, K., Hayden, O., Piu, L., Sikorski, R., *Sensors and Actuators B*, **2001**, *76*, 295-298.
47. Andrea, P., Miroslav, S., Silvia, S., Stanislav, M., *Sensors and Actuators B*, **2001**, *76*, 286-294.
48. Cheng, Z., Wang, E., Yang, Z., *Biosensors and Bioelectronics*, **2001**, *16*, 179-185.
49. Luo, C., Liu, M., Mo, Y., Qu, J., Feng, Y., *Anal. Chim. Acta*, **2001**, *428*, 143-148.

50. Panasyuk-Delaney, T., Mirsky, V. M., Ulbricht, M., Wolfbeis, O.S., *Anal. Chim. Acta*, **2001**, *435*, 157-162.
51. Gao, S., Wang, W., Wang, B., *Bioorganic Chemistry*, **2001**, *29*, 308-320.
52. Yan, M., Kapua, A., *Anal. Chim. Acta*, **2001**, *435*, 163-167.
53. Chow, C. F., Lam, M. H. W., Leung, M. K. P., *Anal. Chim. Acta*, **2002**, *466*, 17-30.
54. Tong, A., Dong, H., Li, L., *Anal. Chim. Acta*, **2002**, *466*, 31-37.
55. Douglas, B.E., McDaniel, D.H., Alexander, J.J., *Concepts and Models of Inorganic Chemistry*, 3rd edition, Wiley & Sons, New York, 1994.
56. Brüggemann, O., *Biomolecular Engineering*, **2001**, *18*, 1-7.
57. Yamazaki, T., Yilmaz, E., Mosbach, K., Sode, K., *Anal. Chim. Acta*, **2001**, *435*, 209-214.
58. Ohkubo, K., Sawakuma, K., Sagawa, T., *J. Molecular Catalysis A: Chemical*, **2001**, *165*, 1-7.
59. Brüggemann, O., *Anal. Chim. Acta*, **2001**, *435*, 197-207.
60. Ohkubo, K., Urata, Y., Hirota, S., Funakoshi, Y., Sagawa, T., Usui, S., Yoshinaga, K., *J. Molecular Catalysis A: Chemical*, **1995**, *101*, L111-L114.
61. Strikovskiy, A., Hradil, J., Wulff, G., *Reactive and Functional Polymers*, **2003**, *54*, 49-61.
62. Gamez, P., Dunjie, B., Pinel, C., Lemaire, M., *Tetrahedron Letters*, **1995**, *36*, 8779-8782.
63. Ohkubo, K., Sawakuma, K., Sagawa, T., *Polymer*, **2001**, *42*, 2263-2266.
64. Karmalkar, R. N., Kulkari, M. G., Mashelkar, R. A., *J. Controlled Release*, **1997**, *43*, 235-243.

65. Masqué, N., Marcé, R. M., Borrull, F., *Trends in Analytical Chemistry*, **1998**, *17*, 384-394.
66. Ferrer, I., Barceló, D., *Trends in Analytical Chemistry*, **1999**, *18*, 180-192.
67. Hennion, M. C., *J. Chromatogr. A*, **1999**, *856*, 3-54.
68. Andersson, L. I., *J. Chromatogr. B*, **2001**, *739*, 163-173.
69. Masqué, N., Marcé, R. M., Borrull, F., *Trends in Analytical Chemistry*, **2001**, *20*, 477-486.
70. Ensing, K., Berggren, C., Majors, R. E., *LC-GC*. **2001**, *19*, 942-954.
71. Olsen, J., Martin, P., Wilson, I. D., *Anal. Commun.*, **1998**, *35*, 13H-14H.
72. Sellergren, B., *Anal. Chem.*, **1994**, *66*, 1578-1582.
73. Mullet, W. M., Lai, E. P. C., *J. Pharmaceutical and Biomedical Analysis*, **1999**, *21*, 835-843.
74. Xie, J., Zhu, L., Luo, H., Zhou, L., Li, C., Xu, X., *J. Chromatogr. A*, **2001**, *934*, 1-11.
75. Zi-hui, M., Qin, L., *Anal. Chem. Acta*, **2001**, *435*, 121-127.
76. Jodlbauer, J., Maier, N. M., Linder, W., *J. Chromatogr. A*, **2002**, *945*, 45-63.
77. Caro, E., Masqué, N., Marcé, R. M., Borrull, F., Cormack, P. A. G., Sherrington, D. C., *J. Chromatogr. A*, **2002**, *963*, 169-178.
78. Chianella, I., Piletsky, S. A., Tothill, I.E., Chen, B., Turner, A.P.F., *Biosensors and Bioelectronics*, **2003**, *18*, 119-127.
79. Matsui, J., Okada, M., Tsuruoka, M., Takeuchi, T., *Anal. Commun.*, **1997**, *34*, 85-87.

80. Walshe, M., Howarth, J., Kelly, M.T., O'Kennedy, R., Smyth, M.R., *J. Pharmaceutical and Biomedical Analysis*, **1997**, *16*, 319-325.
81. Martin, P., Wilson, I.D., Morgan, D.E., Jones, G.R., Jones, K., *Anal. Commun.*, **1997**, *34*, 45-47.
82. Muldoon, M.T., Stanker, L.H., *Anal. Chem.*, **1997**, *69*, 803-808.
83. Andersson, L.I., Paprica, A., Arvidsson, T., *Chromatographia*, **1997**, *46*, 57-62.
84. Rashid, B.A., Briggs, R.J., Hay, J.N., Stevenson, D., *Anal. Commun.* **1997**, *34*, 303-305.
85. Mullet, W.M., Lai, E.P.C., *Anal. Chem.*, **1998**, *70*, 3636-3641.
86. Zander, A., Findlay, P., Renner, T., Sellergren, B., *Anal. Chem.*, **1998**, *70*, 3304-3314.
87. Bjarnson, B., Chimuka, L., Ramström, O., *Anal. Chem.*, **1999**, *71*, 2152-2156.
88. Olsen, J., Martin, P., Wilson, I.D., Jones, G.R., *Analyst*, **1999**, *124*, 467-471.
89. Matsui, J., Fujiwara, K., Ugata, S., Takeuchi, T., *J. Chromatogr. A*, **2000**, *889*, 25-31.
90. Mullet, W.M., Dirie, M.F., Lai, E.P.C., Guo, H., He, X., *Anal. Chim. Acta*, **2000**, *414*, 123-131.
91. Martin, P., Wilson, I.D., Jones, G.R., *J. Chromatogr. A*, **2000**, *889*, 143-147.
92. Berggren, C., Bayouh, S., Sherrington, D.C., Ensing, K., *J. Chromatogr. A*, **2000**, *889*, 105-110.
93. Adbo, K., Nicholls, I.A., *Anal. Chim. Acta*, **2001**, *435*, 115-120.
94. Bereczki, A., Tolokan, A., Horvai, G., Horváth, Lanza, F., Hall, A.J., Sellergren, B., *J. Chromatogr. A*, **2001**, *930*, 31-38.

95. Brambilla, G., Fiori, M., Rizzo, B., Crescenzi, V., Masci, G., *J. Chromatogr. A*, **2001**, *759*, 27-32.
96. Segeyeva, T.A., Matuschewski, H., Piletsky, S.A., Bendig, J., Schedler, U., Ulbricht, M., *J. Chromatogr. A*, **2001**, *907*, 89-99.
97. Möller, K., Nilsson, U., Crescenzi, C., *J. Chromatogr. A*, **2001**, *938*, 121-130.
98. Baggiani, C., Giovannoli, C., Anfossi, L., Tozzi, C., *J. Chromatogr. A*, **2001**, *938*, 35-44.
99. Mena, M.L., Martínez-Ruiz, P., Reviejo, A.J., Pingarrón, J.M., *Anal. Chim. Acta*, **2002**, *451*, 297-304.
100. Moring, S.E., Wong, O.S., Stobaugh, J.F., *J. Pharmaceutical and Biomedical Analysis*, **2002**, *27*, 719-728.
101. Pap, T., Horváth, V., Tolokán, A., Horvai, G., Sellergren, B., *J. Chromatogr. A*, **2002**, *973*, 1-12.
102. Theodoridis, G., Manesiotis, P., *J. Chromatogr. A*, **2002**, *948*, 163-169.
103. Stevenson, D., *Trends in Analytical Chemistry*, **1999**, *18*, 154-158.
104. Kempe, M., Mosbach, K., *J. Chromatogr. A*, **1994**, *664*, 276-279.
105. Lin, J.M., Nakagama, T., Uchiyama, K., Hobo, T., *J. Pharmaceutical and Biomedical Analysis*, **1997**, *15*, 1351-1358.
106. Scheitz, L., Andersson, L.I., Nilsson, S., *J. Chromatogr. A*, **1997**, *792*, 401-409.
107. Brüggermann, O., Freitag, R., Whitcombe, M.J., Vulfson, E.N., *J. Chromatogr. A*, **1997**, *781*, 43-53.
108. Schweitz, L., Andersson, L.I., Nilsson, S., *J. Chromatogr. A*, **1998**, *817*, 5-13.
109. Vallano, P.T., Remcho, V. T., *J. Chromatogr. A*, **2000**, *887*, 125-135.

110. Ellwanger, A., Owens, P.K., Karlsson, L., Bayouhd, S., Cormack, P., Sherrington, D., Sellergren, B., *J. Chromatogr. A*, **2000**, *897*, 317-327.
111. Suedee, R., Songkram, C., Petmoreekul, A., Sangkunakup, S., Sankasa, S., Kongyarit, N., *J. Pharmaceutical and Biomedical Analysis*, **1999**, *19*, 519-527.
112. Andersonn, L.I., O'Shannessy, D.J., Mosbach, K., *J. Chromatogr.*, **1990**, *513*, 167-179.
113. Lepisto, M., Sellergren, B., *J. Org. Chem.*, **1989**, *54*, 6010-6012.
114. Lu, Y., Li, C., Liu, X., Huang, W., *J. Chromatogr. A*, **2002**, *950*, 89-97.
115. Yu, C., Mosbach, K., *J. Mol. Recog.*, **1998**, *11*, 69-74.
116. Nicholls, I.A., Ramström, O., Mosbach, K., *J. Chromatogr. A*, **1995**, *691*, 349-353.
117. O'Brien, T.P., Snow, N.H., Grinberg, N., Crocker, L., *J. Liq. Chrom. and Rec. Technol.*, **1999**, *22*, 183-204.
118. O'Brien, T. Ph.D. Thesis, Seton Hall University, May 1999.
119. Sellergren, B., Shea, K.J., *J. Chromatogr*, **1993**, *635*, 31-49.
120. O'Shannessy, D.J., Ekberg, B., Mosbach, K., *Anal. Biochem.*, **1989**, *177*, 144-149.
121. Spivak, D., Gilmore, M.A., Shea, K.J., *J. Am. Chem. Soc.*, **1997**, *119*, 4388-4393.
122. Sellergren, B., Dauwe, C., Schneider, T., *Macromolecules*, **1997**, *30*, 2454-2459.
123. Ramström, O., Andersson, L.I., Mosbach, K., *J. Org. Chem.*, **1993**, *58*, 7562-7564.
124. Matsui, J., Takeuchi, T., *Anal. Commun.*, **1997**, *34*, 199-200.
125. Matsui, J., Doblhoff-Dier, O., Takeuchi, T., *Anal. Chim. Acta*, **1997**, *343*, 1-4.
126. Zander, A., Findlay, P., Renner, T., Sellergren, B., *Anal. Chem.*, **1998**, *70*, 3304-3314.
127. Yu, C., Mosbach, K., *J. Org. Chem.*, **1997**, *62*, 4057-4064.

158. Mullet. W.M., Dirie, M.F., Lai, E.P.C., Guo, H., He, X., *Anal. Chim. Acta*, **2000**, *414*, 123-131.
159. Duffy, D.J., Das, K., Hsu, S.L., Penelle, J., Rotello, V.M., *Polym. Mater. Sci. Eng.*, **2000**, 69-70.
160. Katz, A., Davis, M.E., *Macromolecules*, **1999**, *32*, 4113-4121.
161. *The Merck Index Tenth Edition*; Windholz, M., Ed., Budavari, S., Ed., Blumetti, R.F., Ass. Ed., Otterbein, E.S., Ass. Ed., Merck & Co., New Jersey, 1983.
162. Crews, P., Rodríguez, J., Jaspars, M., *Organic Structure Analysis*, Oxford University Press, New York, 1998.
163. Calorimetry Sciences Corporation, Model 4200 Isothermal Titration Calorimeter User Manual.
164. Fritz, J.S., *Analytical Solid-Phase Extraction*, Wiley-VCH, New York, 1999.
165. Kazakevich, Y., McNair, H.M., *Basic Liquid Chromatography*, <http://hplc.chem.shu.edu/HPLC/index.html>, 2002.
166. Snyder, L.R., Kirkland, J.J., Glajch, J.L., *Practical HPLC Method Development 2nd ED*. John Wiley & Sons, New York, 1997.
167. Hennion, M.C., Coquart, V.J., *J. Chromatogr.*, **1993**, *642*, 211.